

# UNCLASSIFIED

AD NUMBER
AD480402
NEW LIMITATION CHANGE
TO Approved for public release, distribution unlimited
FROM Distribution authorized to U.S. Gov't. agencies and their contractors; Critical Technology; 20 MAY 1964. Other requests shall be referred to Commanding Officer, Air Force Technical Applications Center, Patrick AFB, FL 32925.
AUTHORITY
USAF ltr, 25 Jan 1972

THIS PAGE IS UNCLASSIFIED

480402

2

# Atlas of Signals and Noise

## Project VT/036

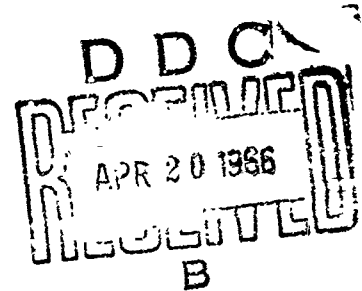
The Geotechnical Corporation

3401 Shiloh Rd • Garland, Texas

VEOTECH

TECHNICAL REPORT NO. 64-50

ATLAS OF SIGNALS AND NOISE



THIS DOCUMENT IS SUBJECT TO SPECIAL  
EXPORT CONTROLS AND EVEN TRANSFER  
TO FOREIGN GOVERNMENTS OF FOREIGN  
NATIONALS MAY BE MADE ONLY WITH PRIOR  
APPROVAL OF CHIEF, AFSA.

THE GEOTECHNICAL CORPORATION  
3401 Shiloh Road  
Garland, Texas

20 May 1964

## CONTENTS

1. INTRODUCTION
  - 1.1 Authority
  - 1.2 Purpose
  - 1.3 Orientation of instrument arrays
2. EARTHQUAKE PHASES
3. P AND PKP PHASES FROM VARIOUS DISTANCES AND AZIMUTHS
  - 3.1 Distance =  $0^{\circ}$  to  $16^{\circ}$
  - 3.2 Distance =  $17^{\circ}$  to  $40^{\circ}$
  - 3.3 Distance =  $41^{\circ}$  to  $60^{\circ}$
  - 3.4 Distance =  $61^{\circ}$  to  $80^{\circ}$
  - 3.5 Distance =  $81^{\circ}$  to  $100^{\circ}$
  - 3.6 Distance =  $101^{\circ}$  to  $120^{\circ}$
  - 3.7 Distance =  $121^{\circ}$  to  $140^{\circ}$
  - 3.8 Distance =  $141^{\circ}$  to  $160^{\circ}$
4. NOISE SAMPLES

## INDEX

Best Available Copy



## ILLUSTRATIONS

### Figure

- 1-1      Orientation of instrument arrays at WMSO
- 1-2      Normalized response characteristics of seismographs at WMSO
- 2-1      WMSO seismogram illustrating P and pP phase arrivals from the Kermadec Islands
- 2-2      WMSO seismogram illustrating P and pP phase arrivals from Central Peru
- 2-3      P-wave arrival recorded on all systems at WMSO. Epicenter: Kurile Islands
- 2-4      WMSO primary short-period seismogram illustrating a "Lonesome P." Epicenter: near the east coast of Kamchatka
- 2-5      WMSO seismogram illustrating S and sS phase arrivals (see figures 2-6 and 2-7 for the corresponding phase arrivals on the short-period system). Epicenter: Northern Chile
- 2-6      WMSO seismogram illustrating an S phase arrival on the short-period system. Epicenter: Northern Chile
- 2-7      WMSO seismogram illustrating an sS phase arrival on the short-period system. Epicenter: Northern Chile
- 2-8      WMSO seismogram illustrating an S phase arrival from Western Bolivia (see figure 2-9 for corresponding phase on the short-period system)
- 2-9      WMSO seismogram illustrating an S phase arrival from Western Bolivia
- 2-10     WMSO seismogram illustrating S and ScS phase arrivals from the Easter Islands region
- 2-11     WMSO seismogram illustrating S and SP phase arrivals from the Kurile Islands

### ILLUSTRATIONS, Continued

#### Figure

- 2-12 WMSO seismogram illustrating a PP phase arrival from the New Hebrides Islands (see figure 2-13 for the corresponding phase on the short-period system)
- 2-13 WMSO primary short-period seismogram illustrating a PP phase from the New Hebrides Islands
- 2-14 WMSO seismogram illustrating a PP phase arrival from Western New Guinea (see figure 2-15 for the corresponding phase on the short-period system)
- 2-15 WMSO seismogram illustrating a PP phase arrival from Western New Guinea
- 2-16 WMSO seismogram illustrating PP and PPP phases from the Kurile Islands
- 2-17 WMSO seismogram illustrating SS and SSS phases from the Fiji Islands region
- 2-18 WMSO seismogram illustrating a PcP phase arrival. Epicenter: Northern Peru
- 2-19 WMSO seismogram illustrating an ScP phase arrival from the Peru-Bolivia border
- 2-20 WMSO seismogram illustrating ScP, S, and ScS phase arrivals from Northern Chile
- 2-21 ScS as recorded on the WMSO short-period seismogram. Epicenter: Northern Chile
- 2-22 WMSO seismogram illustrating PKP<sub>1</sub> and PKP<sub>2</sub> phase arrivals. Epicenter: near the west coast of Sumatra
- 2-23 WMSO seismogram illustrating an SKP phase arrival. Epicenter: near north coast of Java

### ILLUSTRATIONS, Continued

#### Figure

- 2-24 WMSO seismogram illustrating  $SKP_1$  and  $SKP_2$  phase arrivals. Epicenter: Western Macquarie Islands
- 2-25 WMSO primary short-period seismogram illustrating  $PKKP_1$  and  $PKKP_2$  phase arrivals from the Sandwich Islands
- 2-26  $FKKP_1$ - $PKKP_2$ - $PKKP_3$  as recorded on the WMSO short-period seismogram. Epicenter: Santa Cruz Island region
- 2-27 WMSO primary short-period seismogram illustrating an SKKP phase arrival. Epicenter: near north coast of Java
- 2-28 WMSO seismogram illustrating a FKPPKP (P'P') phase arrival. Epicenter: off the east coast of Kamchatka
- 2-29 WMSO seismogram illustrating a PKPPKPPKF (P'P'P') phase arrival. Epicenter: Kermadec Islands
- 2-30 WMSO seismogram illustrating a PKPPKPPKPPKP (P'P'P'P') phase arrival. Epicenter: Kermadec Islands
- 2-31 WMSO seismogram illustrating a PcPPKP phase arrival. Epicenter: Loyalty Islands region
- 2-32 WMSO seismogram illustrating SKS, S<sub>1</sub>, and FS phase arrivals from the Fiji Islands region (see figure 2-33 for the corresponding short-period recording of SKS)
- 2-33 WMSO seismogram illustrating an SKS phase arrival from the Fiji Islands region
- 2-33a WMSO seismogram illustrating an SKS phase arrival from the Fiji Islands region
- 2-34 WMSO seismogram illustrating SKS, FS, and PPS phase arrivals from the New Hebrides Islands
- 2-35 WMSO seismogram illustrating SKS, SP, and SPP phases from the Fiji Islands region

### ILLUSTRATIONS, Continued

#### Figure

- 2-36 WMSO seismogram illustrating SKS and SKKS phase arrivals from Western New Guinea
- 2-37 WMSO seismogram illustrating PKKS and SKKS phase arrivals from the New Hebrides Islands
- 2-38 WMSO seismogram illustrating a PKPKS phase arrival from the Kermadec Islands
- 2-39 SKKKS as recorded on the WMSO short-period seismogram. Epicenter: Kermadec Islands
- 2-40 WMSO seismogram illustrating Love and Rayleigh phase arrivals from Sonora, Mexico
- 2-41 WMSO seismogram illustrating the broad-band system response to surface waves. Epicenter: off the coast of Central Mexico
- 2-42 WMSO seismogram illustrating a Rayleigh<sub>1</sub> phase arrival (see figure 2-43 for Rayleigh<sub>2</sub> arrival from the same event). Epicenter: Kermadec Islands
- 2-43 WMSO seismogram illustrating a Rayleigh<sub>2</sub> phase arrival. Epicenter: Kermadec Islands
- 2-44 Rayleigh waves as recorded on the WMSO short-period seismogram. Epicenter: Santa Cruz Island region
- 3-1 WMSO seismogram illustrating a P phase arrival from the Gulf of California
- 3-2 WMSO short-period seismogram illustrating a P phase arrival from Central Idaho
- 3-3 WMSO seismogram illustrating a P phase arrival from Guerrero, Mexico

### ILLUSTRATIONS, Continued

#### Figure

- 3-4 WMSO seismogram illustrating a P phase arrival from the Revilla Gigedo Island region
- 3-5 WMSO short-period seismogram illustrating a P phase arrival. Epicenter: Jalisco, Mexico
- 3-6 WMSO short-period seismogram illustrating a P phase arrival from the Ontario-Quebec border
- 3-7 WMSO seismogram illustrating a P phase arrival from off the coast of Oregon
- 3-8 WMSO seismogram illustrating a P phase arrival from off the coast of Oregon
- 3-9 WMSO short-period seismogram illustrating a P phase arrival. Epicenter: near the north coast of Venezuela
- 3-10 WMSO seismogram illustrating a P phase arrival from the Galapagos Islands
- 3-11 WMSO seismogram illustrating a P phase arrival. Epicenter: near the coast of Southern Chile
- 3-12 WMSO short-period seismogram illustrating a P phase arrival from Ecuador
- 3-13 WMSO seismogram illustrating a P phase arrival from the North Atlantic Ocean
- 3-14 An event from Western Brazil as recorded at WMSO
- 3-15 WMSO seismogram illustrating a P phase arrival. Epicenter: south of Hawaii Island
- 3-16 WMSO seismogram illustrating a P phase arrival from the Andreanof Islands region

### ILLUSTRATIONS, Continued

#### Figure

- 3-17 WMSO seismogram illustrating a P phase arrival from the Andreanof Islands region
- 3-18 WMSO primary short-period seismogram illustrating a P phase arrival from the Andreanof Islands region
- 3-19 WMSO seismogram illustrating a P phase arrival. Epicenter: near the coast of Northern Chile
- 3-20 WMSO seismogram illustrating a P phase arrival from the Bolivia-Brazil border
- 3-21 WMSO seismogram illustrating a P phase arrival from the Easter Island region
- 3-22 WMSO seismogram illustrating a P phase arrival from the Kurile Islands
- 3-23 WMSO seismogram illustrating a P phase arrival from the mid-Atlantic Ocean
- 3-24 WMSO seismogram illustrating a P phase arrival. Epicenter: near the east coast of Hokkaido
- 3-25 WMSO short-period seismogram illustrating a P phase arrival from the Ionian Sea
- 3-26 WMSO short-period seismogram illustrating a P phase arrival from the Aegean Sea
- 3-27 WMSO seismogram illustrating a P phase arrival from the Fiji Islands
- 3-28 WMSO seismogram illustrating a P phase arrival from the Fiji Islands
- 3-29 WMSO seismogram illustrating a P phase arrival from off the coast of Turkey

### ILLUSTRATIONS, Continued

#### Figure

- 3-30 WMSO seismogram illustrating a PKP phase arrival from New Britain
- 3-31 WMSO seismogram illustrating a PKP phase arrival. Epicenter: near the coast of Southern Iran
- 3-32 WMSO short-period seismogram illustrating a PKP phase arrival. Epicenter: near the north coast of Luzon
- 3-33 WMSO short-period seismogram illustrating a PKP phase arrival from the Banda Sea
- 3-34 WMSO short-period seismogram illustrating a PKP phase arrival. Epicenter: off the southern coast of Java
- 3-35 WMSO seismogram illustrating a PKP phase arrival. Epicenter: off southern coast of Sumatra
- 3-36 WMSO seismogram illustrating a PKP phase arrival from the Sunda Strait
- 3-37 WMSO seismogram illustrating a PKP phase arrival from the Prince Edward Island region
- 3-38 WMSO seismogram illustrating a PKP phase arrival from the Chagos Archipelago region
- 3-39 WMSO seismogram illustrating a PKP phase arrival. Epicenter: south of Australia
- 3-40 WMSO short-period seismogram illustrating a PKP phase arrival from the Indian Ocean
- 4-1 WMSO short-period seismogram illustrating 1/2-second microseisms
- 4-2 WMSO seismogram illustrating the occurrence of 4- to 6-second microseisms at a low level on the short-period system

### ILLUSTRATIONS, Continued

#### Figure

- 4-3 WMSO seismogram illustrating the occurrence of 4- to 6-second microseisms at a moderate level on the short-period system
- 4-4 WMSO seismogram illustrating the occurrence of 4- to 6-second microseisms at a high level on the short-period system
- 4-5 WMSO seismogram illustrating wind-generated noise on the short-period system. Wind speed is approximately 38 mph
- 4-6 WMSO seismogram illustrating the short-period system response to train noise
- 4-7 WMSO seismogram illustrating lightning spikes on the short-period system
- 4-8 WMSO seismogram illustrating overlining and a generally noisy condition caused by barometric pressure changes
- 4-9 WMSO seismogram illustrating artillery generated acoustic signals. No corresponding seismic signals were recorded
- 4-10 Seismic signal and corresponding acoustics from artillery fire as recorded on the WMSO short-period seismogram
- 4-11 WMSO seismogram illustrating the seismic signal and acoustics generated by the demolition of outdated ammunition and artillery duds on Fort Sill
- 4-12 WMSO seismogram illustrating a 2500-pound detonation of TNT on Fort Sill
- 4-13 WMSO seismogram illustrating an acoustical signal generated by a blast at Richard's Spur Quarry
- 4-14 WMSO seismogram illustrating the Lg (Sur) phase from a near regional (?) event. The P phase was not recorded



## ATLAS OF SIGNALS AND NOISE

### 1. INTRODUCTION

#### 1.1 AUTHORITY

The data included in this publication were collected under authority contained in Contract AF 33(657)-12007, Project VT/036 dated 1 March 1963. The Air Force Technical Applications Center (AFTAC) has technical supervision of the contract as a part of Project VELA UNIFORM, which is under the overall direction of the Advanced Research Projects Agency (ARPA).

#### 1.2 PURPOSE

This atlas is designed as a guide for those interested in the signals recorded at the Wichita Mountains Seismological Observatory (WMSO). Examples of signals, phases, and noise are included. In many instances, the examples may be considered typical; however, due to the nature of several of the subjects, some of the examples given must be considered atypical. Reference to this atlas should provide assistance to those engaged in routine analysis of WMSO seismograms by illustrating the many different characteristics of signals and noise that appear on the seismograms.

The atlas is published in loose-leaf form so that new data may be readily added as they are encountered.

#### 1.3 ORIENTATION OF INSTRUMENT ARRAYS AT WMSO

Figure 1-1 illustrates the orientation of the arrays and identifies the locations of the individual array elements at the observatory. The short-period horizontal seismometers are located in the walk-in vault with Z6; the three-component broad-band and intermediate-band systems are located in the tank farm; and the three-component long-period system is located in the walk-in vault between Z6 and Z10. All instrument traces are identified and their respective magnifications are shown on the seismograms included in this atlas.

The normalized response characteristics of the WMSO seismographs are shown in figure 1-2.



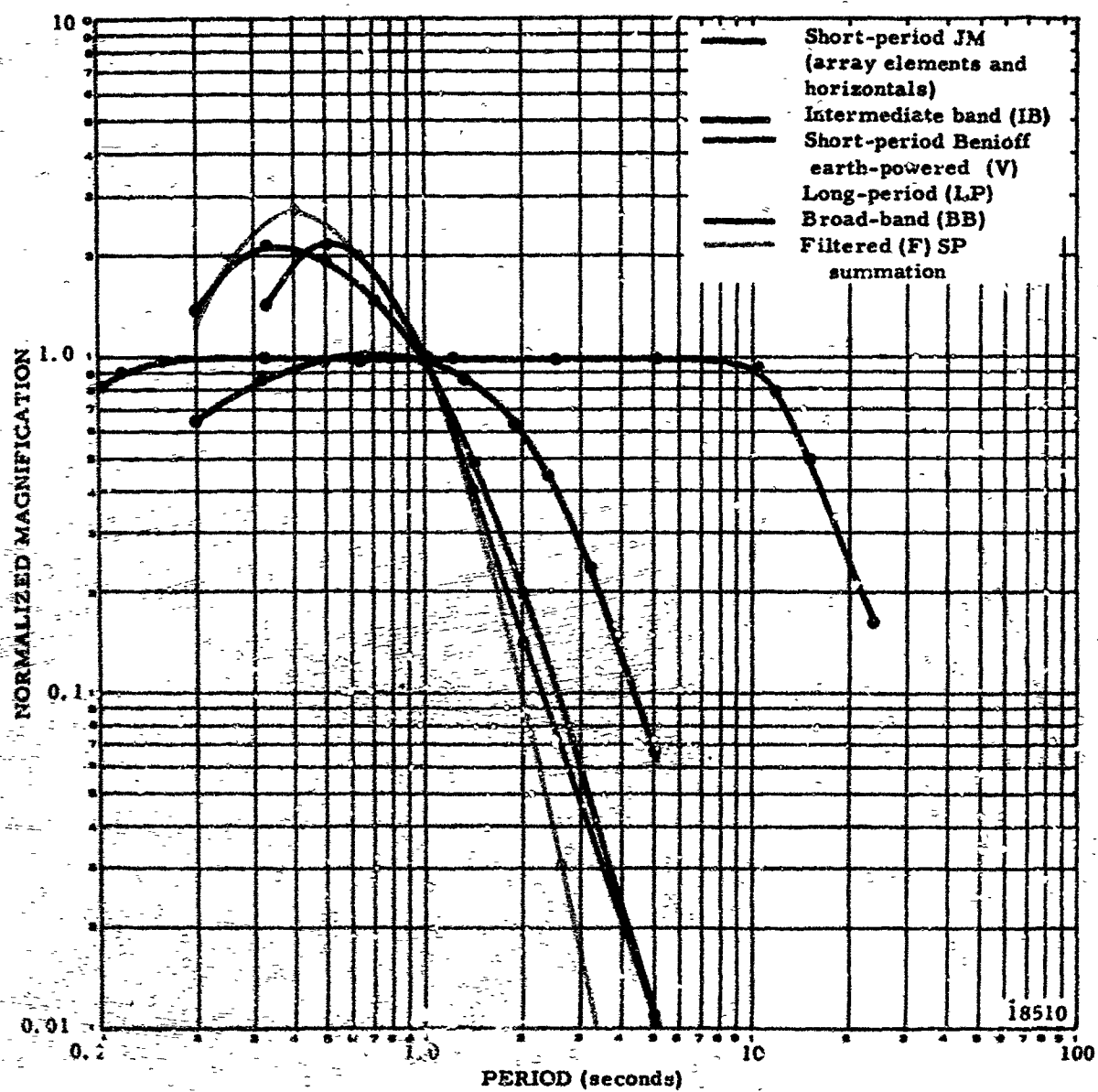


Figure 1-2. Normalized response characteristics of seismographs at WMSO

## 2. EARTHQUAKE PHASES

TR 64-50

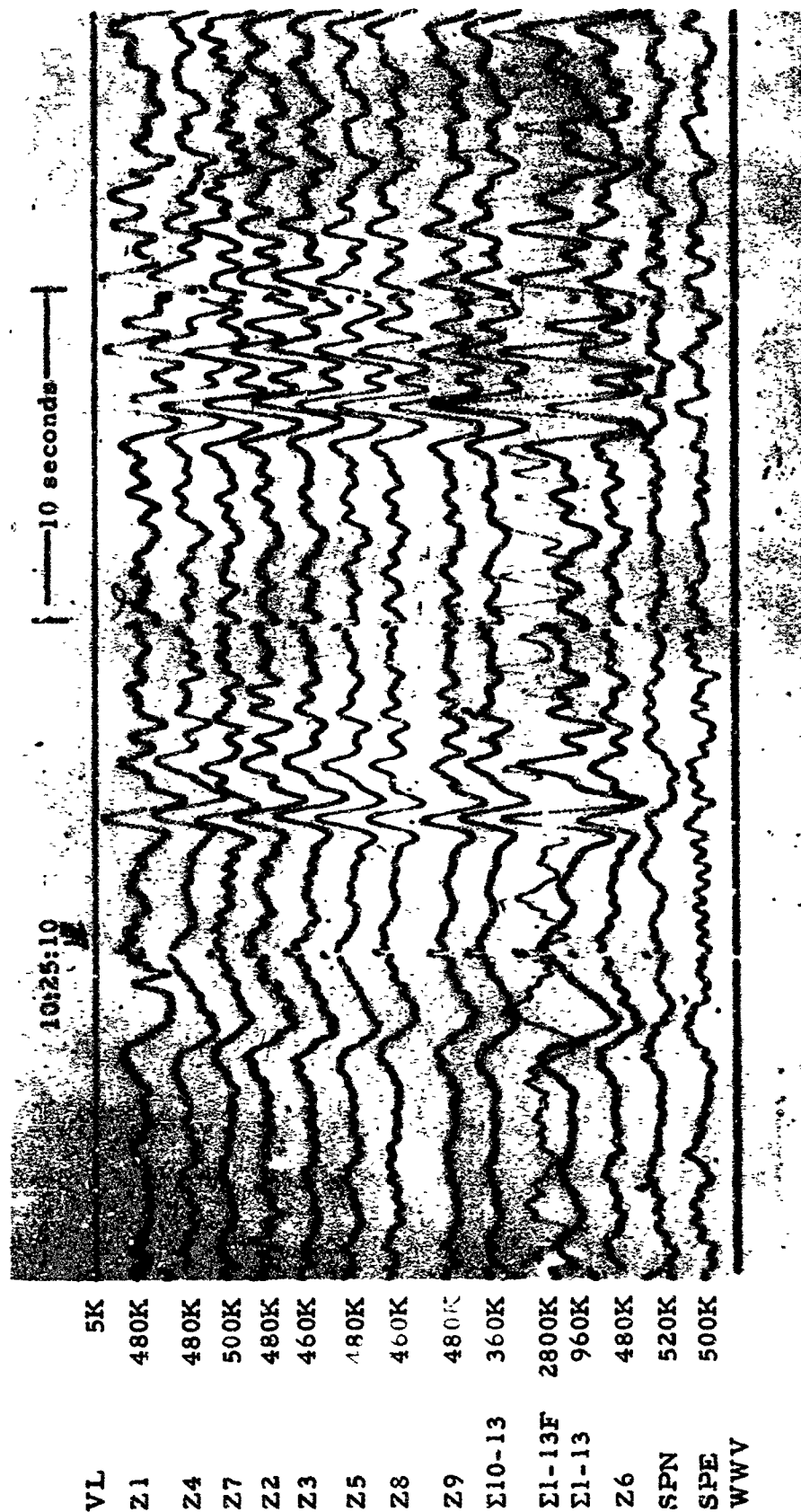


Figure 2-1. WMSO seismogram illustrating P and pP phase arrivals from the Kermadec Islands. Epicentral data:  $\Delta \approx 95^\circ$ ,  $h \approx 31$  km, azimuth  $\approx 241^\circ$ , magnitude  $\approx 5.1$  (X10 enlargement of 16-mm film)

WMSO  
Run 005  
5 Jan 1964  
Data Group 311

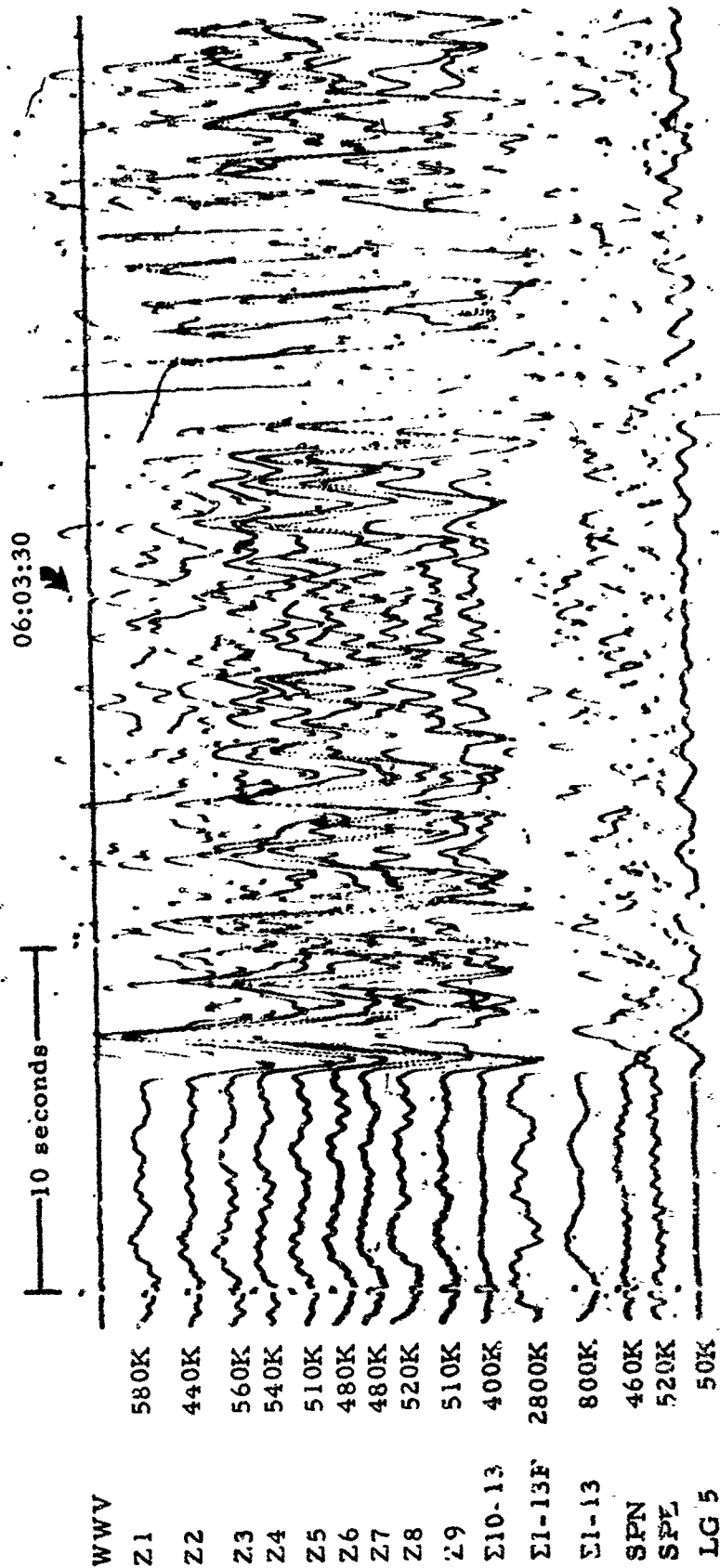


Figure 2-2. WMSO seismogram illustrating P and pP phase arrivals from Central Peru. Epicentral data:  $\Delta \approx 49^\circ$ ,  $h \approx 61$  km, azimuth  $\approx 153^\circ$ , magnitude  $\approx 6.7$  (X10 enlargement of 16-mm film)

WMSO  
Run 260  
17 Sep 1963

TR 64-50

WVV  
 RPZ 4.6K  
 BBK 4.2K  
 BBZ 4.2K  
 1/10 LPZ 1.5K  
 1/10 LPN 2.0K  
 1/1 LPE 2.0K  
 LPZ 17.3K  
 LPN 19.5K  
 LPE 20.5K  
 E1-10 260K  
 M  
 A



Figure 2-3. P-wave arrival recorded on all systems at WMSO. Epicenter: Kurile Islands,  $\Delta \approx 80^\circ$ ,  $h \approx 40$  km, azimuth  $\approx 318^\circ$ , magnitude  $\approx 5.5$  (X10 enlargement of 16-mm film)

WMSO  
 Run 214  
 10 Nov 1963  
 Data Group 304

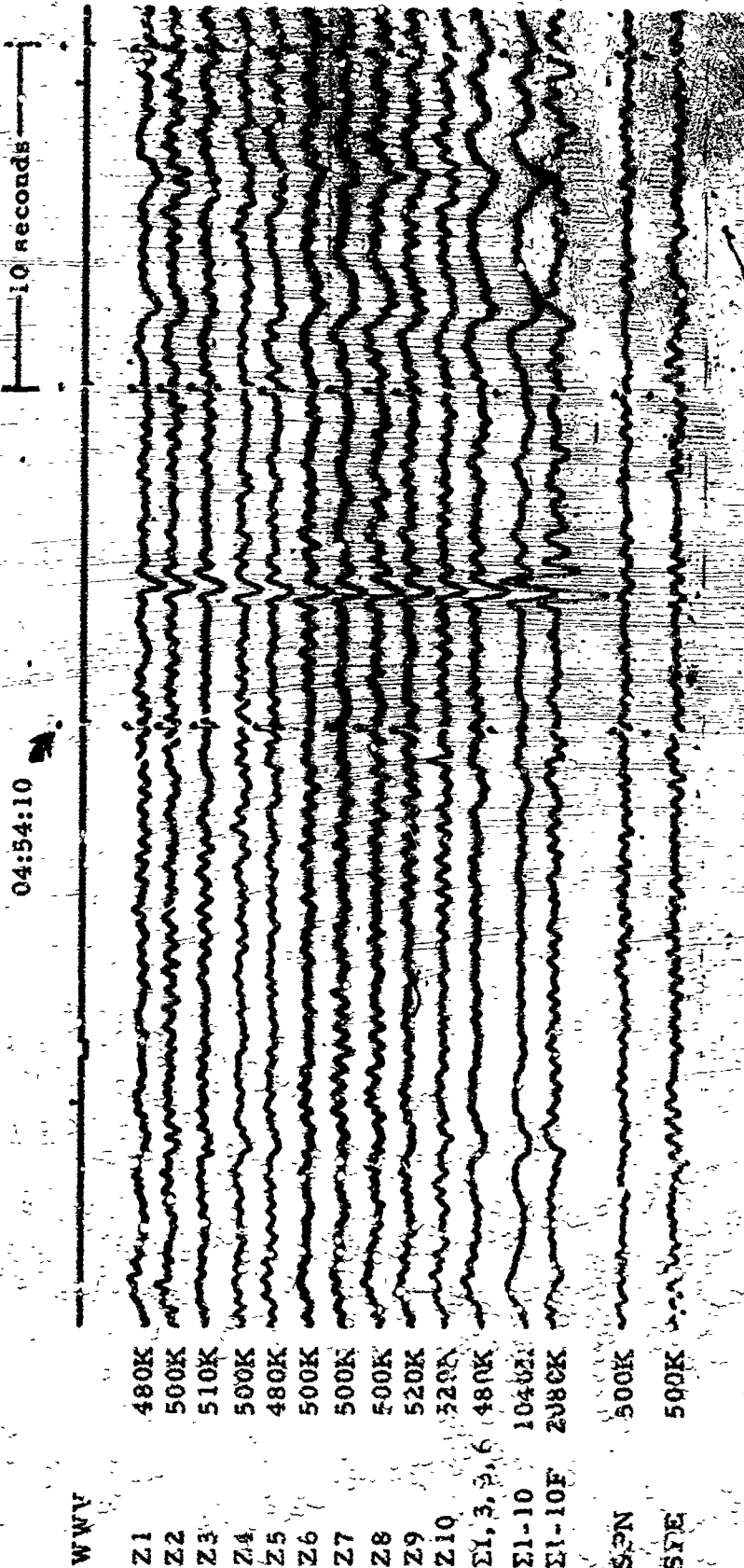


Figure 2-4. WMSO primary short-period seismogram illustrating a "Lonesome P." Epicenter: near the east coast of Kamchatka,  $\Delta \approx 69^\circ$ ,  $h \approx 33$  km, azimuth  $\approx 321^\circ$ , magnitude  $\approx 4.6$  (X10 enlargement of 16-mm film)

WMSO  
Run 146  
26 May 1963



TR 64-50

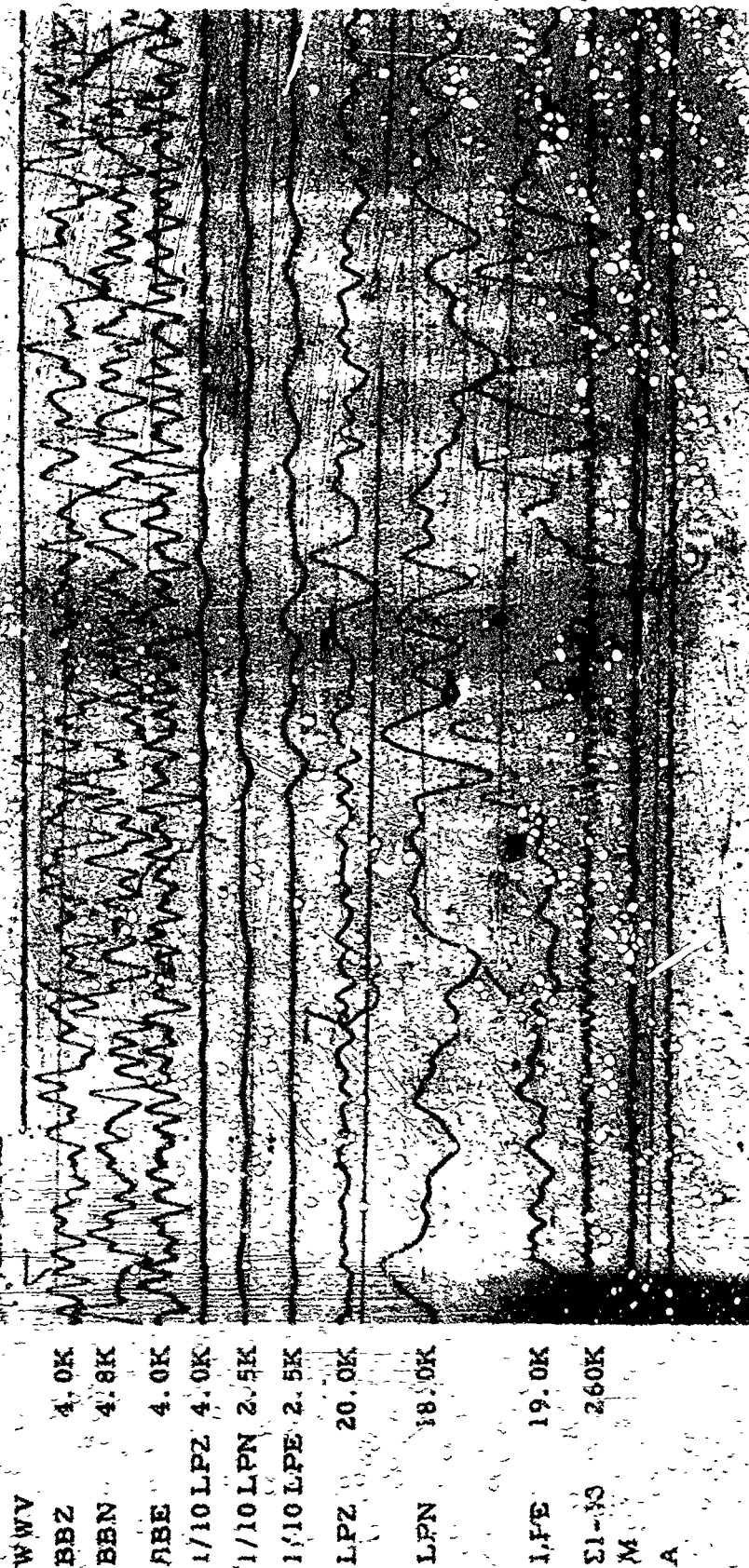


Figure 2-5. WMSO seismogram illustrating S and sQ phase arrivals. See figures 2-4 and 2-7 for the corresponding phase arrivals on the short-period system. Epicenter: Northern Chile,  $\Delta \approx 60^\circ$ ,  $h \approx 213$  km, azimuth  $\approx 48^\circ$ , magnitude  $\approx 5.5$  (X19 enlargement of 16-mm film)

WMSO  
Run 360  
29 Dec 1963  
Data Group 304

TR 64-50

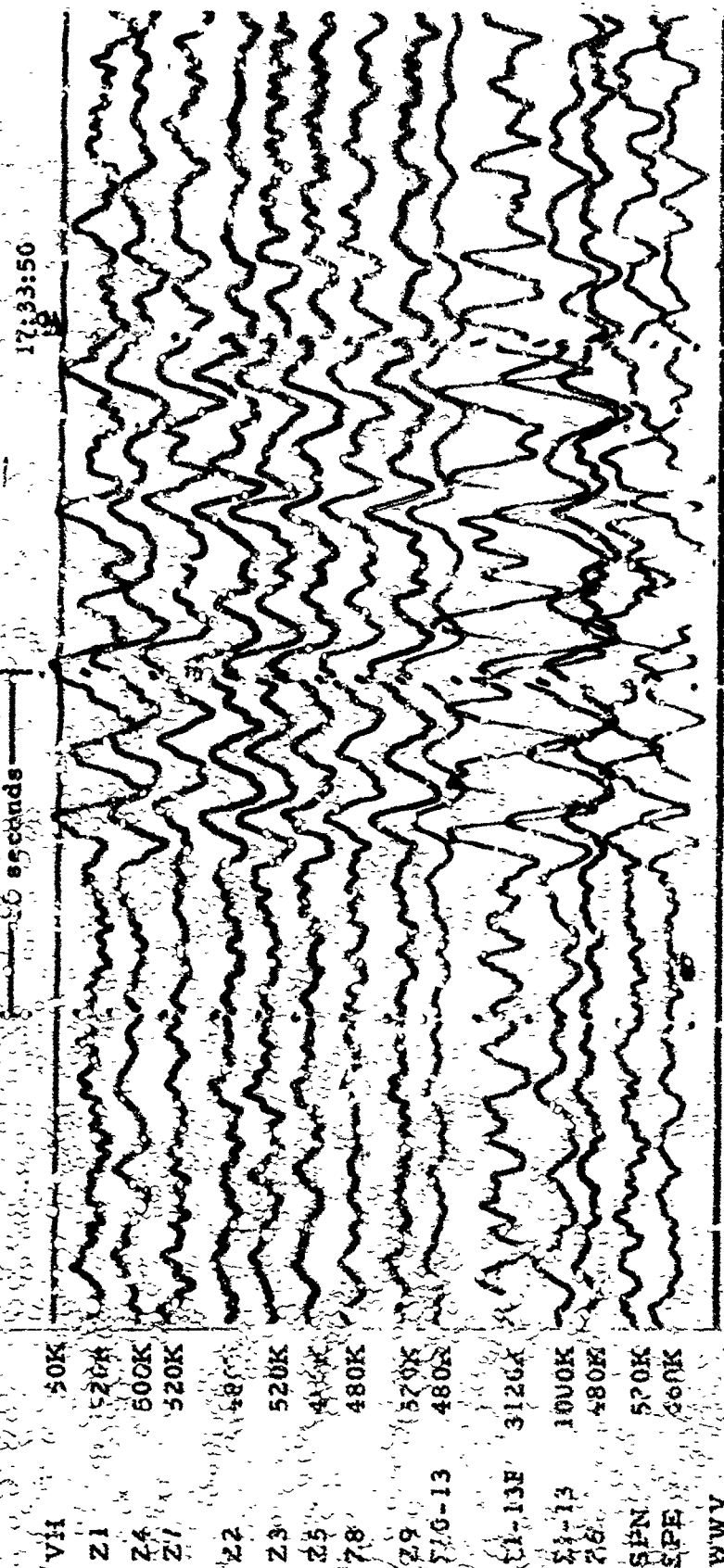


Figure 2-6. WMSO smogram illustrating an S phase arrival on the short-period system. Epicenter: Northern Chile,  $\Delta \sim 60^\circ$ ,  $h \sim 13$  km, azimuth  $\sim 148^\circ$ , magnitude  $\sim 5.5$  (X10 enlargement of 16-mm film)

WMSO  
Run 353  
29 Dec 1963  
Data Group 311

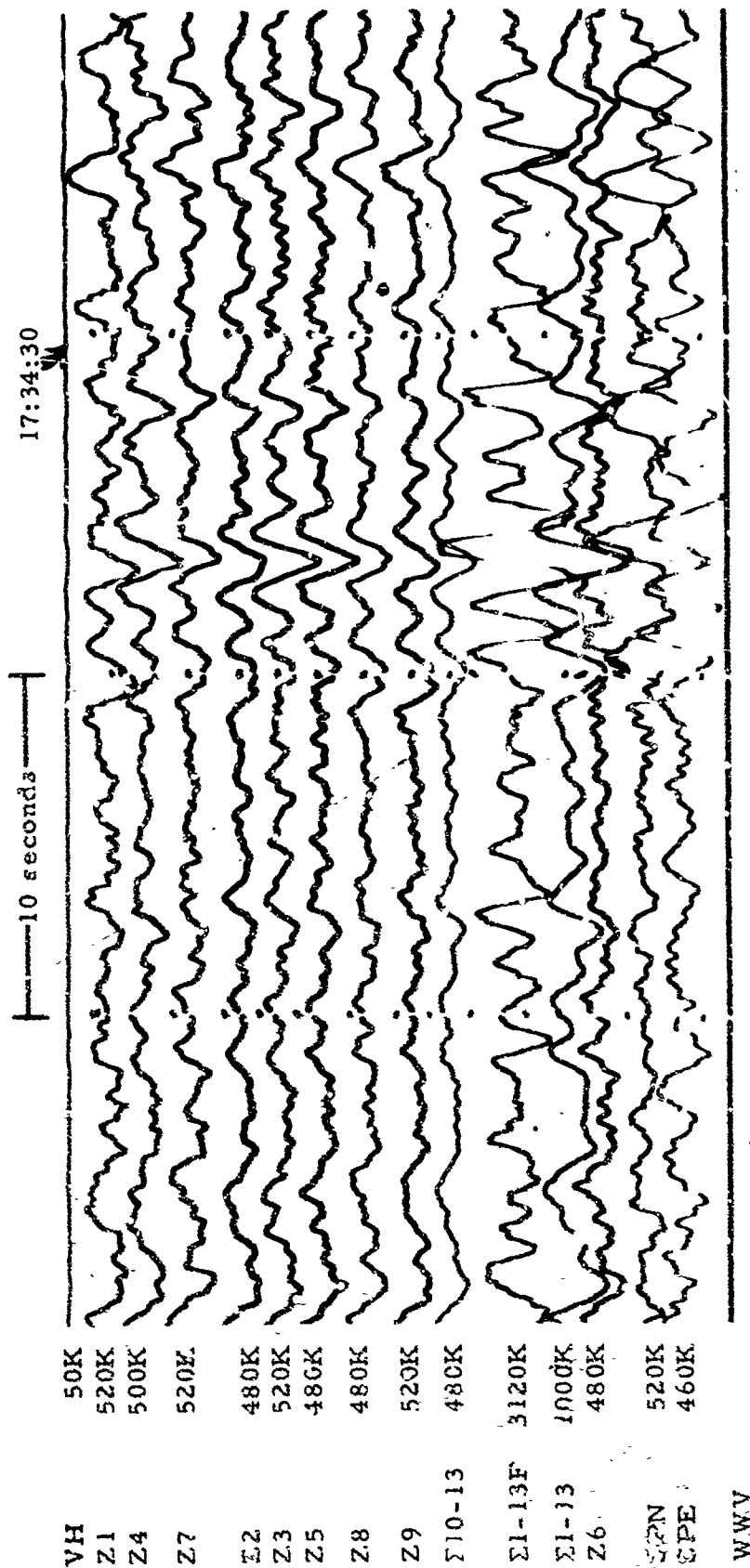


Figure 2-7. WMSO seismogram illustrating an sS phase arrival on the short-period system. Epicenter: Northern Chile,  $\Delta \approx 60^\circ$ ,  $h \approx 113$  km, azimuth  $\approx 148^\circ$ , magnitude  $\approx 5.5$  (X10 enlargement of 16-mm film)

WMSO  
Run 363  
29 Dec 1963  
Data Group 311

TR 64-50

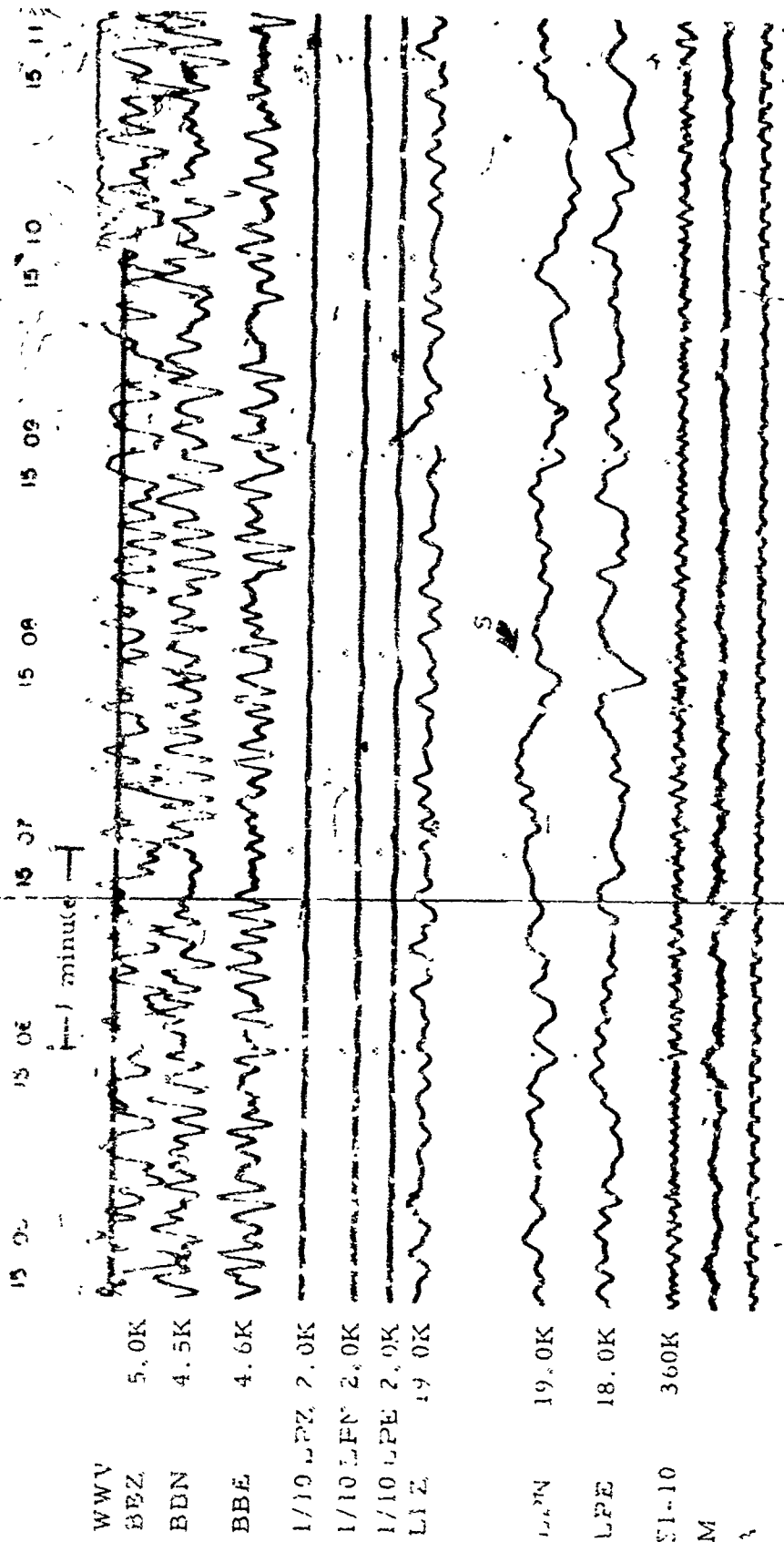


Figure 2-3. WMSO seismogram illustrating an S phase arrival from Western Bolivia.  
See figure 2-9 for corresponding phase on the short-period system. Epicentral  
data:  $\Delta \approx 60^\circ$ ,  $h \approx 79$  km, azimuth  $\approx 147^\circ$ , magnitude  $\approx 5.3$   
(X10 enlargement of 16-mm film)

WMSO  
Run 344  
10 Dec 1963  
Data Group 304

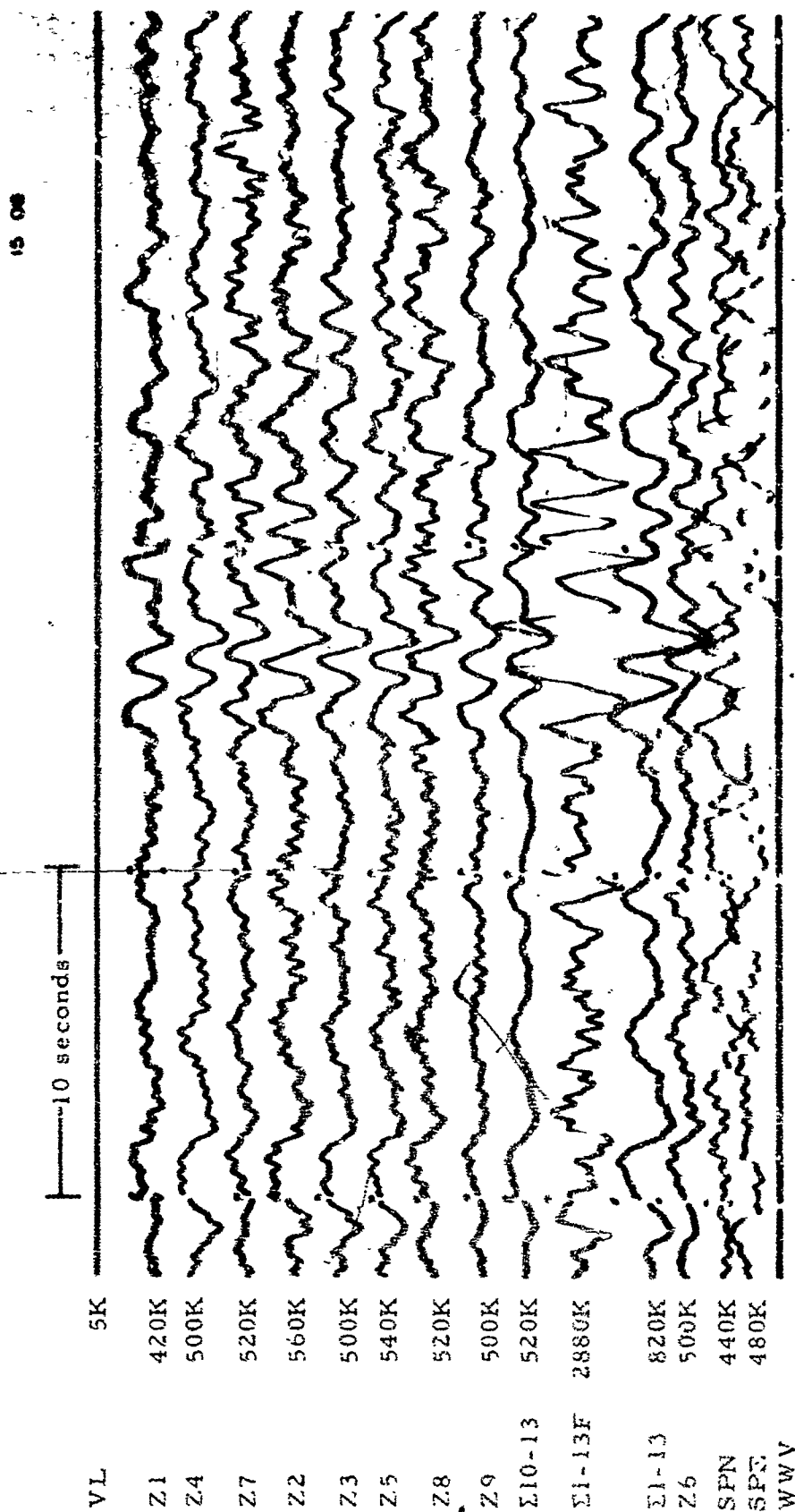


Figure 2-9. WMSO seismogram illustrating an S phase arrival from Western Bolivia.  
 Epicentral data:  $\Delta \approx 60^\circ$ ,  $h \approx 79$  km, azimuth  $\approx 147^\circ$ , magnitude  $\approx 5.3$   
 (X10 enlargement of 16-mm film)

WMSO  
 Run 344  
 10 Dec 1963  
 Data Group 311

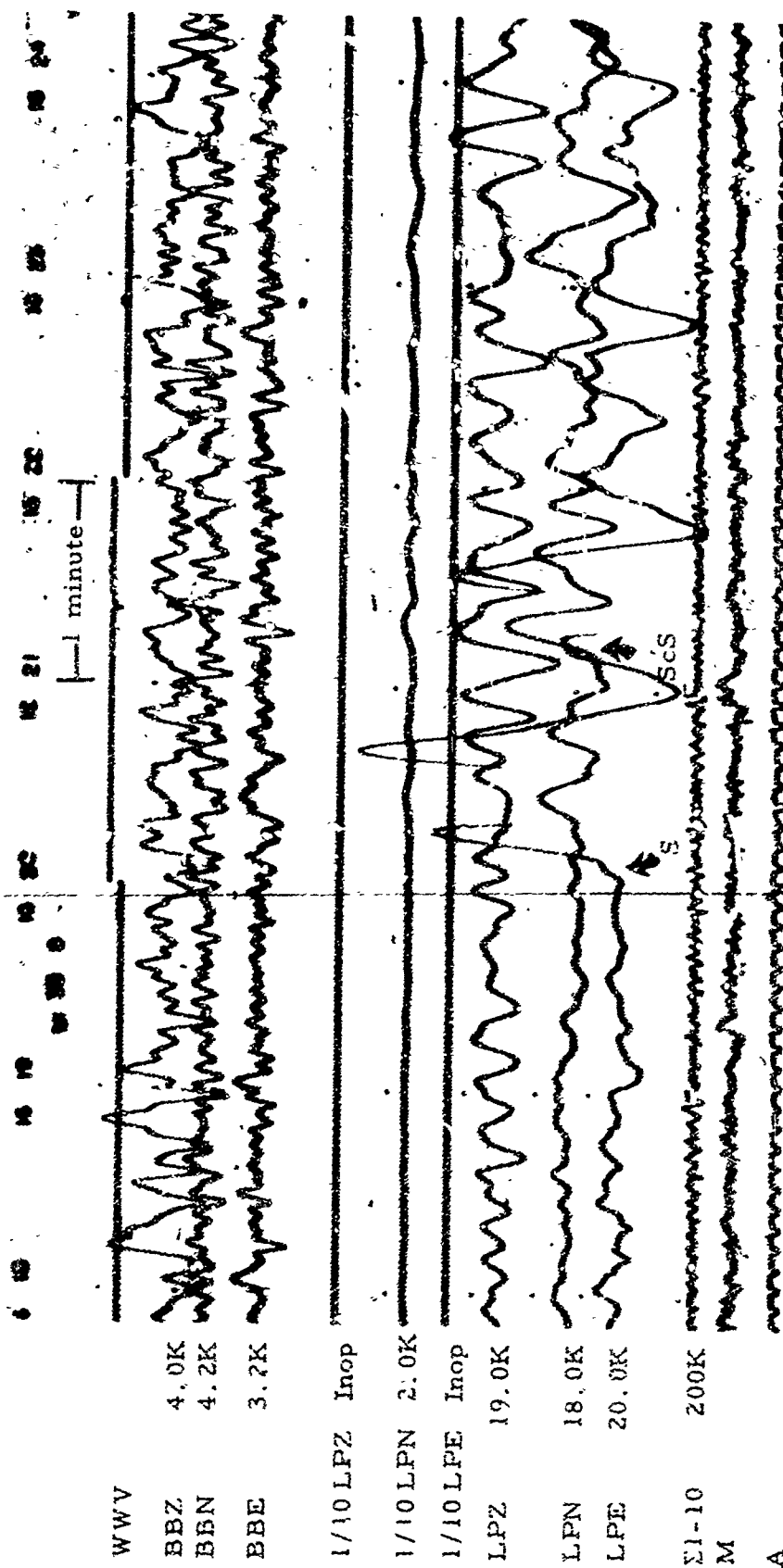


Figure 2-10. WMSO seismogram illustrating S and ScS phase arrivals from the Easter Island's region. Epicentral data:  $\Delta \approx 70^\circ$ ,  $h \approx 33$  km azimuth  $\approx 181^\circ$ , magnitude  $\approx 4.6$  (2:10 enlargement of 16-mm film)

WMSO  
Run 338  
4 Dec 1963  
Data Group 304

TP 54-50

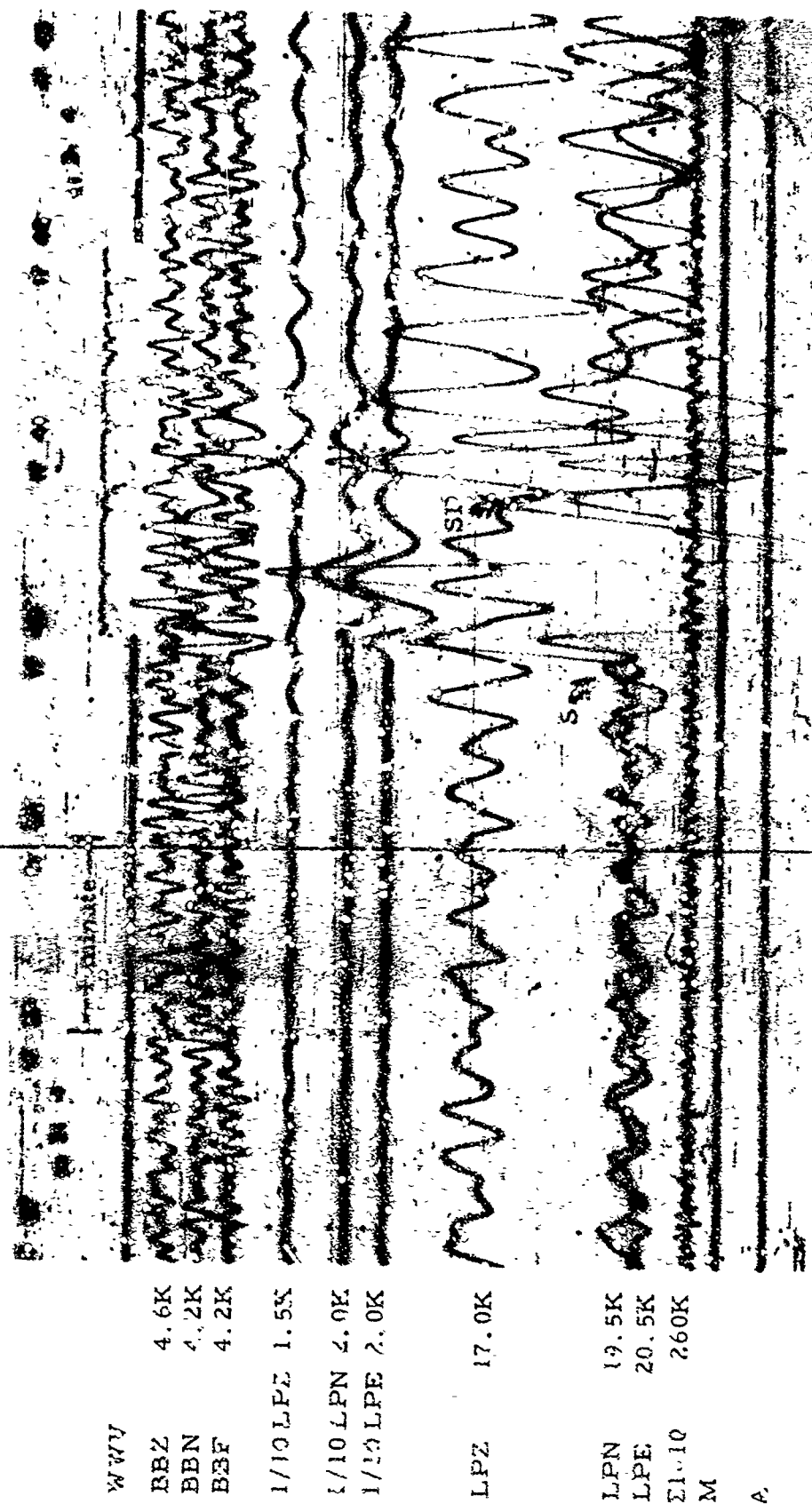


Figure 2-11. WMSO seismogram illustrating S and SP phase arrivals from the Kurile Islands. Epicentral data:  $\Delta \approx 80^\circ$ ,  $h \approx 40$  km, azimuth  $\approx 318^\circ$ , magnitude  $\approx 5.5$  (X10 enlargement of 16-mm film)

WMSO  
Run 314  
10 Nov 1963  
Data Group 304

WWV	
BBZ	3.0K
SBN	5.8K
BBE	3.4K
1/10 LPZ	2.0K
1/10 LPN	2.0K
1/10 LPE	2.0K
LPZ	18.0K
LPN	20.0K
LPE	18.0K
$\Sigma 1-10$	200K
M	
A	



Figure 2-12. WMSO seismogram illustrating a PP phase arrival from the New Hebrides Islands. See figure 2-13 for the corresponding phase on the short-period system.  
 Epicentral data:  $\Delta \approx 102^\circ$ ,  $h \approx 154$  km, azimuth  $\approx 260^\circ$ , magnitude  $\approx 5.8$   
 (X10 enlargement of 16-mm film)

WMSO  
 Run 308  
 4 Nov 1963  
 Data Group 304



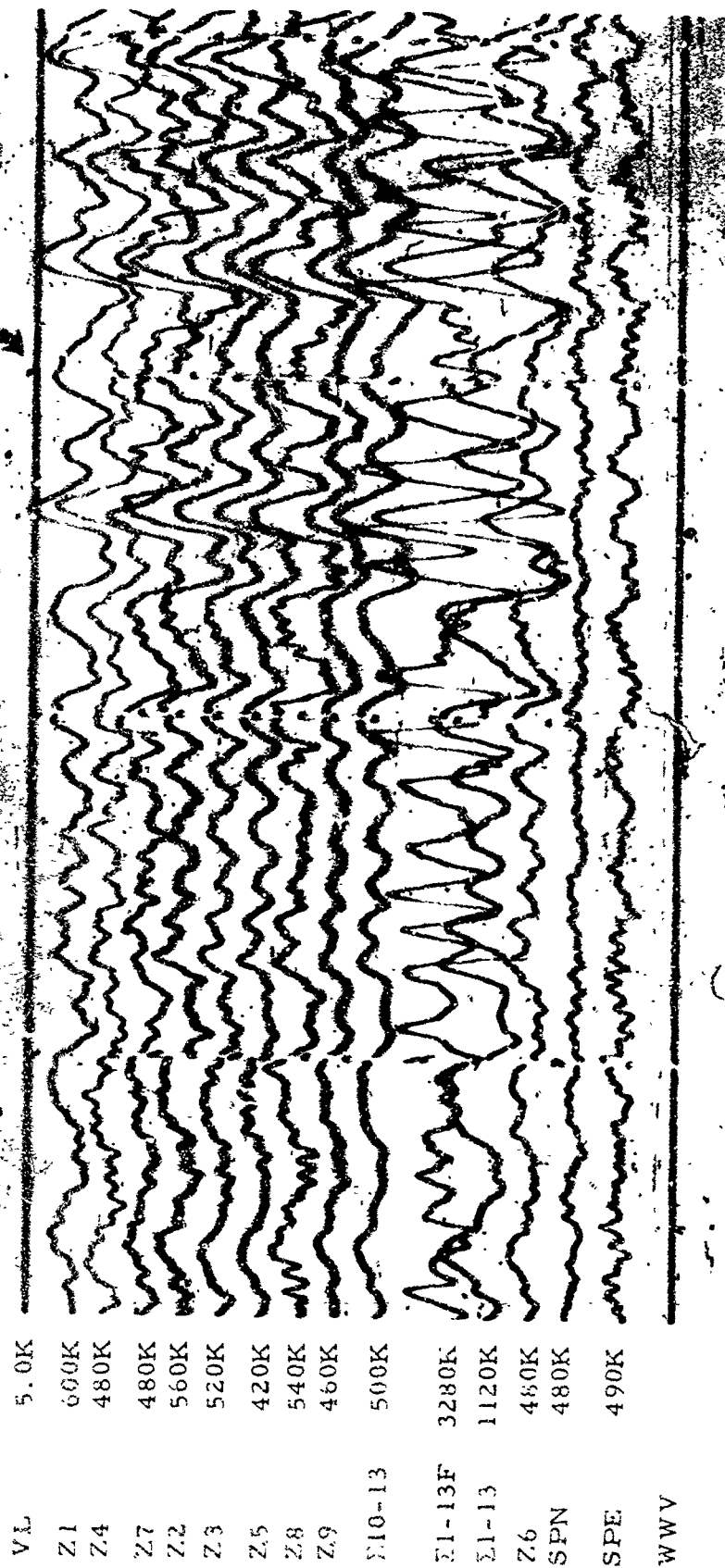


Figure 2-13. WMSO primary short-period seismogram illustrating a PP phase from the New Hebrides Islands. Epicentral data:  $\Delta \approx 102^\circ$ ,  $h \approx 154$  km, azimuth  $\approx 260^\circ$ , magnitude  $\approx 5.8$  (X10 enlargement of 16-mm film)

WMSO  
Run 308  
4 Nov 1963  
Data Group 302

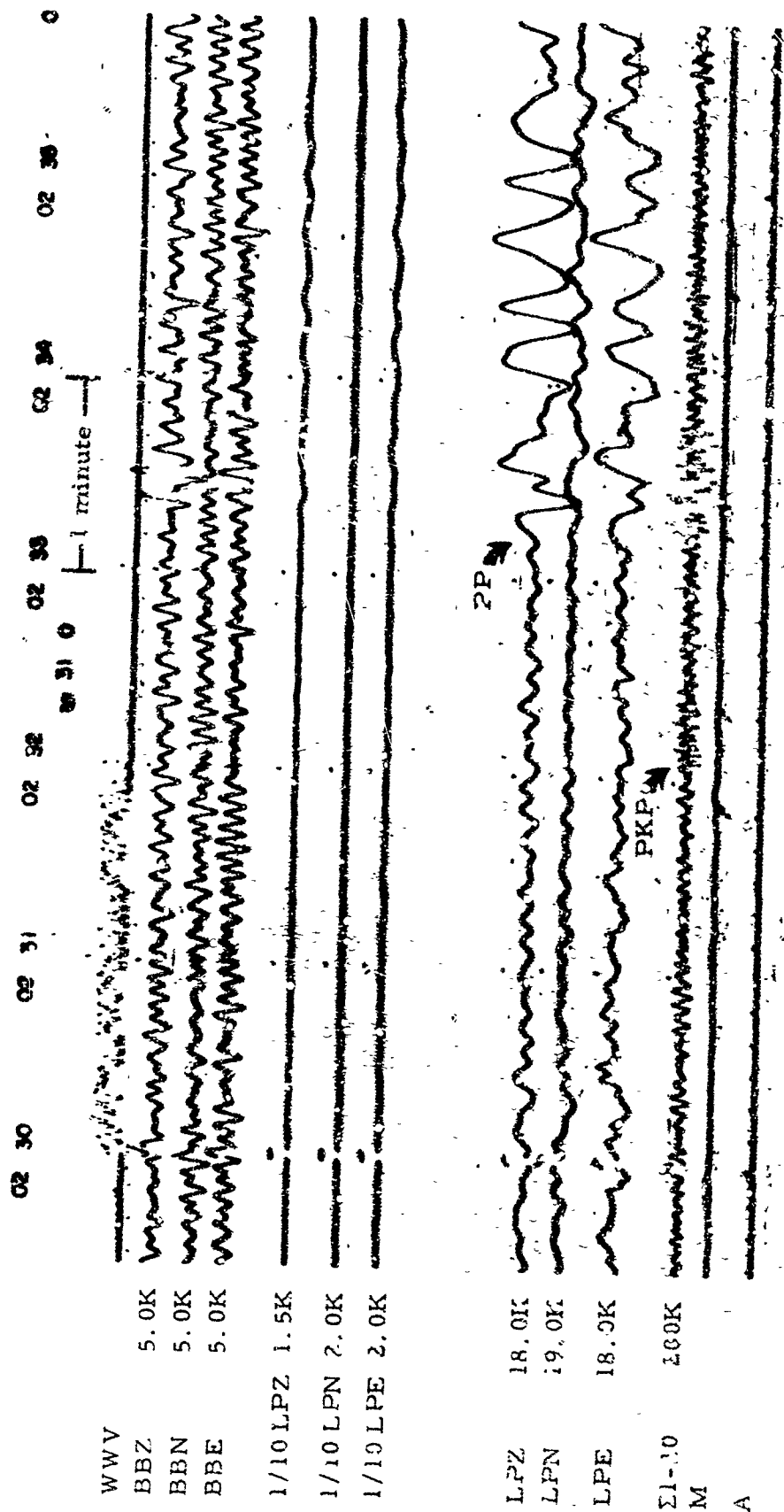


Figure 2-14. WMSO seismogram illustrating a PP phase arrival from Western New Guinea. See figure 2-15 for the corresponding phase on the short-period system. Epicentral data:  $\Delta \approx 118^\circ$ ,  $h \approx 33$  km, azimuth  $\approx 288^\circ$ , magnitude  $\approx 5.7$  (X10 enlargement of 16-mm film)

WMSO  
Run 316  
6 Nov 1963  
Data Group 304

VL	5.0K
Z1	500K
Z4	490K
Z7	500K
Z2	520K
Z3	520K
Z5	480K
Z8	480K
Z9	580K
Σ10-13	500K
Σ1-13F	2720K
Σ1-13	1080K
Z6	490K
SPN	440K
SPE	440K
WVV	

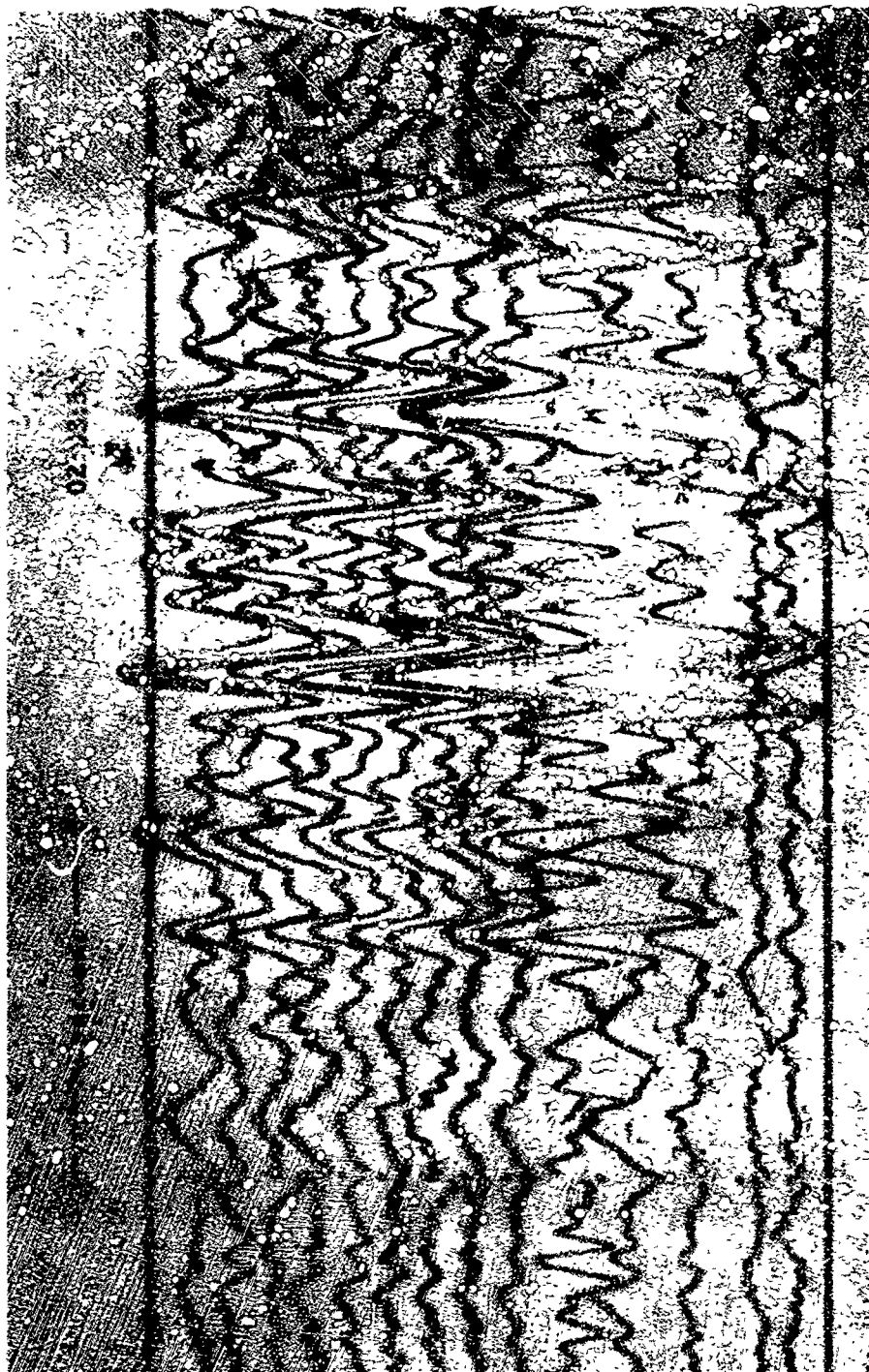


Figure 2-15. WMSO seismogram illustrating a PP phase arrival from Western New Guinea. Epicentral data:  $\Delta \approx 118^\circ$ ,  $h \approx 33$  km, azimuth  $\approx 288^\circ$ , magnitude  $\approx 5.7$  (X10 enlargement of 16-mm film)

WMSO  
Run 310  
6 Nov 1963  
Data Group 302

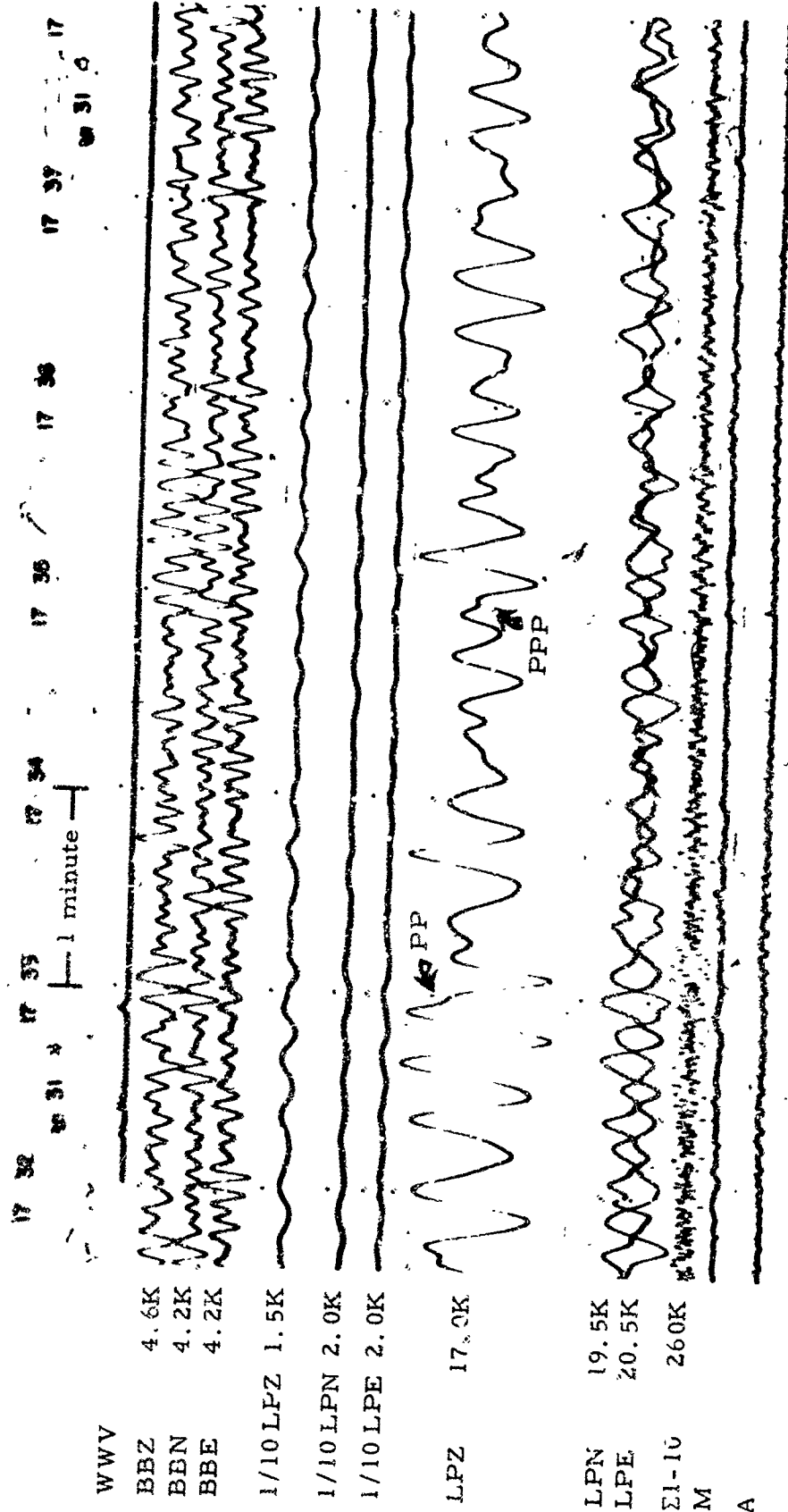


Figure 2.16. WMSO seismogram illustrating PP and PPP phases from the Kurile Islands. Epicentral data:  $\Delta \approx 80^\circ$ ,  $h \approx 40$  km, azimuth  $\approx 318^\circ$ , magnitude  $\approx 5.5$  (510 enlargement of 16-mm film)

WMSO  
Run 314  
10 Nov 1963  
Data Group 304

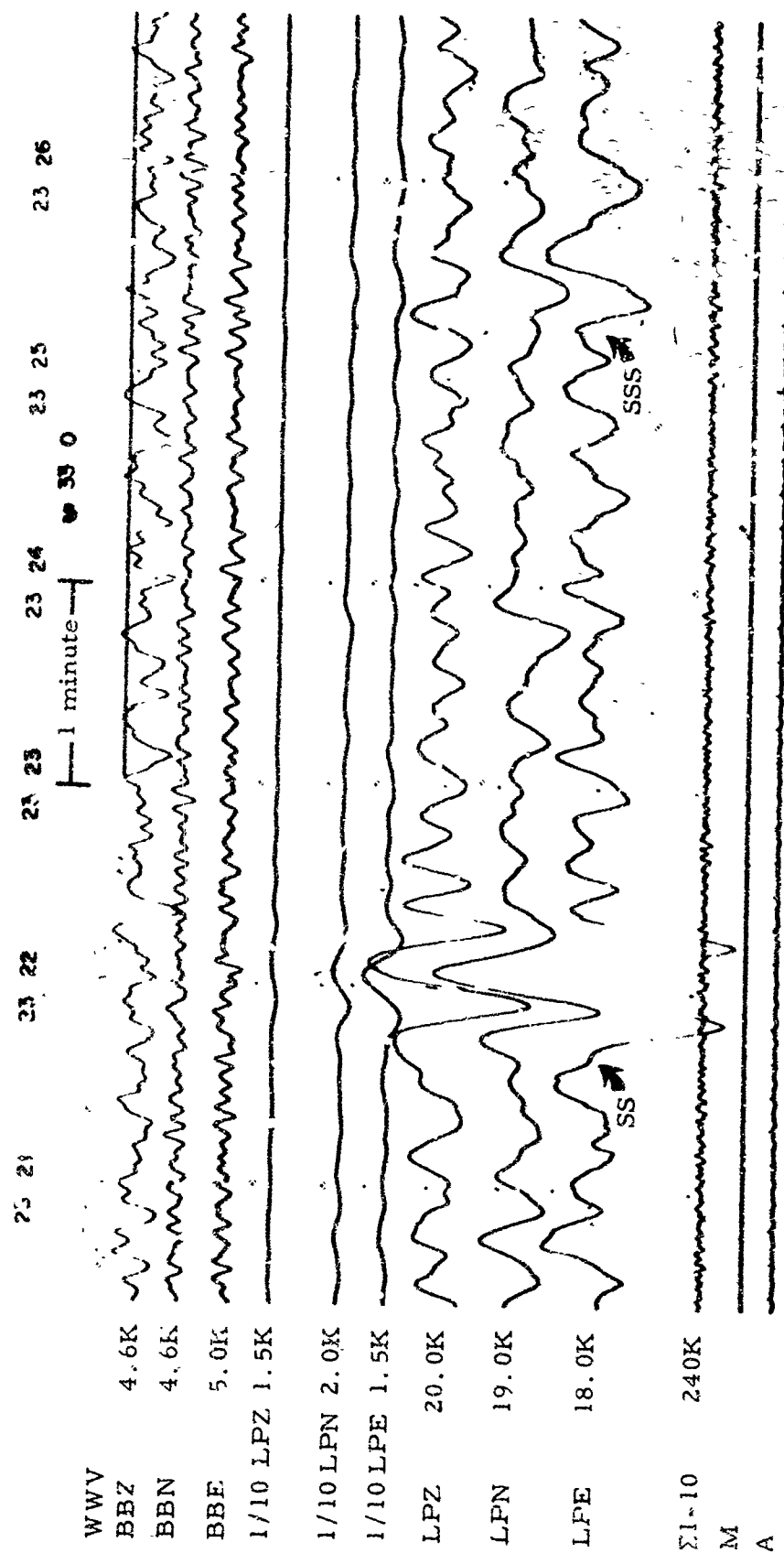


Figure 2-17. WMSO seismogram illustrating SS and SSS phases from the Fiji Islands region. Epicentral data:  $\Delta \approx 96^\circ$ ,  $h \approx 33$  km, azimuth  $\approx 254^\circ$ , magnitude  $\approx 5.2$   
(X10 enlargement of 16-mm film)

WMSO  
Run 330  
26 Nov 1963  
Data Group 304

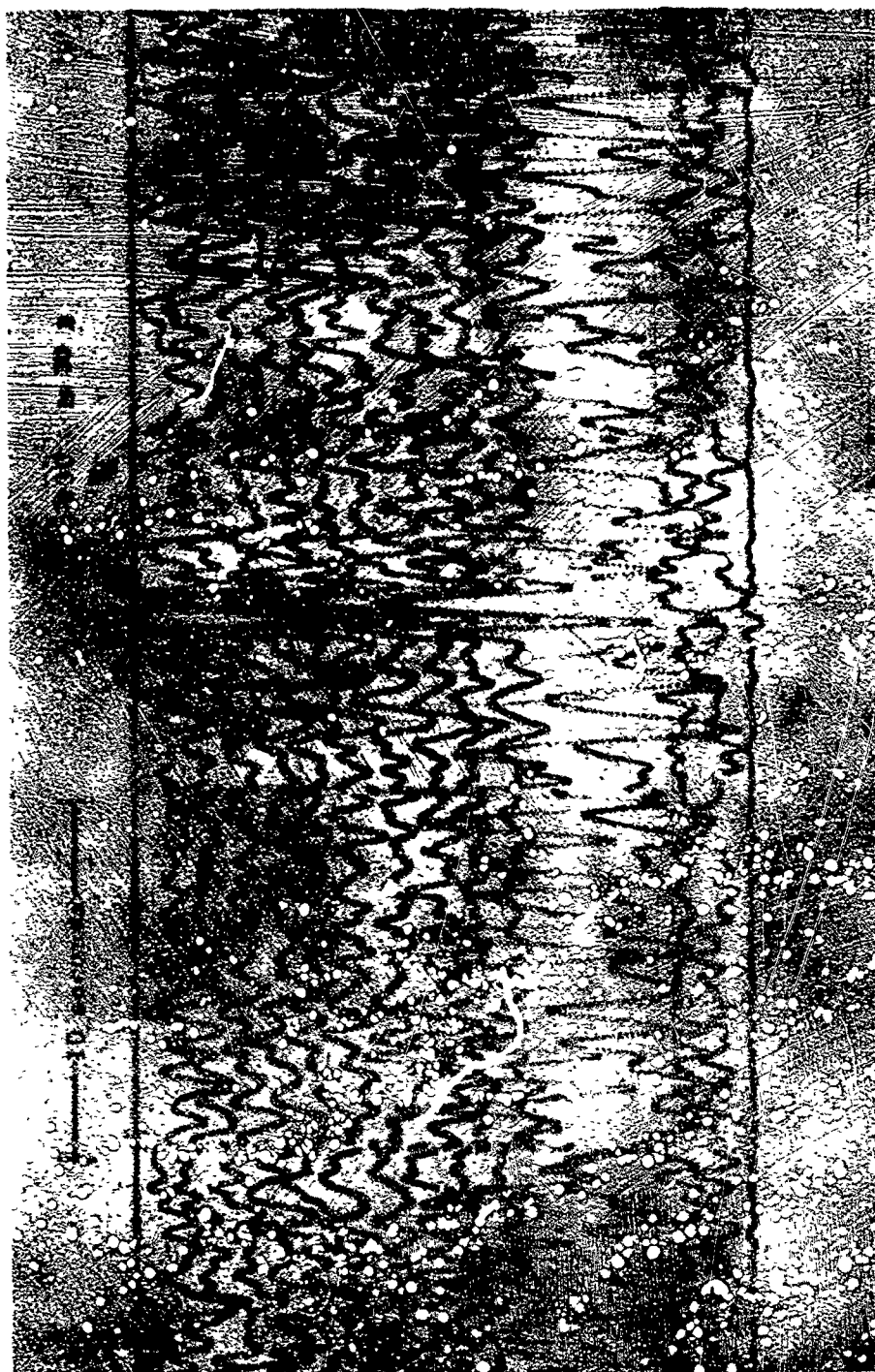


Figure 2-18. WMSO seismogram illustrating a P<sub>c</sub>P phase arrival. Epicenter:  
 Northern P<sub>c</sub>P-1,  $L = 44^\circ$ ,  $h = 20$  km, azimuth  $\approx 149^\circ$ , magnitude  $\approx 5.3$   
 (X10 enlargement of 16-mm film)

WWV	540K
Z1	470K
Z2	480K
Z3	500K
Z4	530K
Z5	520K
Z7	510K
Z8	530K
Z9	570K
ΣJ-13	540K
Σ1-10F	3200K
Σ1-13	1750K
SPN	550K
SPE	530K
LGS	50K

WMSO  
 Run 293  
 30 Oct 1963

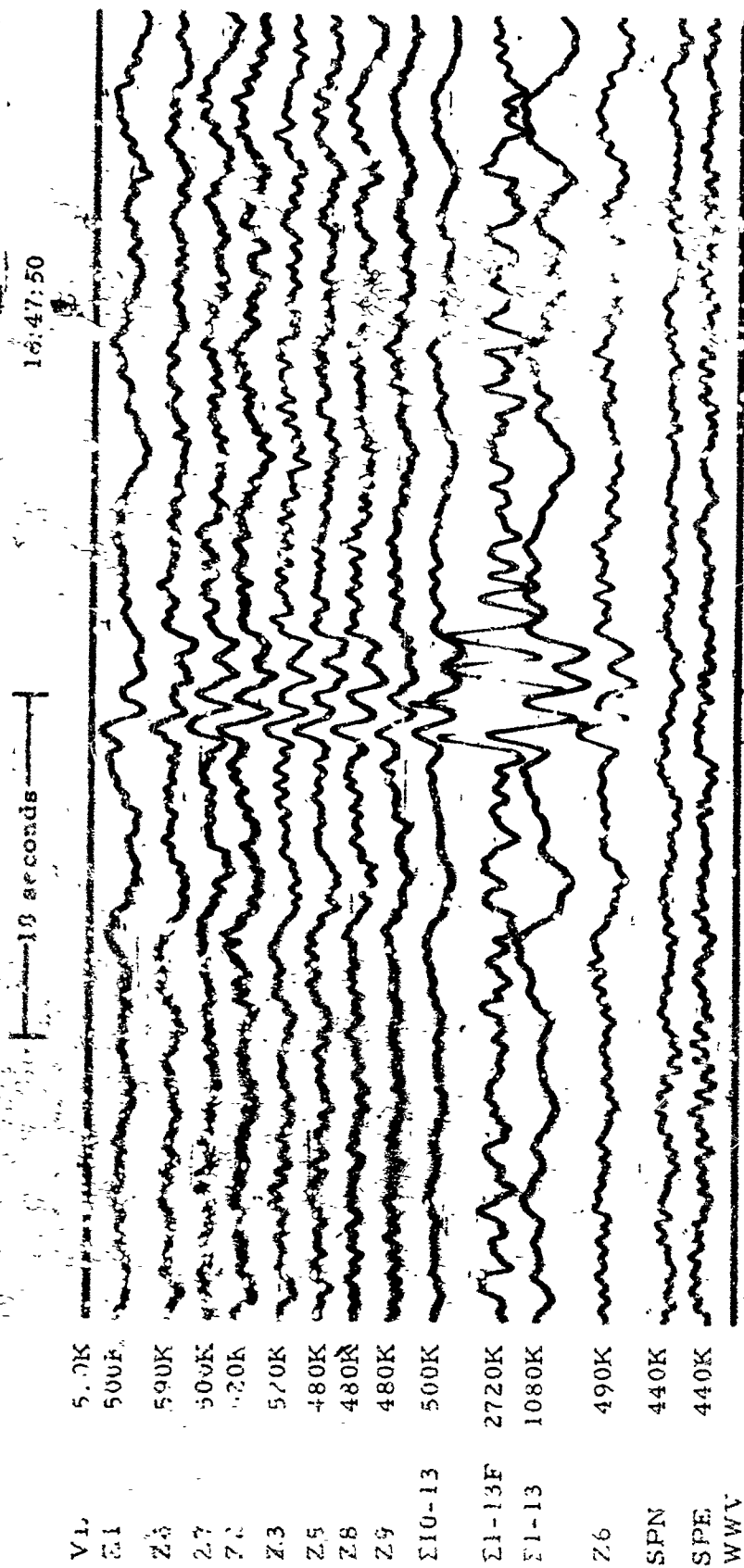


Figure 2-19. WMSO seismogram illustrating an ScP phase arrival from the Peru-Bolivia border. Epicentral data:  $\Delta \approx 58^\circ$ ,  $h \approx 174$  km, azimuth  $\approx 147^\circ$ , magnitude  $\approx 4.7$  (X10 enlargement of 16-mm film)

WMSO  
Run 310  
6 Nov 1963  
Data Group 302

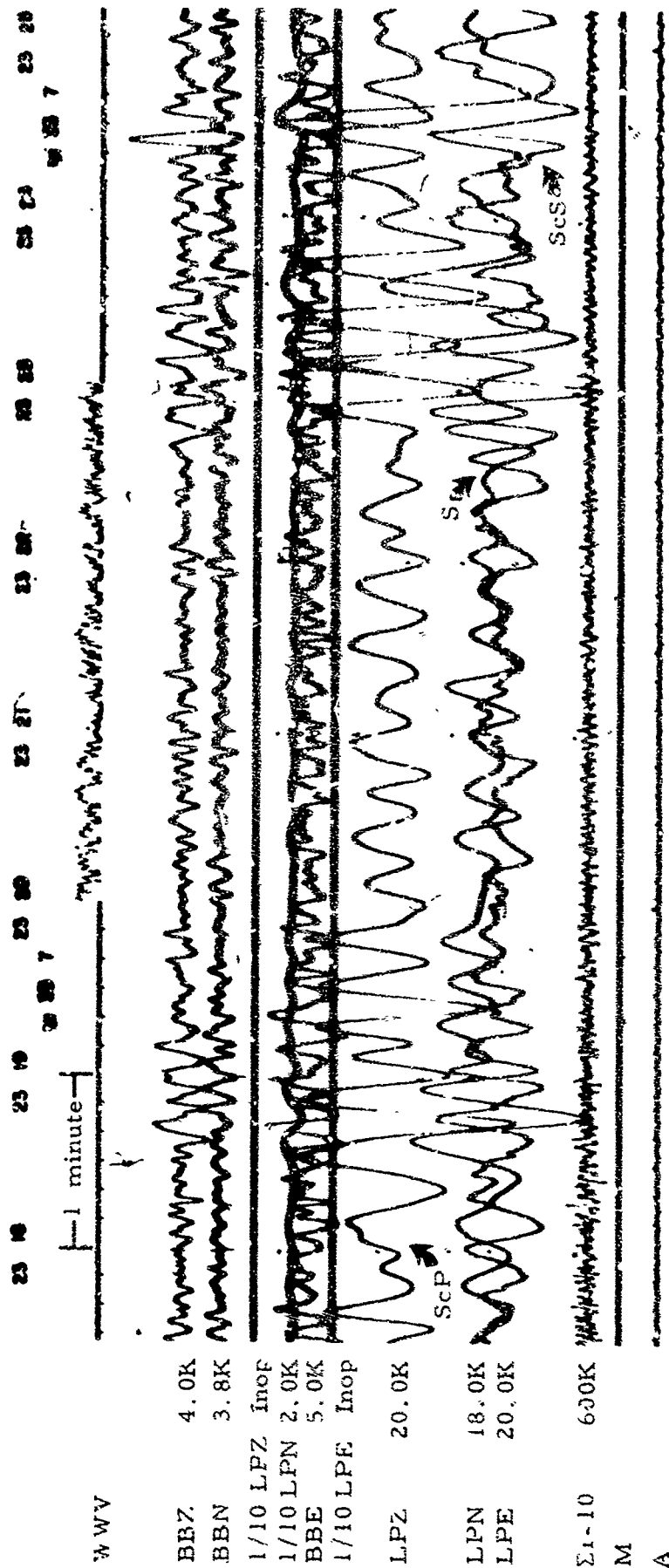


Figure 2-20. WMSO seismogram illustrating ScP, S, and ScS phase arrivals from Northern Chile. Epicentral data:  $\Delta \approx 63^\circ$ ,  $h \approx 13$  km, azimuth  $\approx 150^\circ$ , magnitude  $\approx 6.1$  (X10 enlargement of 16-mm film)

WMSO  
Run 337  
3 Dec 1963  
Data Group 304



TR 64-50

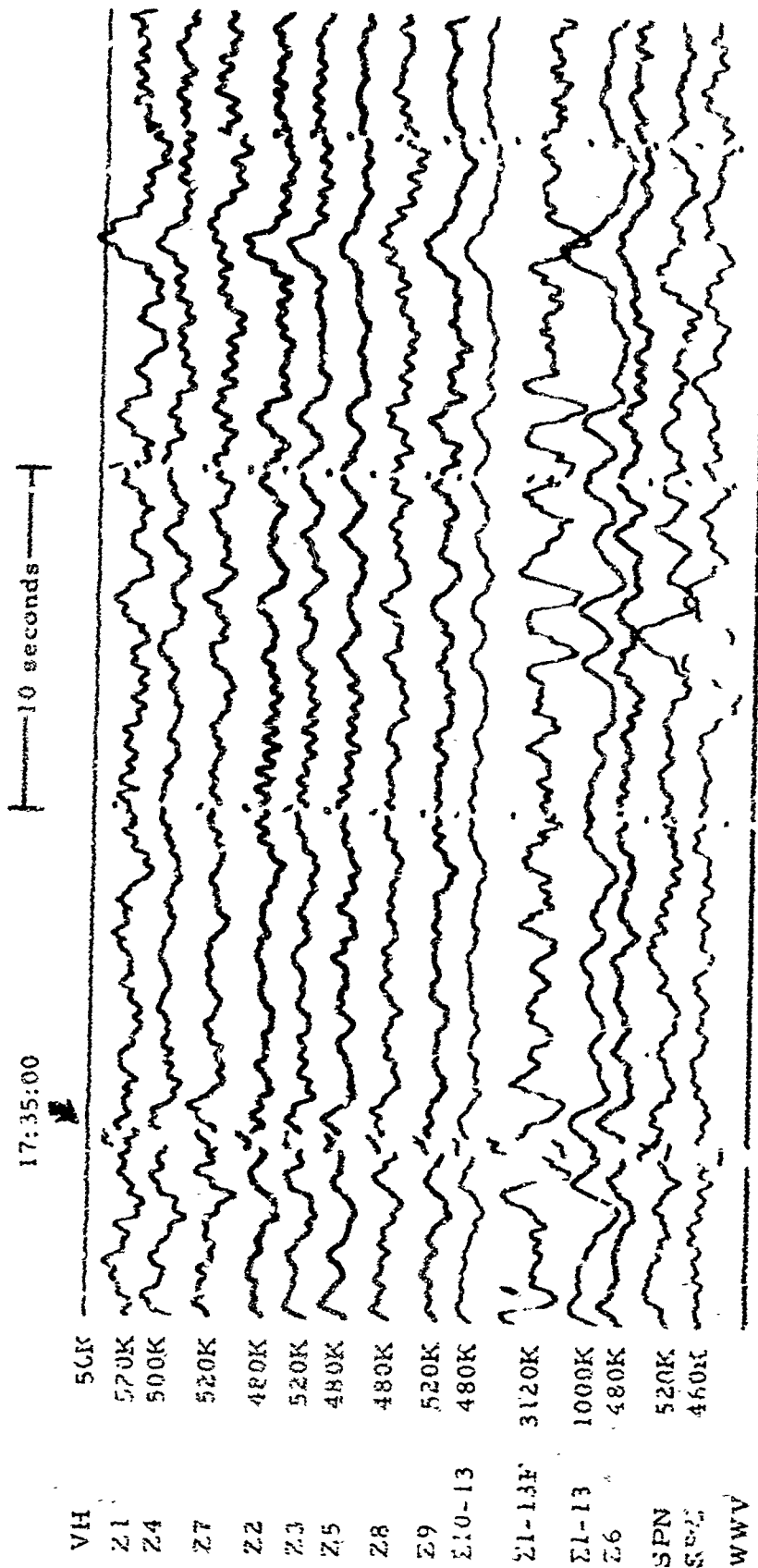


Figure 2-21. ScS as recorded on the WMSO short-period seismogram. Epicenter:  
Northern Chile,  $\Delta \approx 60^\circ$ ,  $h \approx 113$  km, azimuth  $\approx 148^\circ$ , magnitude  $\approx 5.5$   
(X10 enlargement of 16-mm film)

WMSO

Reel 363

29 Dec 1963

Data Group 311

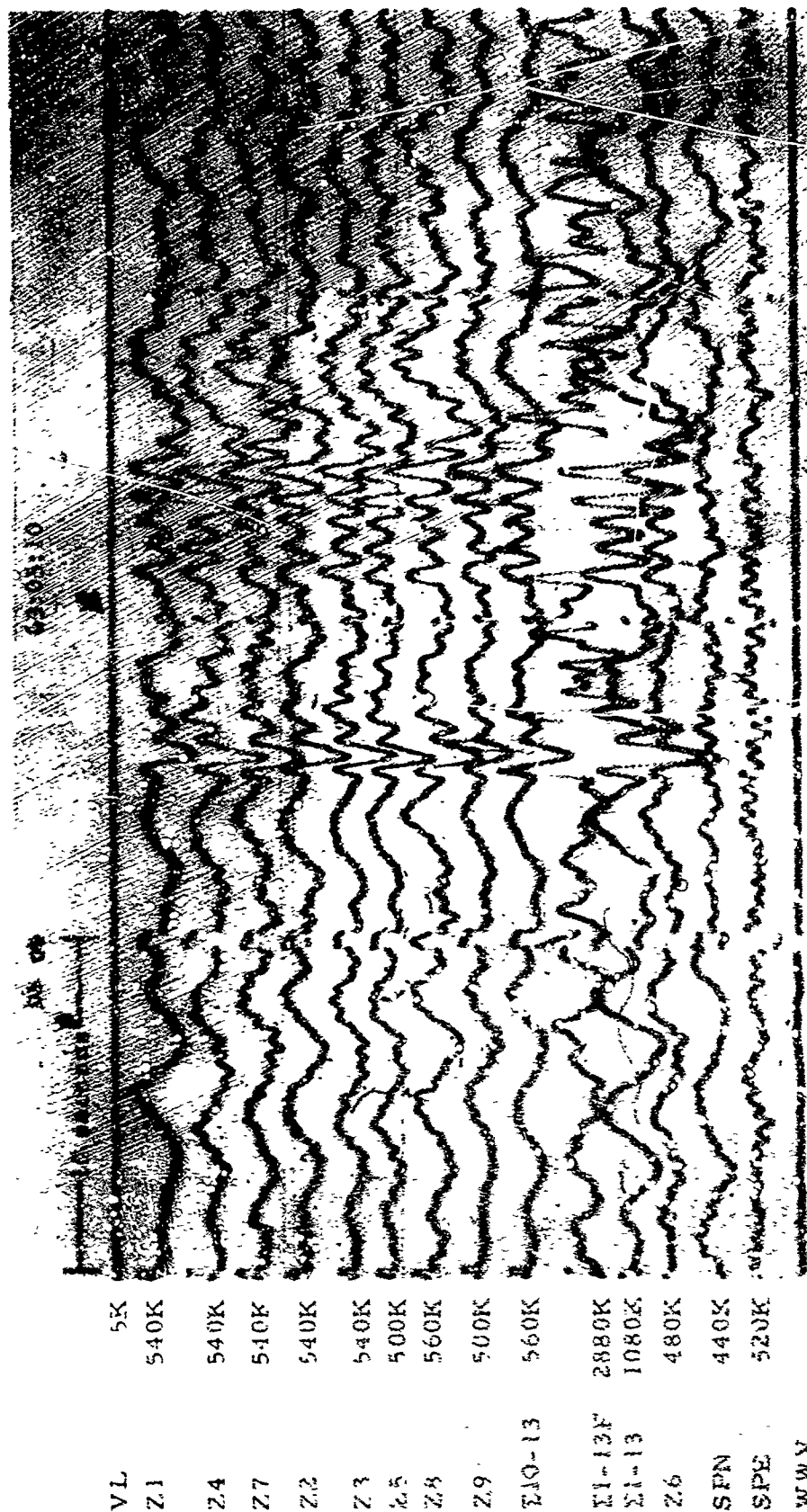


Figure 2-22. WMS-2 seismic, am illustrating PKP<sub>1</sub> and PKP<sub>2</sub> phase arrivals.  
 Epicenter: near the west coast of Sumatra,  $\Delta \approx 144^\circ$ ,  $h \approx 55$  km,  
 azimuth  $\approx 317^\circ$ , magnitude  $\approx 5.0$  (X10 enlargement of  
 16-mm film)

WMS-2

Run 350

16 Dec 1963

Data Group 311

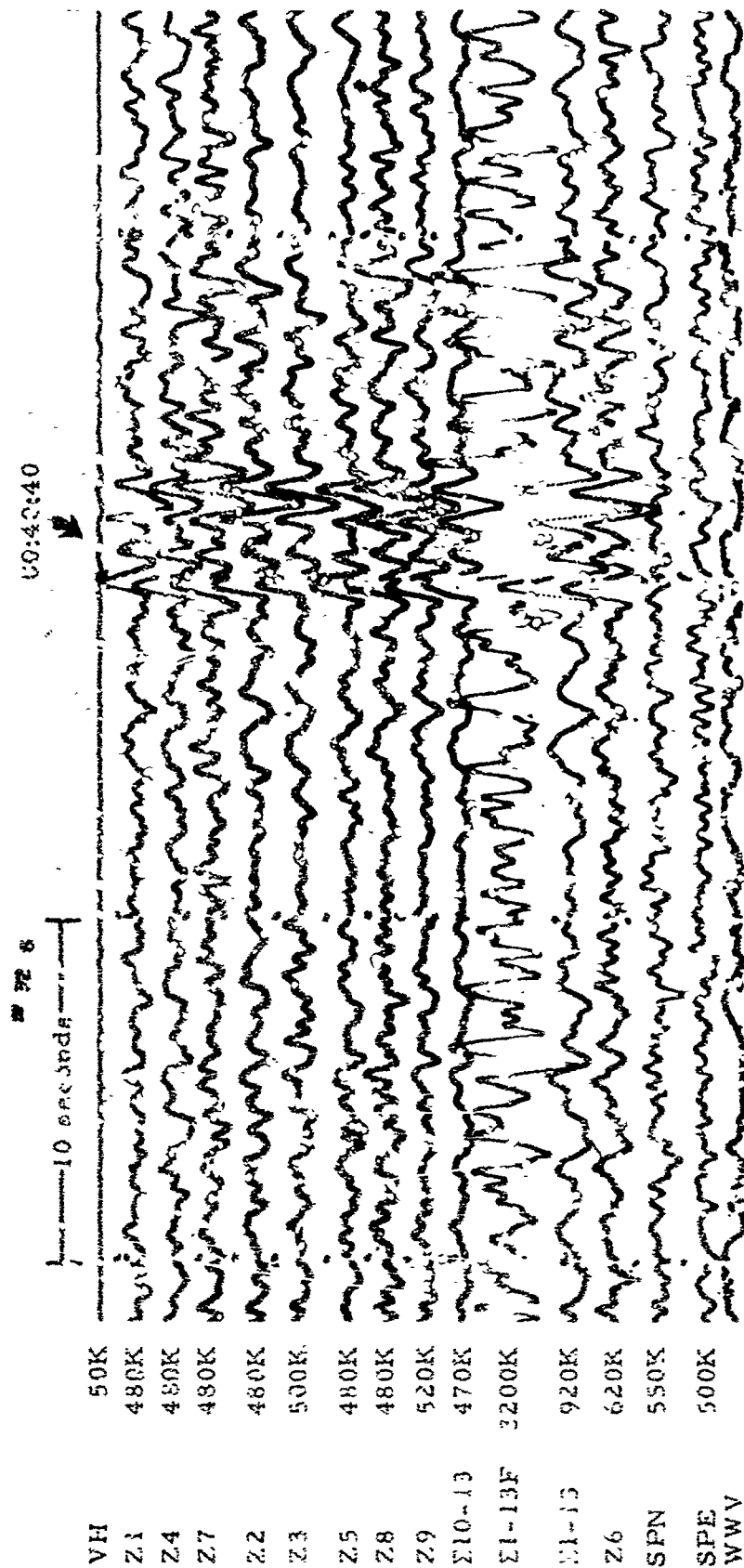


Figure 2-23. WMSO seismogram illustrating an SKP phase arrival. Epi, enter:  
near north const of Java,  $\Delta \approx 142^\circ$ ,  $h \approx 383$  km, azimuth  $\approx 314^\circ$ ,  
magnitude  $\approx 5.1$  (X10 enlargement of 14-min film)

WMSO  
Run 326  
22 Nov 1963  
Data Group 311

TR 64-50

WWV	
Z1	510K
Z2	470K
Z3	520K
Z4	450K
Z5	500K
Z6	540K
Z7	500K
Z8	480K
Z9	490K
Z10	500K
Z13, 5, 6	520K
Z1-10	1080K
Z1-10F	2000K
SFN	500K
SPE	500K



Figure 2-24. WMSO seismogram illustrating SKP1 and SKP2 phase arrivals.  
 Epicenter: Western Macquarie Islands,  $\Delta \approx 132^\circ$ ,  $h \approx 33$  km,  
 azimuth  $\approx 224^\circ$ , magnitude  $\approx 6.1$  (X10 enlargement of  
 16-mm film)

WMSO  
 Run 161  
 10 June 1963

TR 64-50

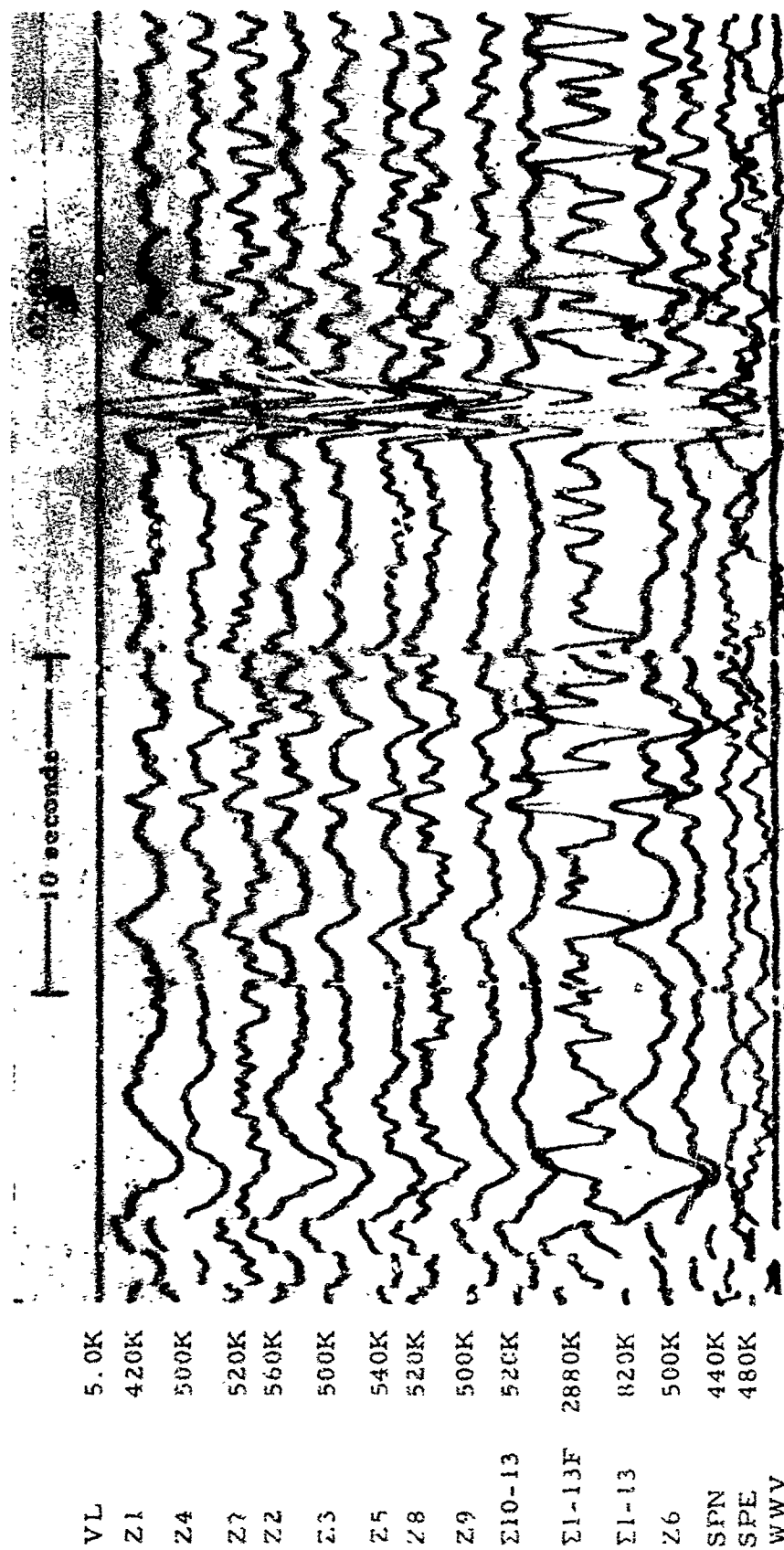


Figure 2-25. WMSO primary short-period seismogram illustrating PKKP<sub>1</sub> and PKKP<sub>2</sub> phase arrivals from the Sandwich Islands. Epicentral data:  $\Delta \approx 110^\circ$ ,  $h \approx 110$  km, azimuth  $\approx 147^\circ$ , no magnitude data available. (X10 enlargement of 16-mm film)

WMSO  
Run 344  
10 Dec 1963  
Data Group 311

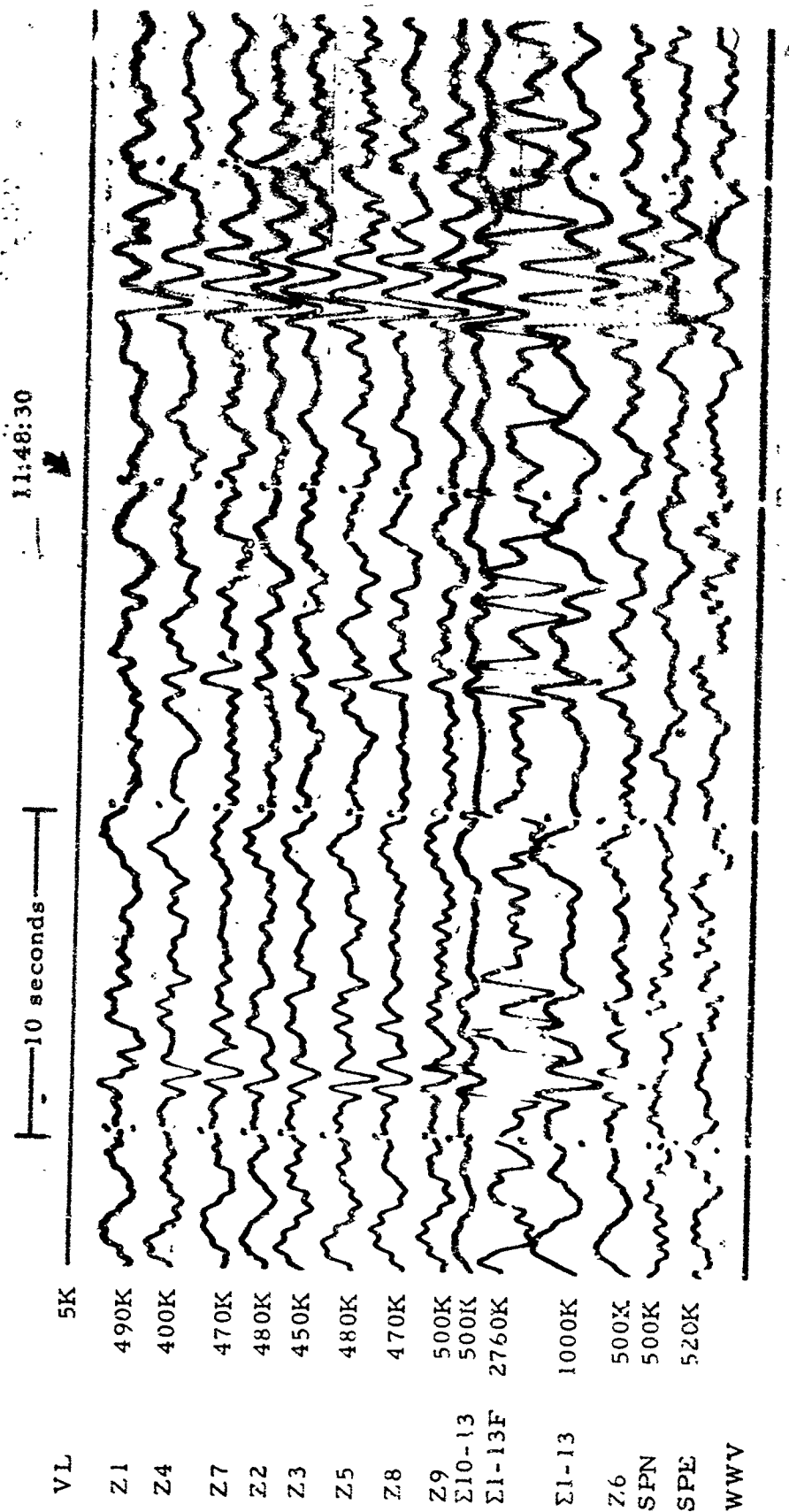


Figure 2-26. PKKP<sub>1</sub>-PKKP<sub>2</sub>-PKKP<sub>3</sub> as recorded on the WMSO short-period seismogram. Epicenter: Santa Cruz Island region,  $\Delta \approx 101^\circ$ ,  $h \approx 61$  km, azimuth  $\approx 262^\circ$ , magnitude  $\approx 5.5$  (X10 enlargement of 16-mm film)

WMSO  
Run 358  
24 Dec 1963  
Data Group 311

TR 64-50

CC 48

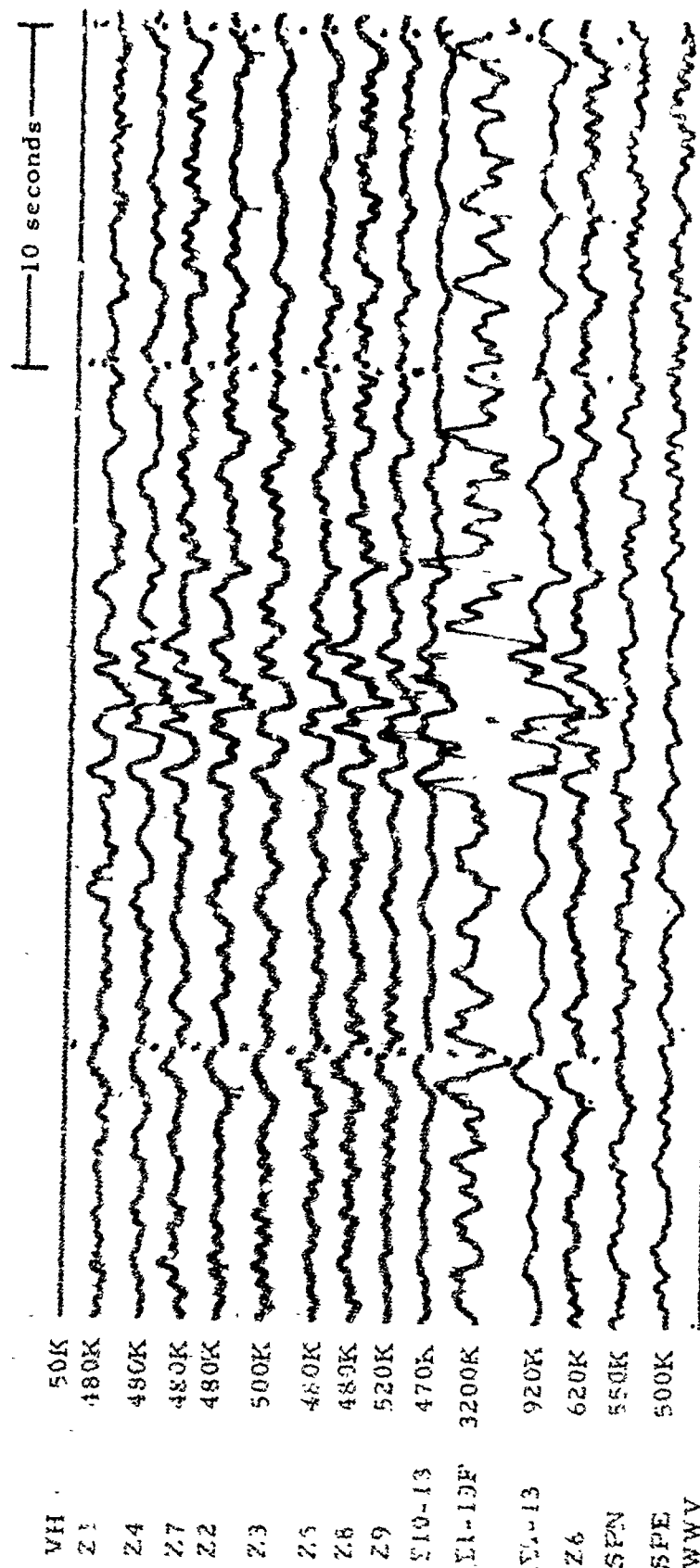


Figure 2-27. WMSO primary short-period seismogram illustrating an SKKP phase arrival.  
 Epicenter: near north coast of Java,  $\Delta \approx 142^\circ$ ,  $h \approx 323$  km, azimuth  $\approx 314^\circ$ ,  
 magnitude  $\approx 5.1$  (X10 enlargement of 16-mm film)

WMSO  
 Run 326  
 22 Nov 1963  
 Data Group 311



WWV

Z1 540K  
 Z2 500K  
 Z3 500K  
 Z4 500K  
 Z5 520K  
 Z6 480K  
 Z7 460K  
 Z8 500K  
 Z9 460K  
 Σ10-13 440K  
 Σ1-13F 3360K  
 Σ1-13 500K  
 SPN 480K  
 SPE 480K  
 LG 5 50K

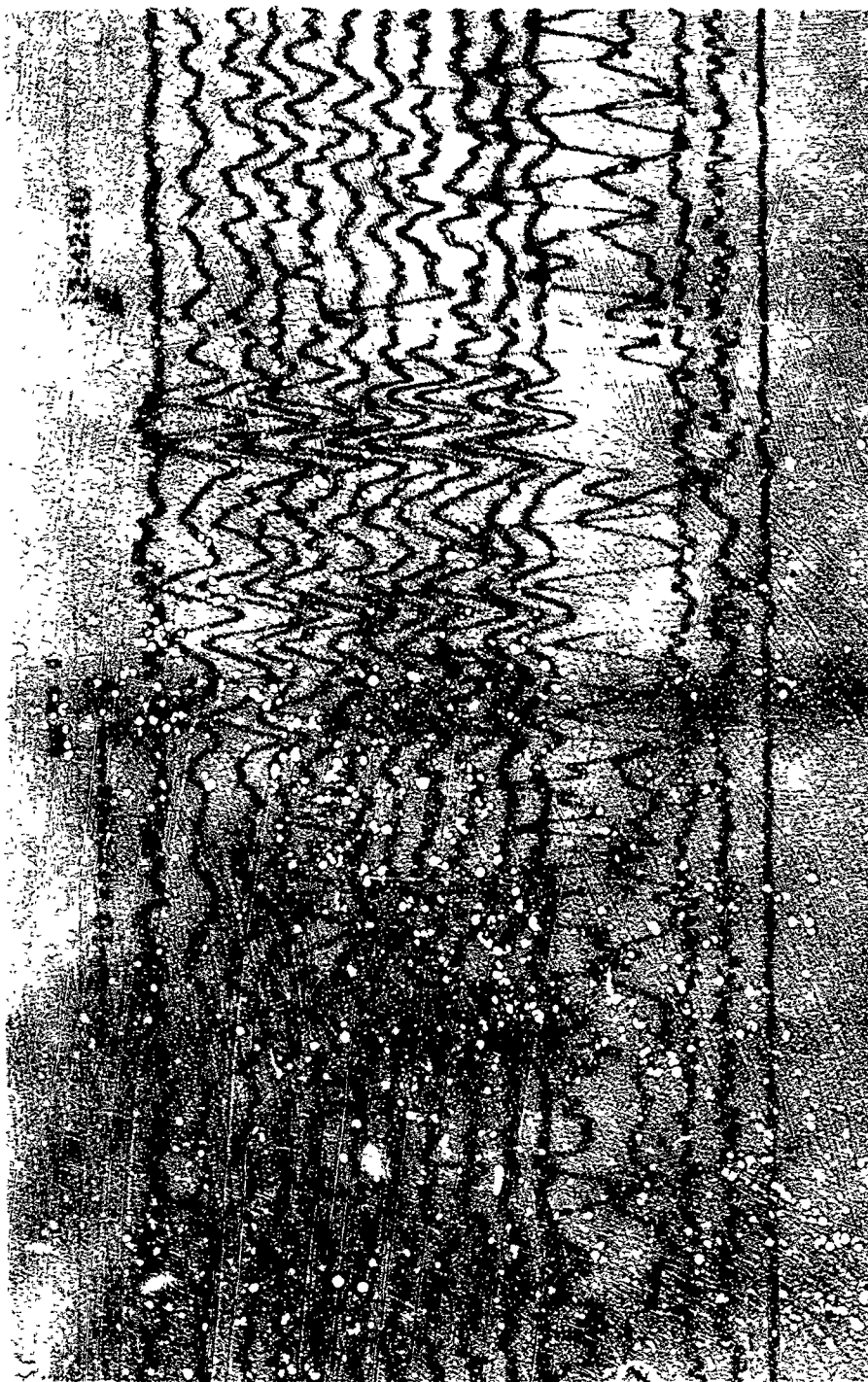


Figure 2-28. WMSO seismogram illustrating a PKPPKP (P'P') phase arrival.

Epicenter: off the east coast of Kamchatka,  $\Delta \approx 70^\circ$ ,  $h \approx 33$  km.  
 azimuth  $\approx 321^\circ$ , magnitude  $\approx 5.7$  (X10 enlargement of  
 16-mm film)

WMSO

Run 301

23 Oct 1963



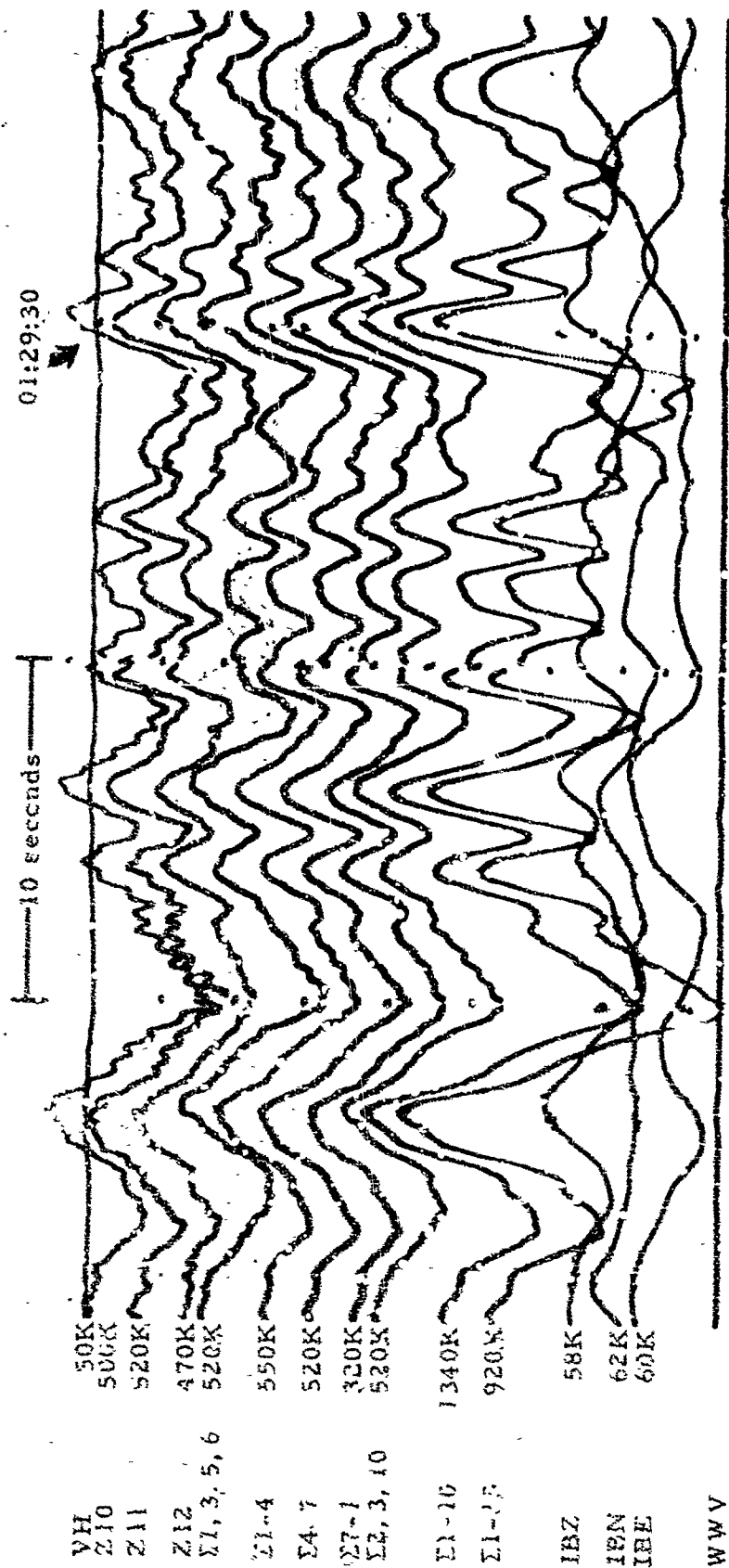


Figure 2-29. WMSO seismogram illustrating a PKPPKPPKP (P'P'P') phase arrival.  
 Epicenter: Kermadec Islands,  $\Delta \approx 95^\circ$ ,  $h \approx 46$  km, azimuth  $\approx 243^\circ$ ,  
 magnitude  $\approx 6.5$  (X10 enlargement of 16-mm film)

WMSO  
 Run 352  
 18 Dec 1963  
 Data Group 307

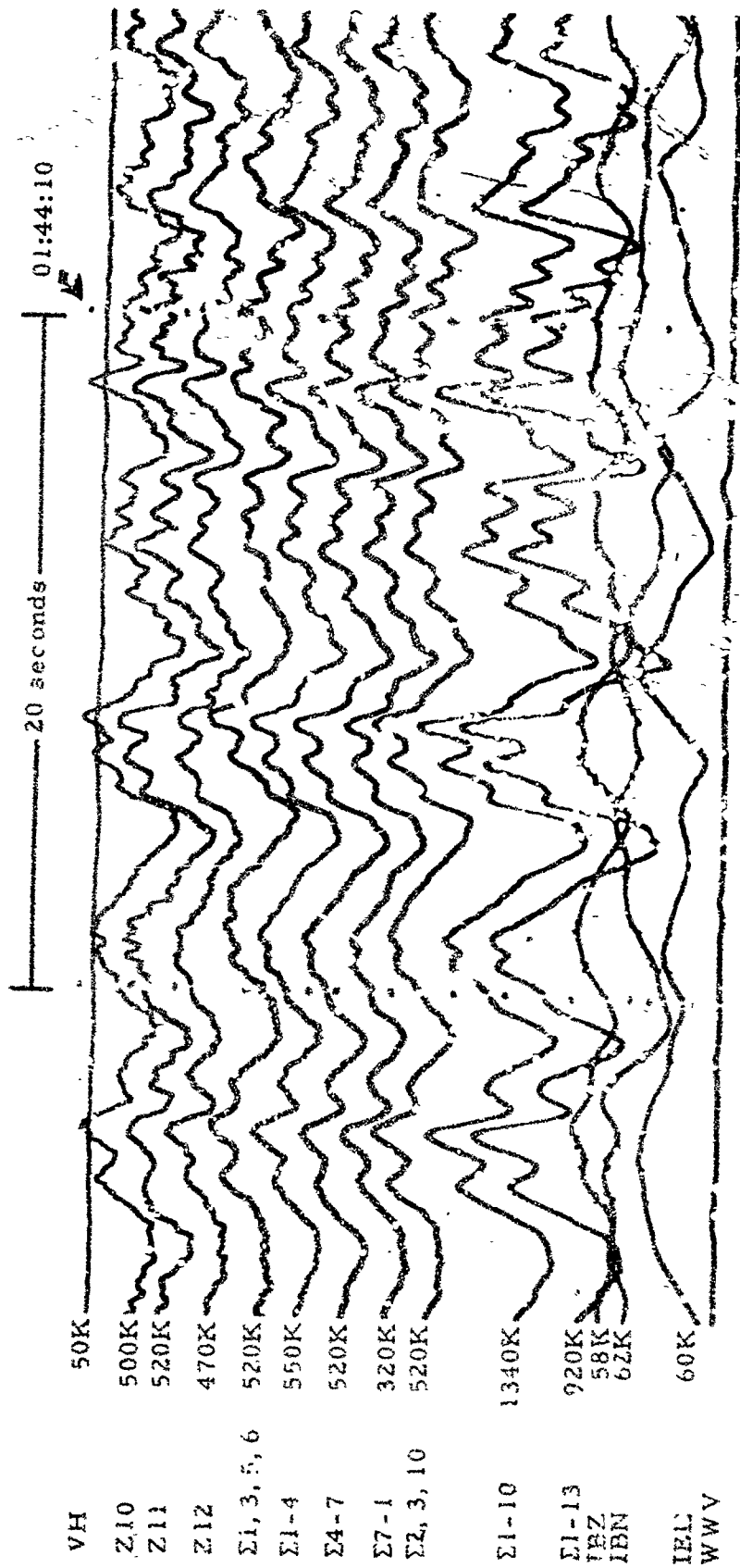


Figure 2-30. WMSO seismogram illustrating a PKPPA (P-wave) phase arrival. Epicenter: Kermadec Islands,  $\Delta \approx 95^\circ$ ,  $h \approx 400$  km, azimuth  $\approx 243^\circ$ , magnitude  $\approx 6.5$  (X10 enlargement of 16-mm film)

WMSO  
 Run 352  
 18 Dec 1963  
 Data Group 307

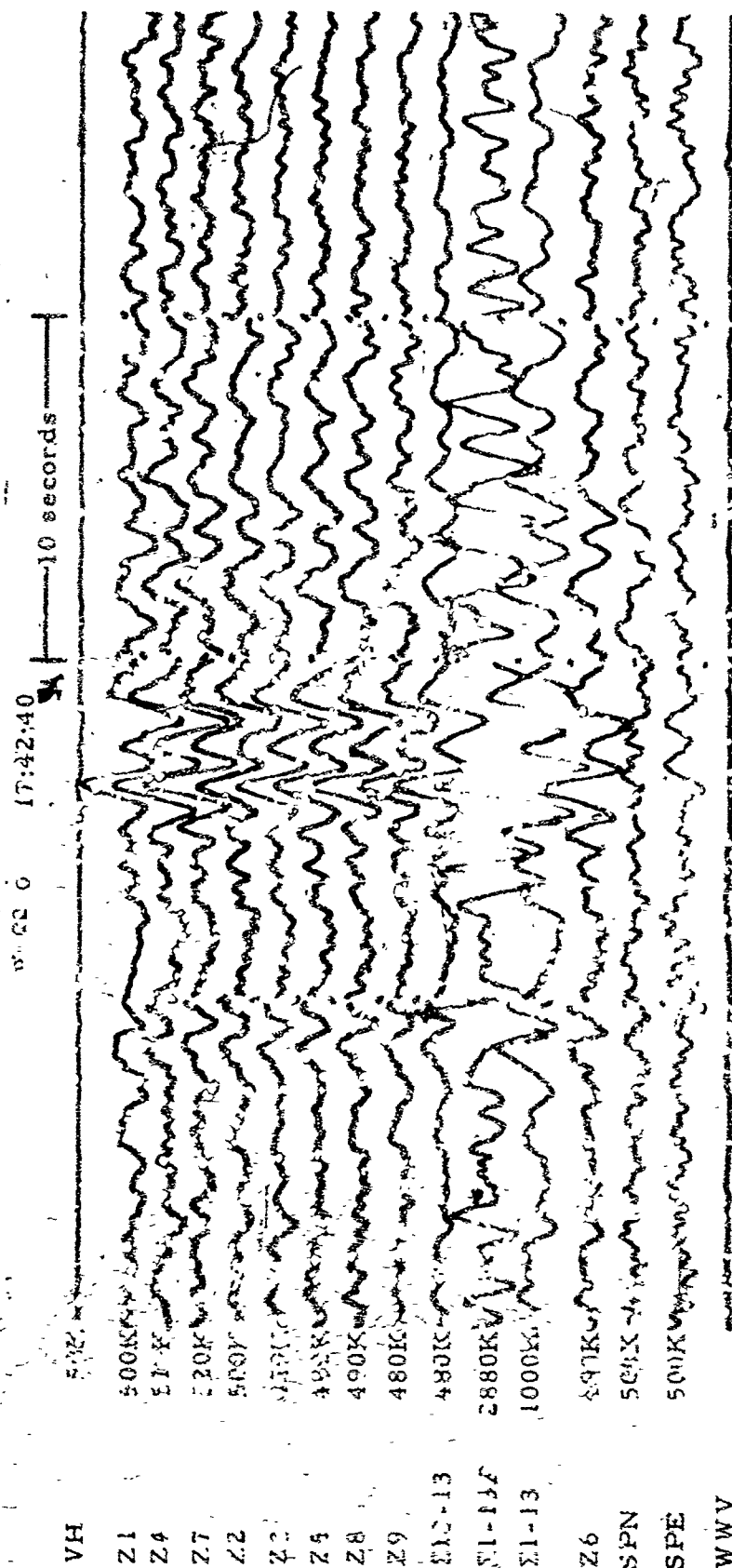


Figure 2-31. WMSO seismogram illustrating a PcPPKP phase arrival. Epicenter: Loyalty Islands region,  $\Delta = 103^\circ$ ,  $L = 141$  km, azimuth  $\approx 254^\circ$ , magnitude  $\approx 6.7$  (X10 enlargement of 6 mm film)

WMSO

Run 020

20 Jan 1964

Data Group 311

TR 64-50

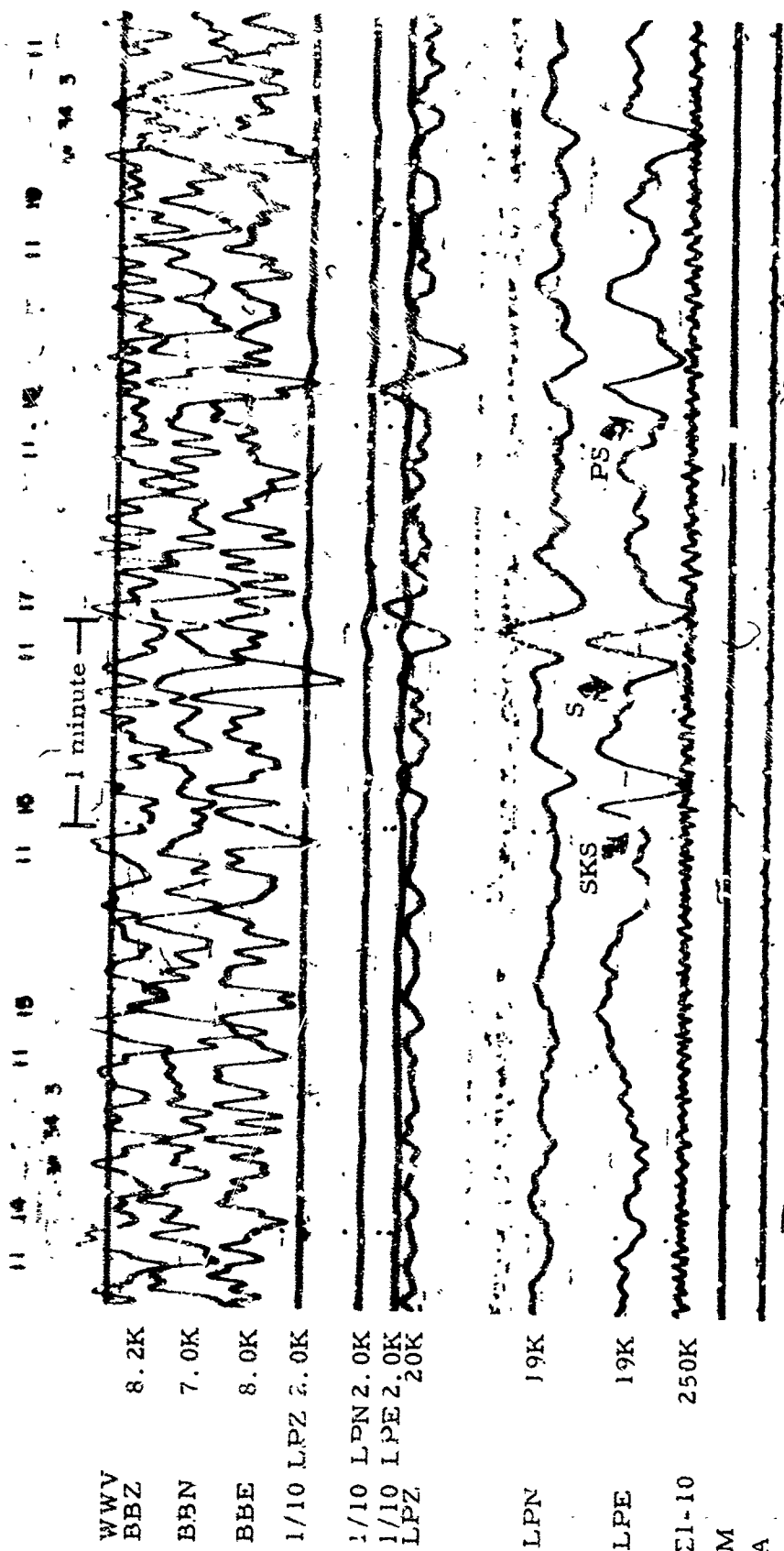


Figure 2-32. WMSO seismogram illustrating SKS, S, and PS phase arrivals from the Fiji Islands region. See figure 2-33 for the corresponding short-period recording of SKS. Epicentral data:  $\Delta \approx 94^\circ$ ,  $h \approx 435$  km,  $t \approx 247^\circ$ , magnitude  $\approx 5.0$  (X10 enlargement of 16-mm film)

WMSO

Run 343

9 Dec 1963

Data Group 204

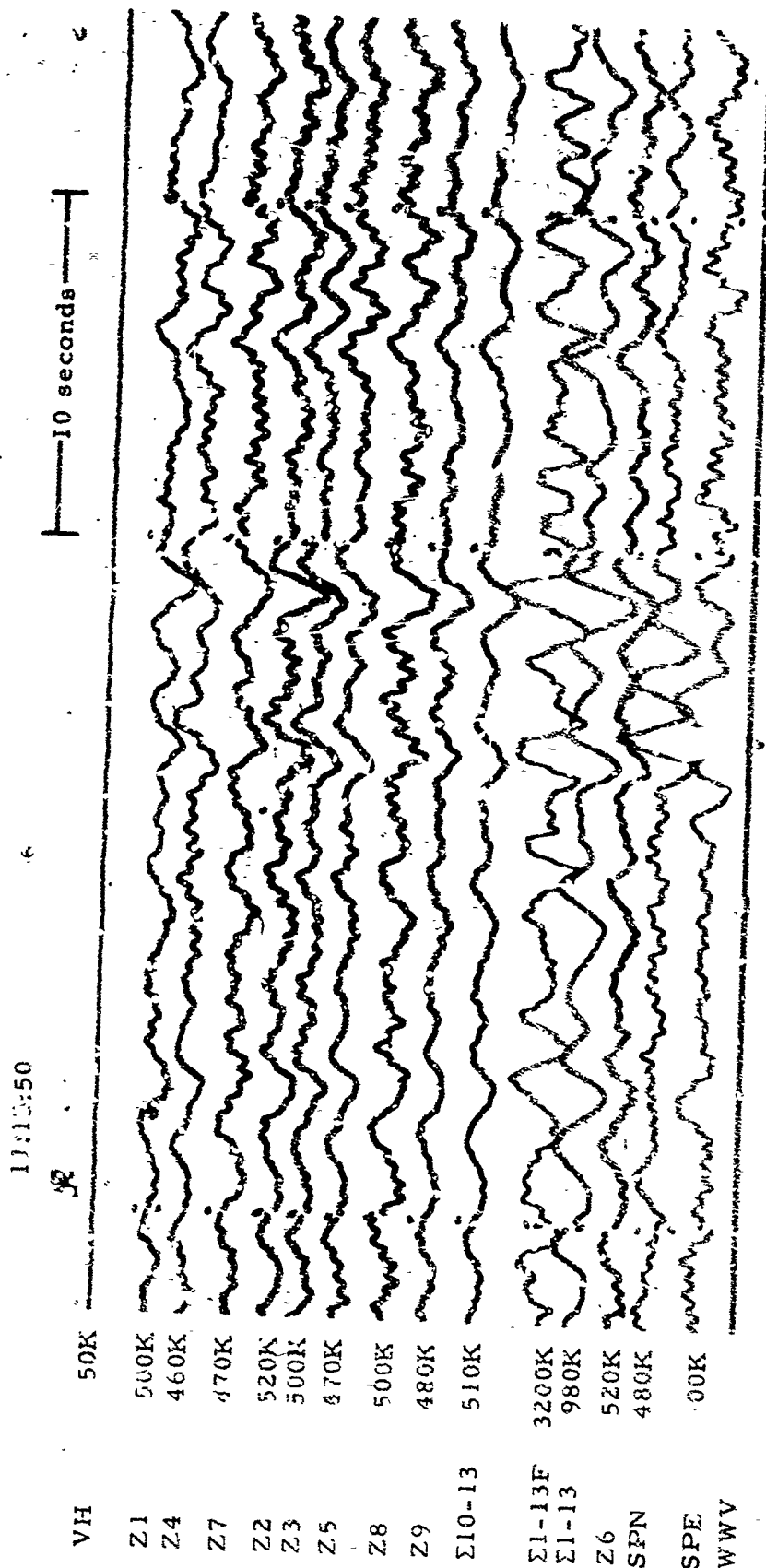
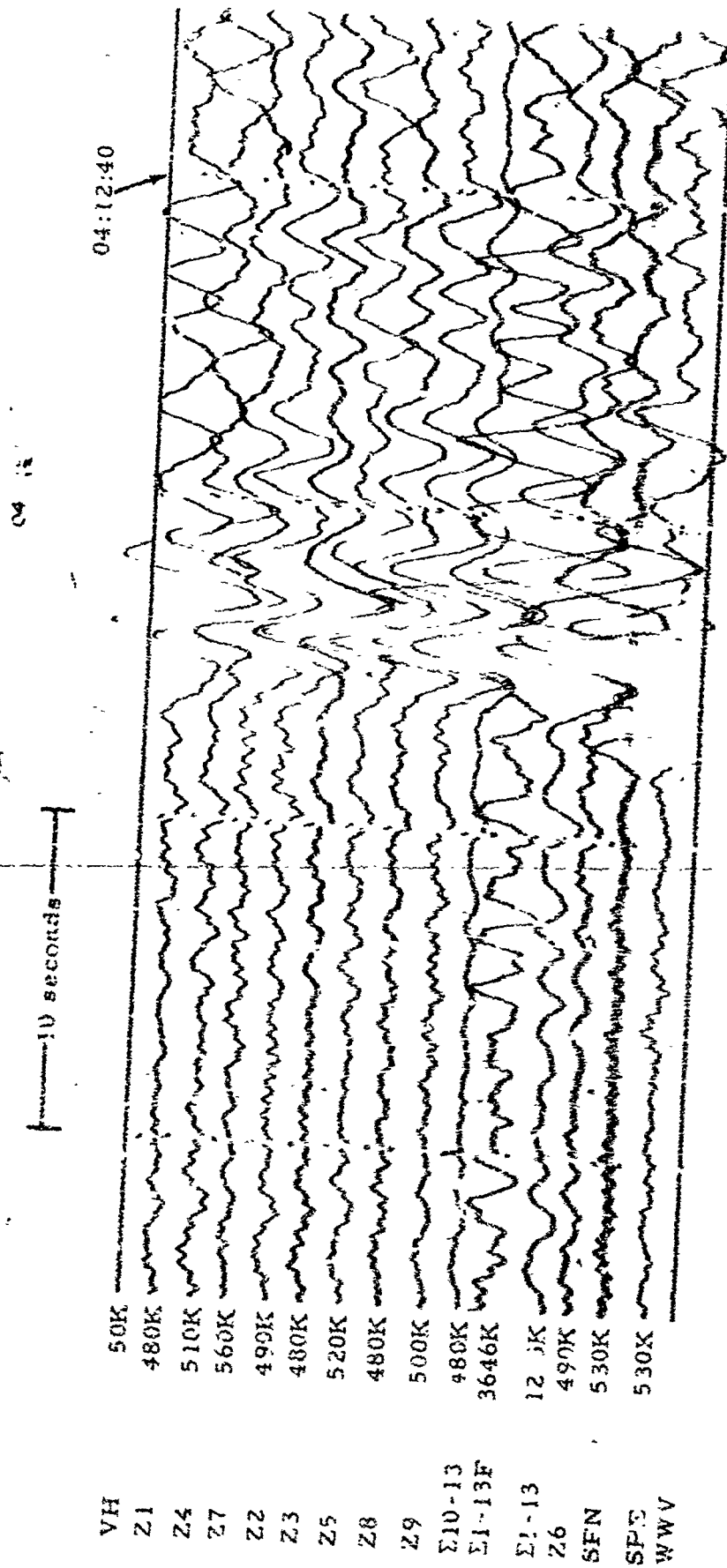


Figure 2-33. WMSO seismogram illustrating an SKS phase arrival from the Fiji Islands region. Epicentral data:  $\Delta \approx 94^\circ$ ,  $h \approx 435$  km, azimuth  $\approx 247^\circ$ , magnitude  $\approx 5.0$  (X10 enlargement of 16-mm film)

WMSO  
Run 342  
9 Dec 1963  
Data Group 312

TR 64-50



WMSO  
Run 203  
21 July 1964  
Data Group 3003

Figure 2-33a. WMSO seismogram illustrating an SKS phase arrival from the Fiji Islands region. Epicentral data:  $\Delta \approx 96^\circ$ ,  $h \approx 222$  km, azimuth  $\approx 243^\circ$ , magnitude  $\approx 5.8$   
(X10 enlargement of 16-mm film)

TR 64-50

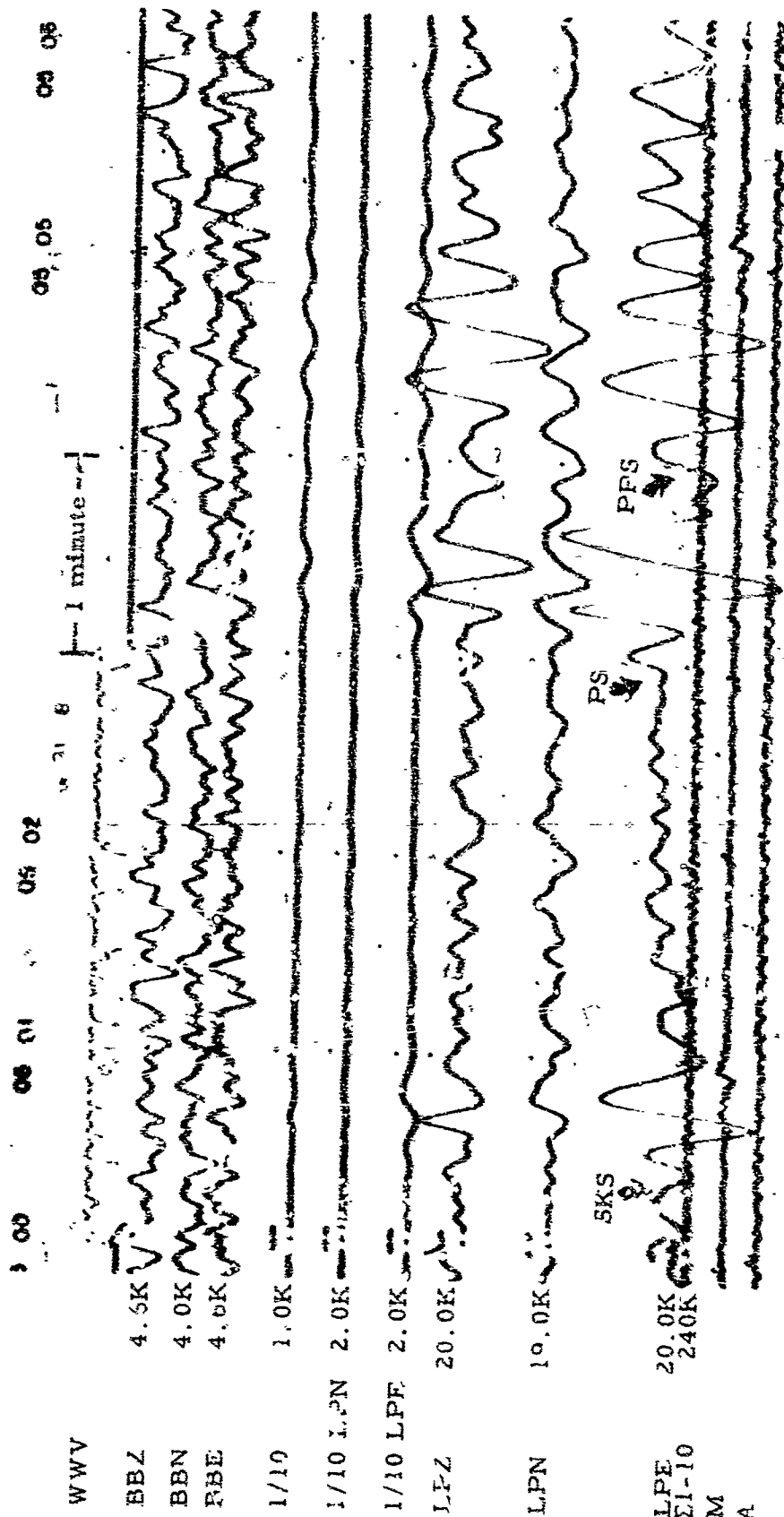


Figure 2-34. WMSO seismogram illustrating SKS, PS, and PPS phase arrivals from the New Hebrides Islands. Epicentral data:  $\Delta \approx 103^\circ$ ,  $h \approx 33$  km, azimuth  $\approx 257^\circ$ , magnitude  $\approx 4.9$  (X10 enlargement of 16-mm film)

WMSO

Rur. 318

14 Nov 1963

Data Group 304

TR 64-50

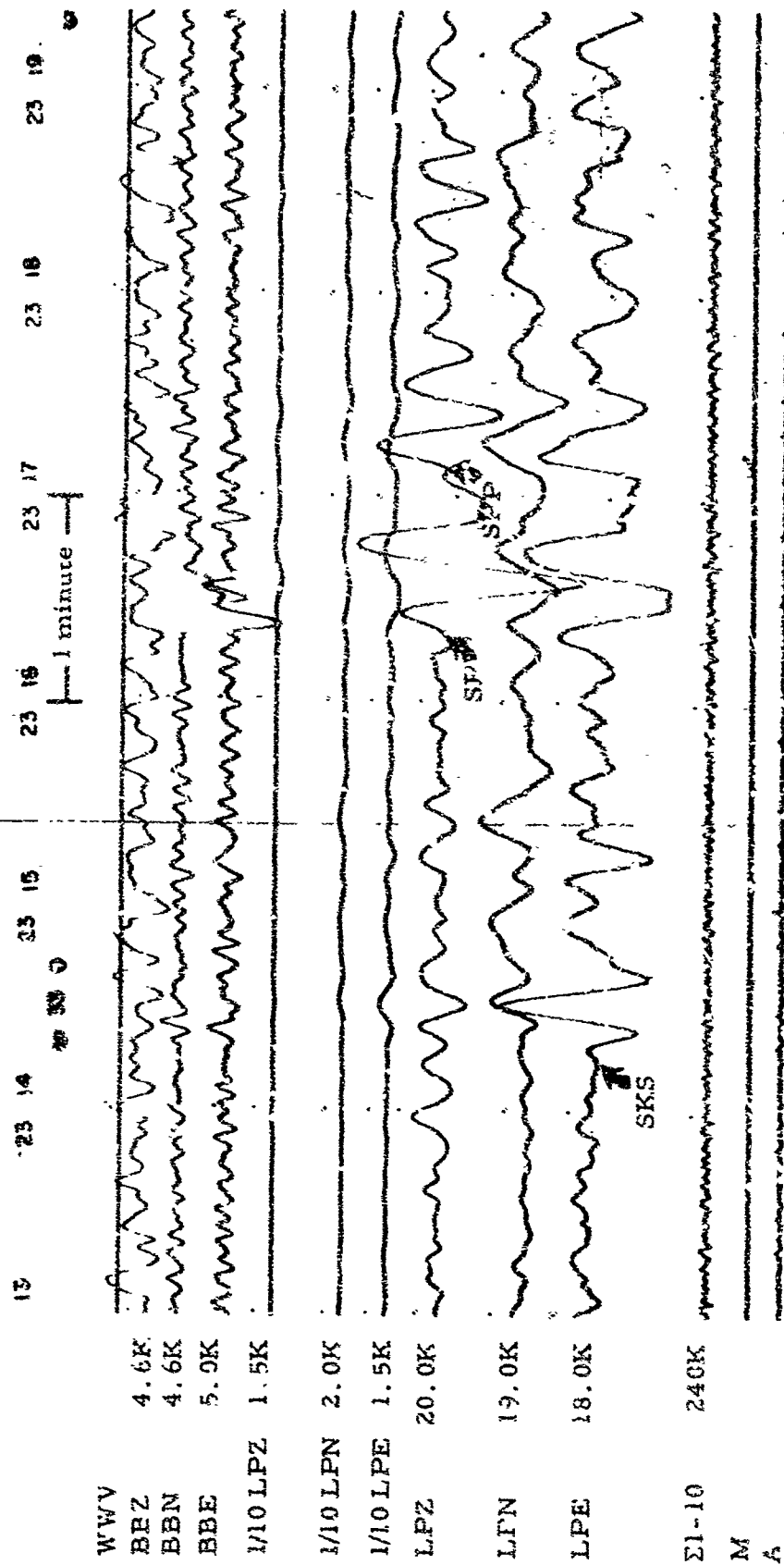


Figure 2-35. WMSO seismogram illustrating SKS, SP, and SPP phases from the Fiji Islands region. Epicentral data:  $\Delta \approx 96^\circ$ ,  $h \approx 33$  km, azimuth  $\approx 254^\circ$ , magnitude  $\approx 5.3$  (X10 enlargement of 16-mm film)

WMSO  
Run 326  
26 Nov 63  
Data Group 304



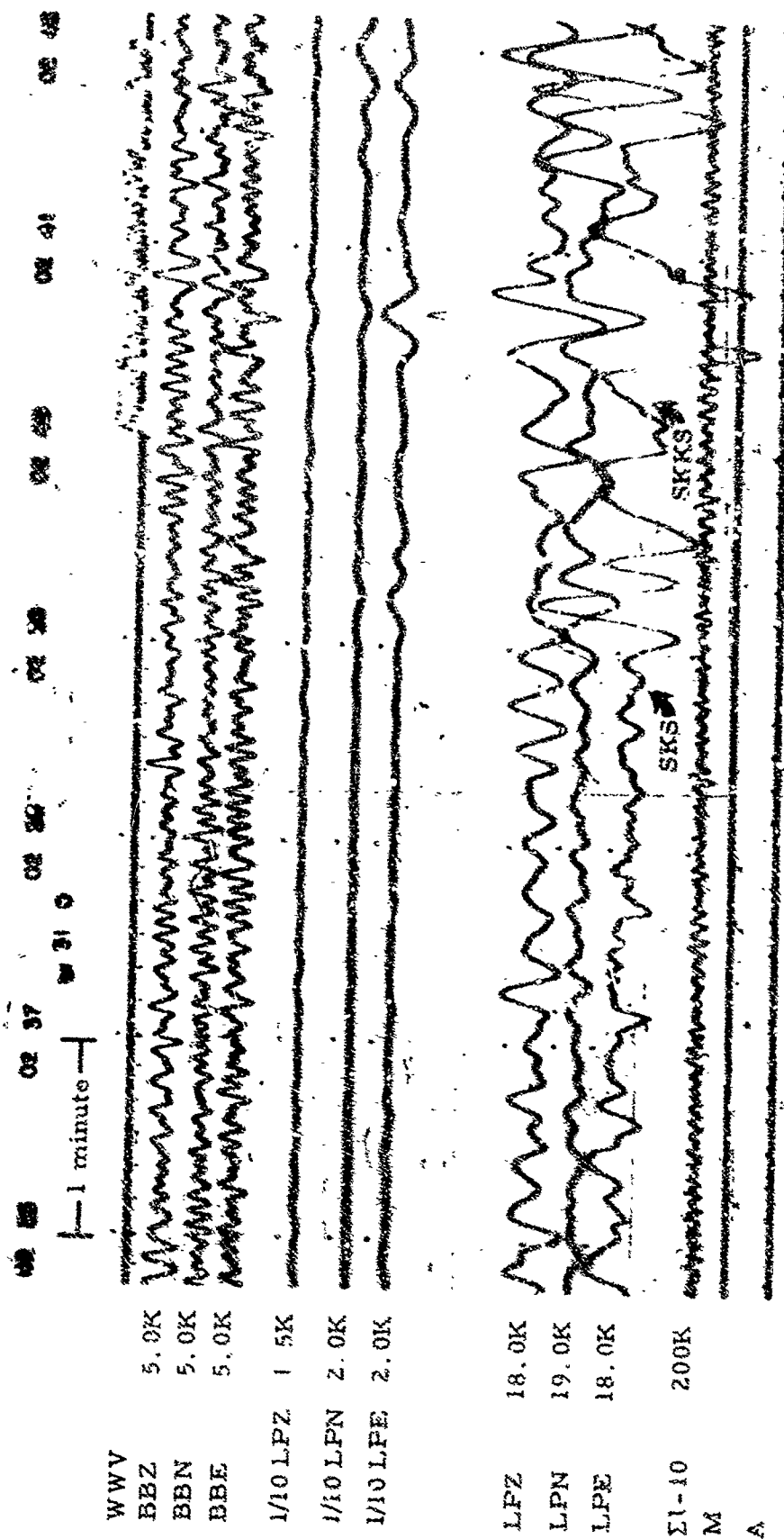


Figure 2-36. WMSO seismogram illustrating SKS and SKKS phase arrivals from Western New Guinea. Epicentral data:  $\Delta \approx 118^\circ$ ,  $h \approx 33$  km, azimuth  $\approx 288^\circ$ , magnitude  $\approx 5.7$  (X10 enlargement of 16-mm film)

WMSO  
Run 310  
6 Nov 1963  
Data Group 304

TR 64-50

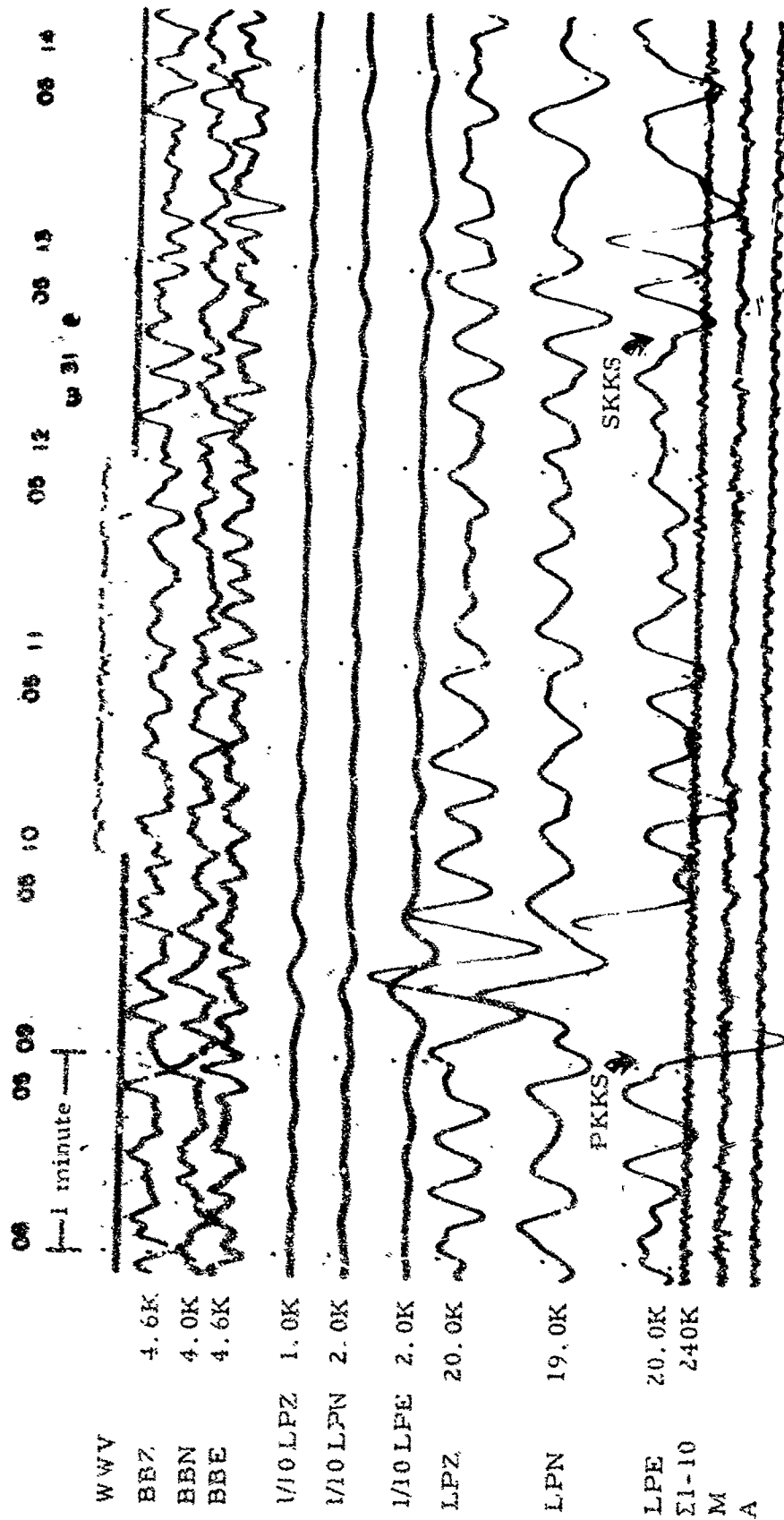


Figure 2-37. WMSO seismogram illustrating PKKS and SKKS phase arrivals from the New Hebrides Islands. Epicentral data:  $\Delta \approx 103^\circ$ ,  $h \approx 33$  km, azimuth  $\approx 257^\circ$ , magnitude  $\approx 4.8$  (X10 enlargement of 16-mm film)

WMSO  
Run 318  
14 Nov 1963  
Data Group 304

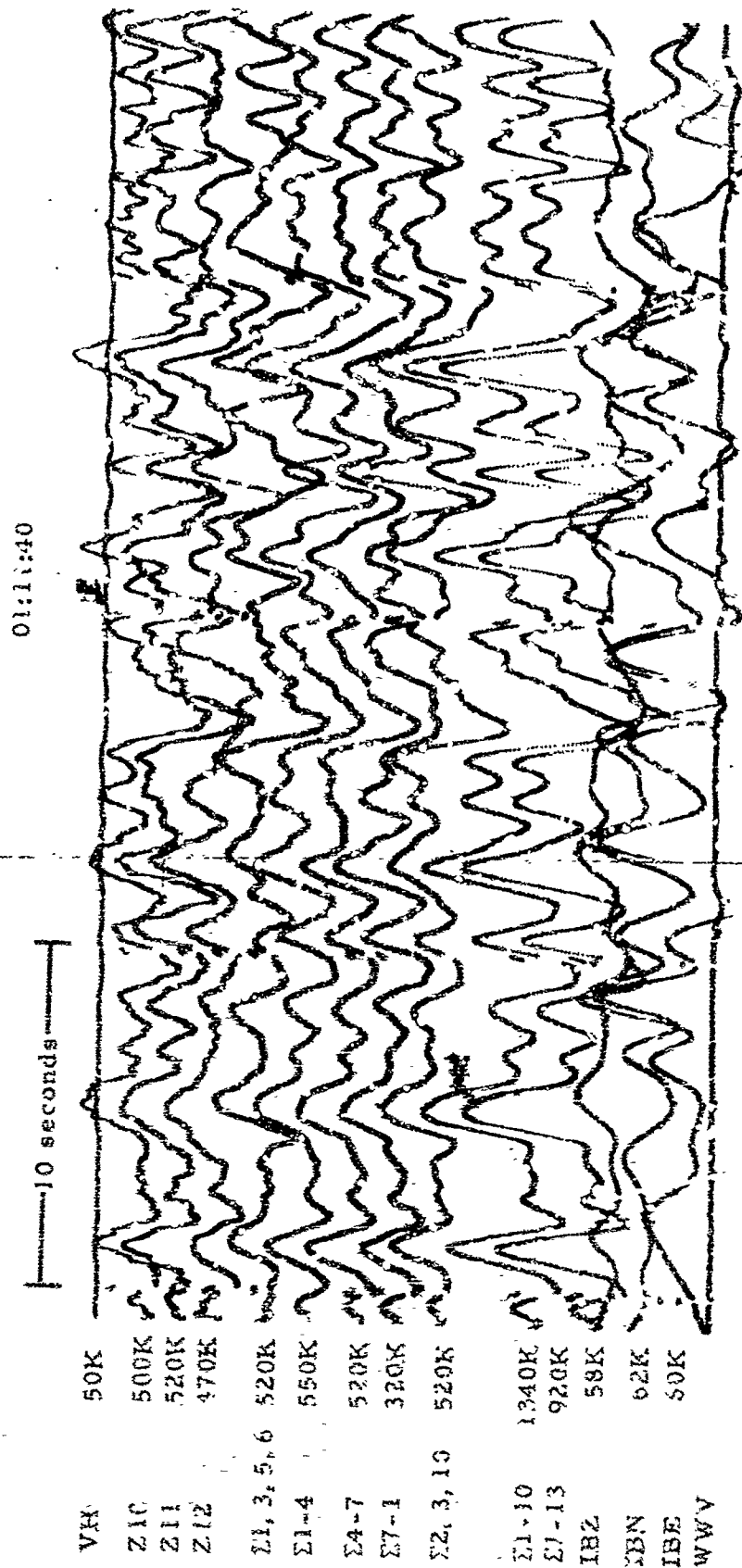


Figure 2-38. WMSO seismogram illustrating a PPKS phase arrival from the  
Kermadec Islands. Epicentral data:  $\Delta \approx 95^\circ$ ,  $h \approx 46$  km, azimuth  $\approx 243^\circ$ ,  
magnitude  $\approx 6.5$  (X10 enlargement of 10-mm film).

WMSO

Run 352

18 Dec 1963

Data Group 307

—10— ॐ नमो भगवते वासुदेवाय

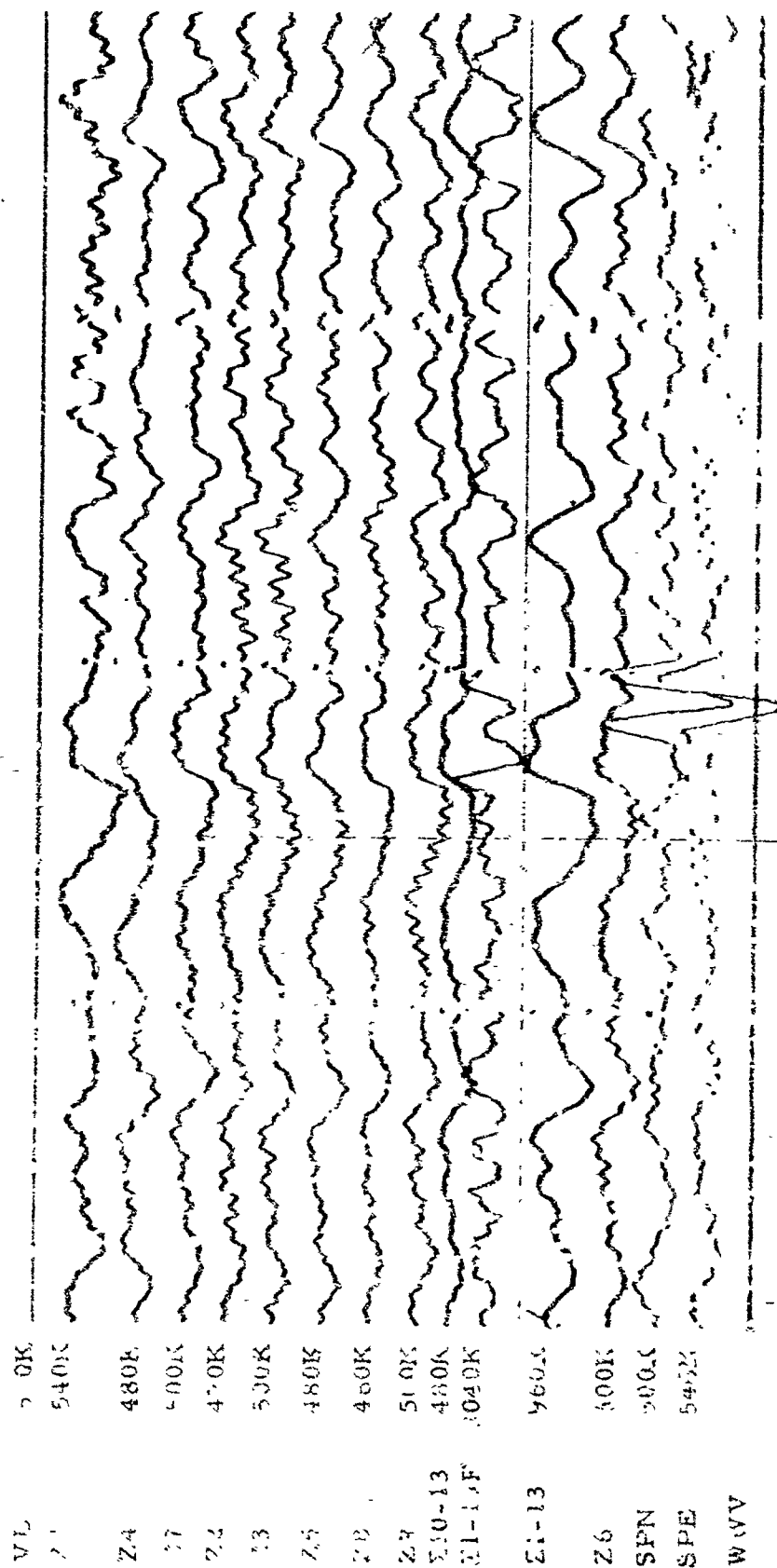


Figure 2-39. GKKKS as recorded on the WMSO short-period seismogram. Epicenter: Kermadec Islands,  $\lambda \approx 101^{\circ}$ ,  $h \approx 33$  km, azimuth  $\approx 238^{\circ}$ , magnitude  $\approx 5.5$  (X10 enlargement of 16-mm film)

Data Group 3:1

WWV  
 PBZ 5.0K  
 EBN 5.0K  
 BBE 5.0K  
 1/10LPZ 1.5K  
 1/10LPN 2.0K  
 1/10LPE 1.5K  
 LPZ 19.0K  
 LPN 19.0K  
 LPE 17.5K  
 Σ1-10 20K  
 1A  
 A

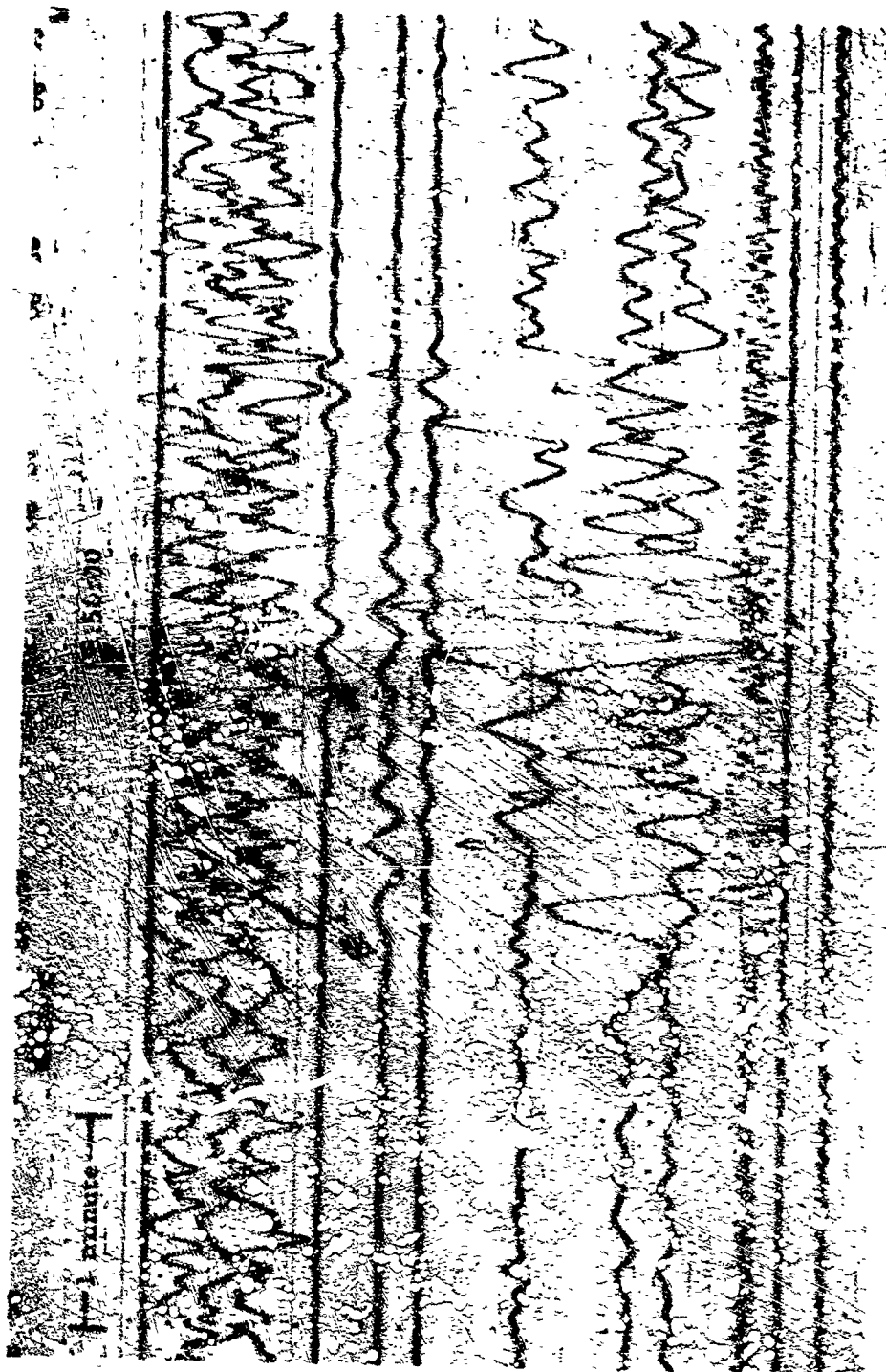


Figure 2-10. WMSO seismic data illustrating Love and Rayleigh phase arrivals from Sonora, Mexico. Epicentral data:  $\Delta \approx 13^\circ$ ,  $h \approx 14$  km, azimuth  $\approx 200^\circ$ , magnitude  $\approx 4.7$  (N10 enlargement of 16-min film)

WMSO  
 Run 338  
 2 Nov 1963  
 Data Group 304

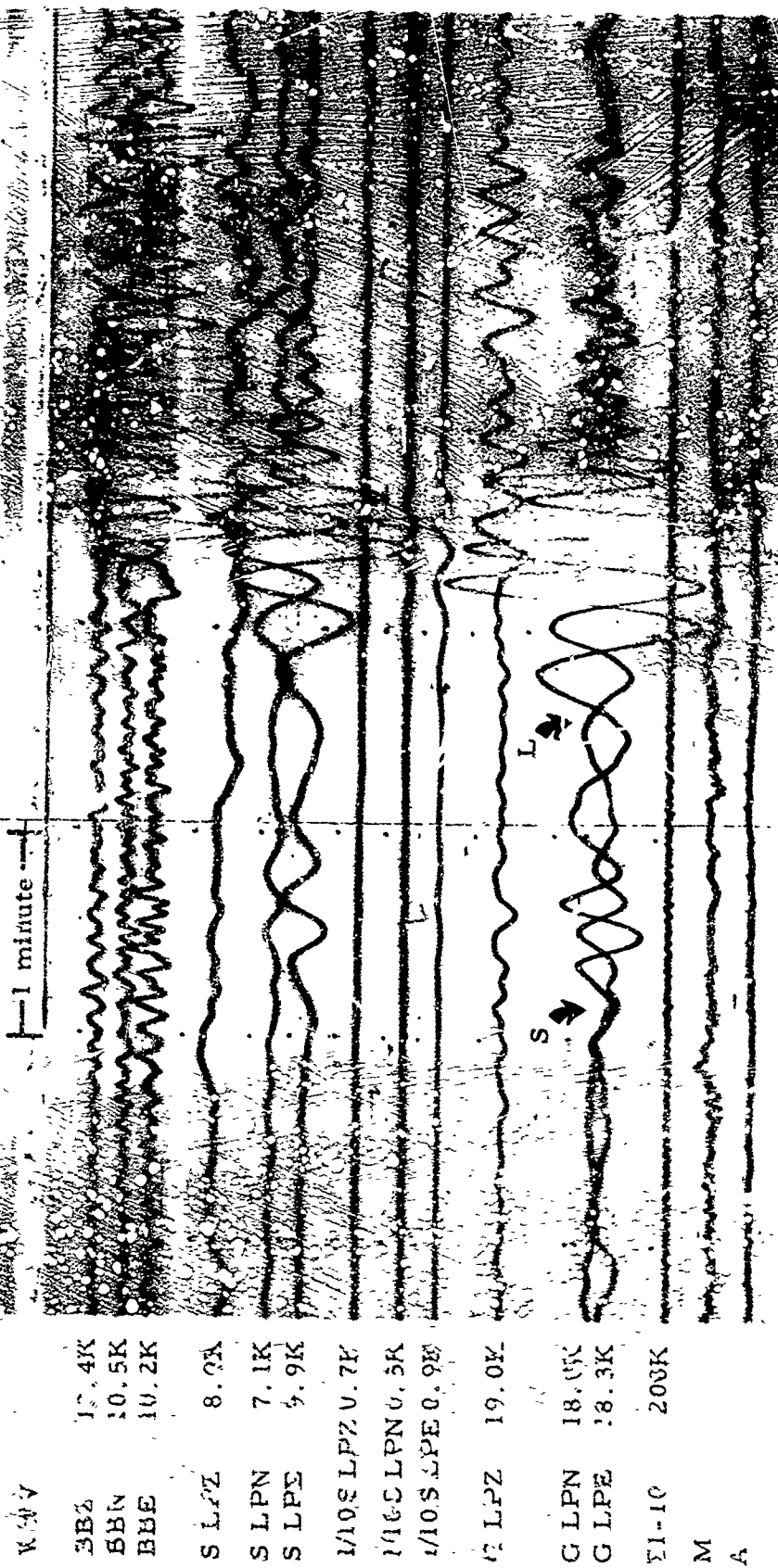


Figure 2-41. WMSO seismogram illustrating the broad-band system response to surface waves. Epicenter: off the coast of Central Mexico,  $\Delta \approx 16^\circ$ ,  $h \approx 33$  km, azimuth  $\approx 214^\circ$ , magnitude  $\approx 3.9$  (X10 enlargement of 16-mm film)

WMSO  
Run 174  
23 Jun 1963

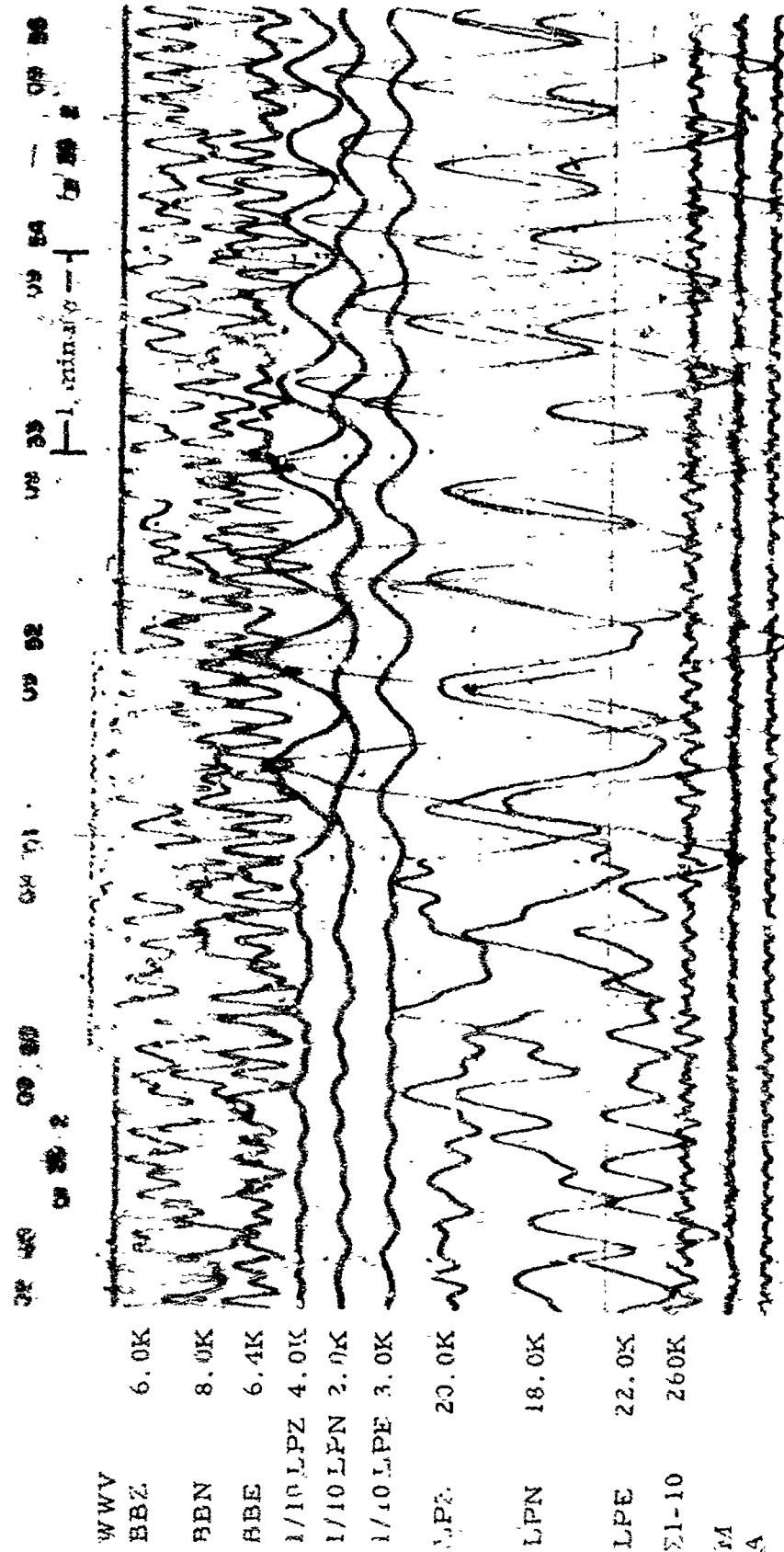


Figure 2-42. WMSO seismogram illustrating a Rayleigh<sub>1</sub> phase arrival. See figure 2-43 for Rayleigh<sub>2</sub> arrival from the same event. Epicenter: Kermadec Islands,  $\Delta \approx 101^\circ$ ,  $h \approx 33$  km, azimuth  $\approx 238^\circ$ , magnitude  $\approx 5.8$  (X10 enlargement of 16-mm film)

WMSO  
Run 362  
23 Dec 1963  
Data Group 304

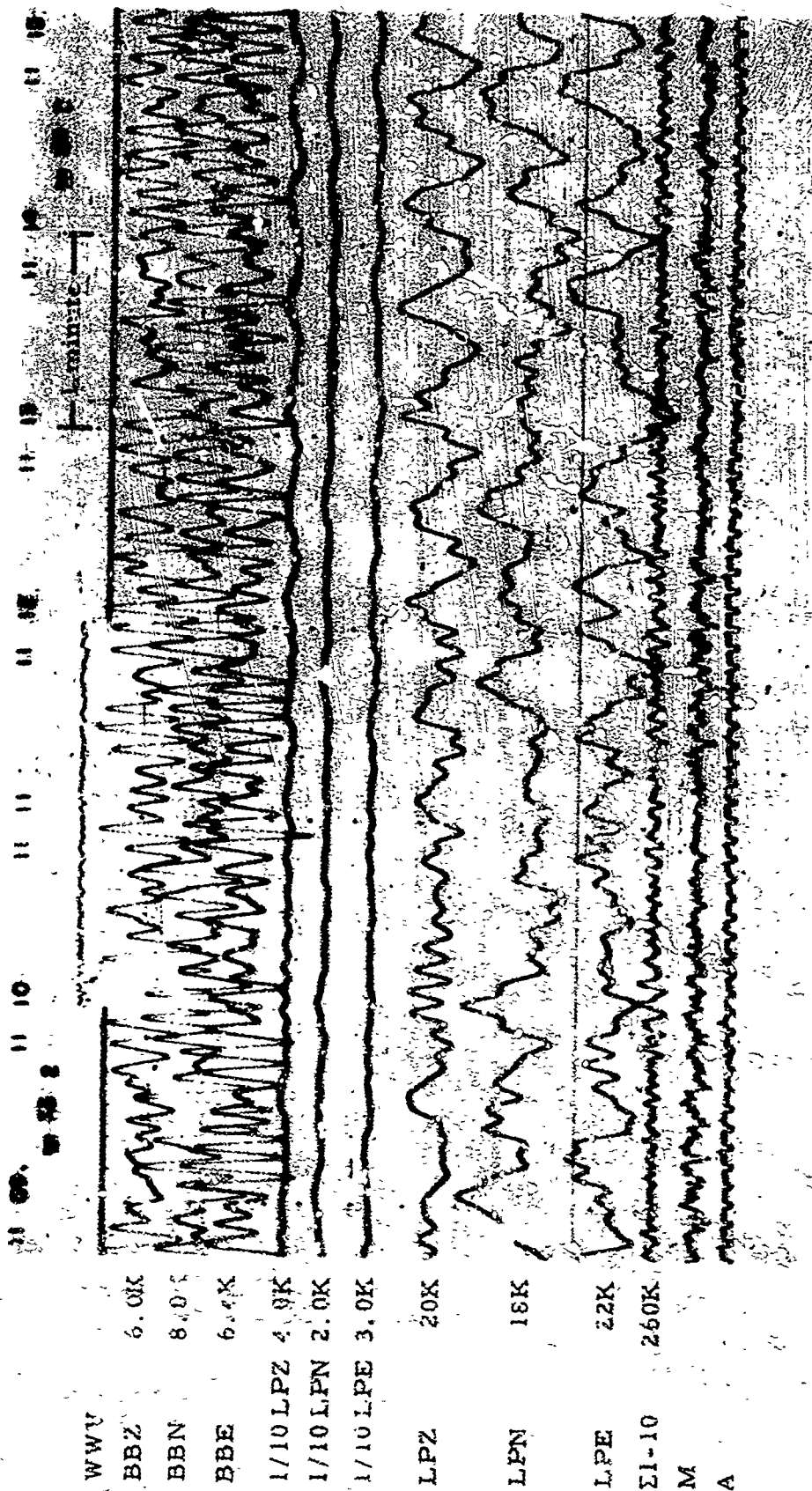


Figure 2-43. WMSO seismogram illustrating a Rayleigh<sub>2</sub> phase arrival.  
 Epicenter: Kermadec Island,  $\Delta = 101^\circ$ ,  $h = 33$  km, azimuth  $\approx 238^\circ$ ,  
 magnitude  $\approx 5.8$  (X10 enlargement of 16-mm film)

WMSO

Run 362

22 Dec 1963

Data Group 304



TR 64-50

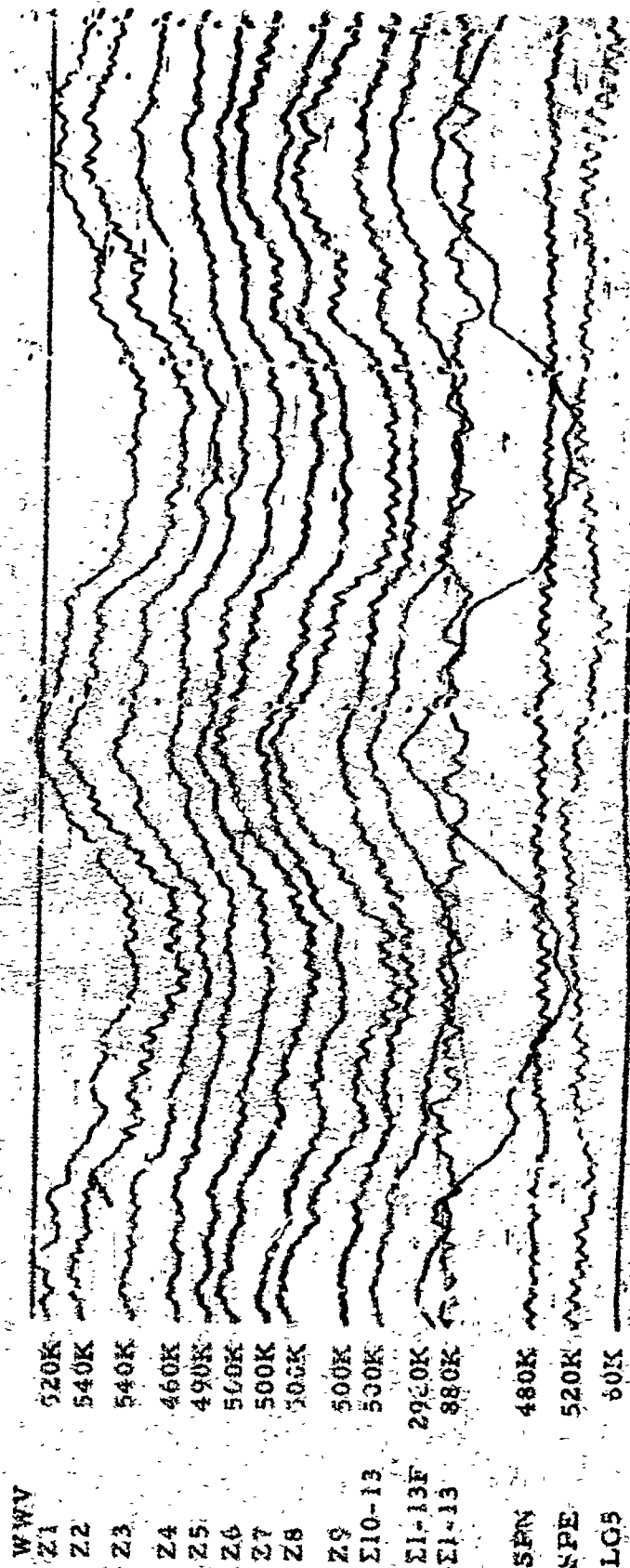


Figure 2-44. Rayleigh waves as recorded on the WMSO short-period seismogram.  
Epicenter: Santa Cruz Island region,  $\Delta \approx 101^\circ$ ,  $h \approx 43$  km, azimuth  $\approx 265^\circ$ ,  
magnitude  $\approx 6.3$  (X10 enlargement of 16-mm film)

WMSO  
Run 258  
15 Sep 1963

10 seconds

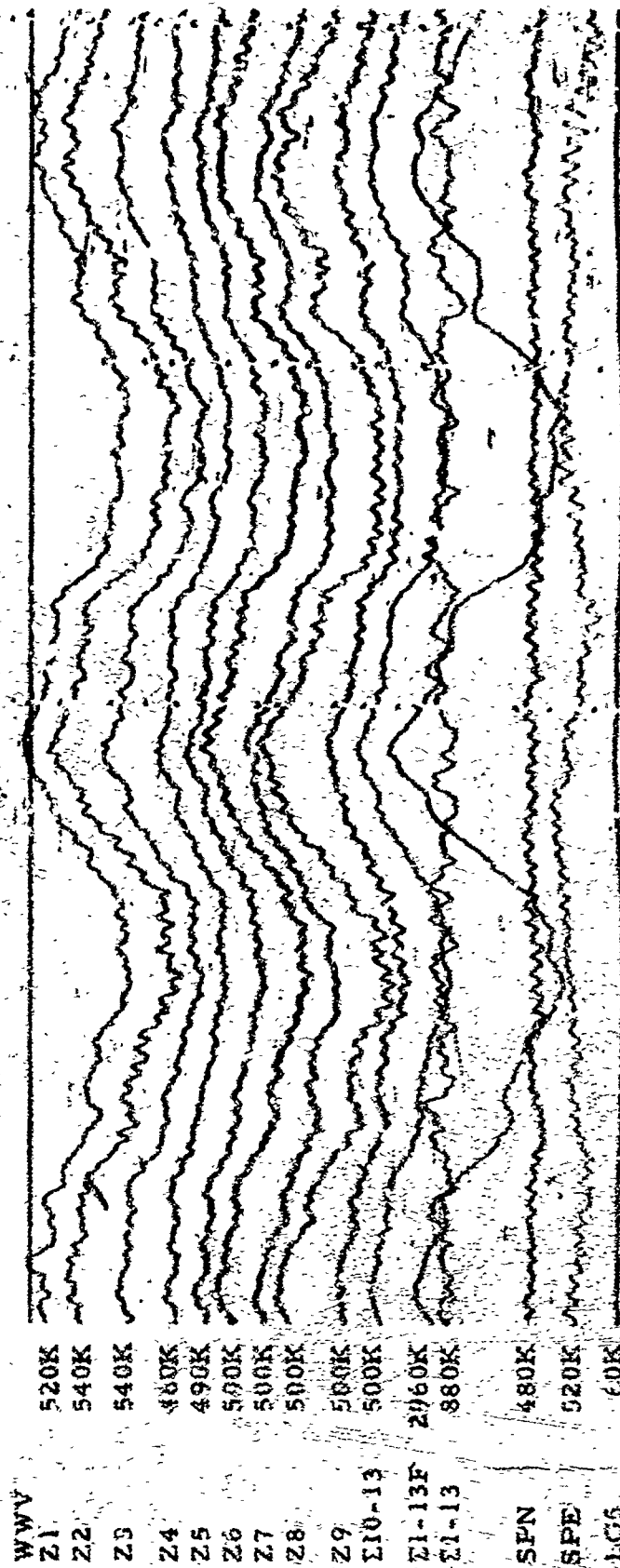


Figure 2-24. Rayleigh waves as recorded on the WMSO short-period seismogram.  
Epicenter: Santa Cruz Island region,  $\Delta \approx .01^\circ$ ,  $h \approx 43$  km, azimuth  $\approx 265^\circ$ ,  
magnitude  $\approx 6.3$  (X10 enlargement of 16-mm film)

WMSO  
Run 252  
15 Sep 1963

3. P AND PKP PHASES FROM VARIOUS  
DISTANCES AND AZIMUTHS

3.1 DISTANCE =  $0^{\circ}$  to  $16^{\circ}$

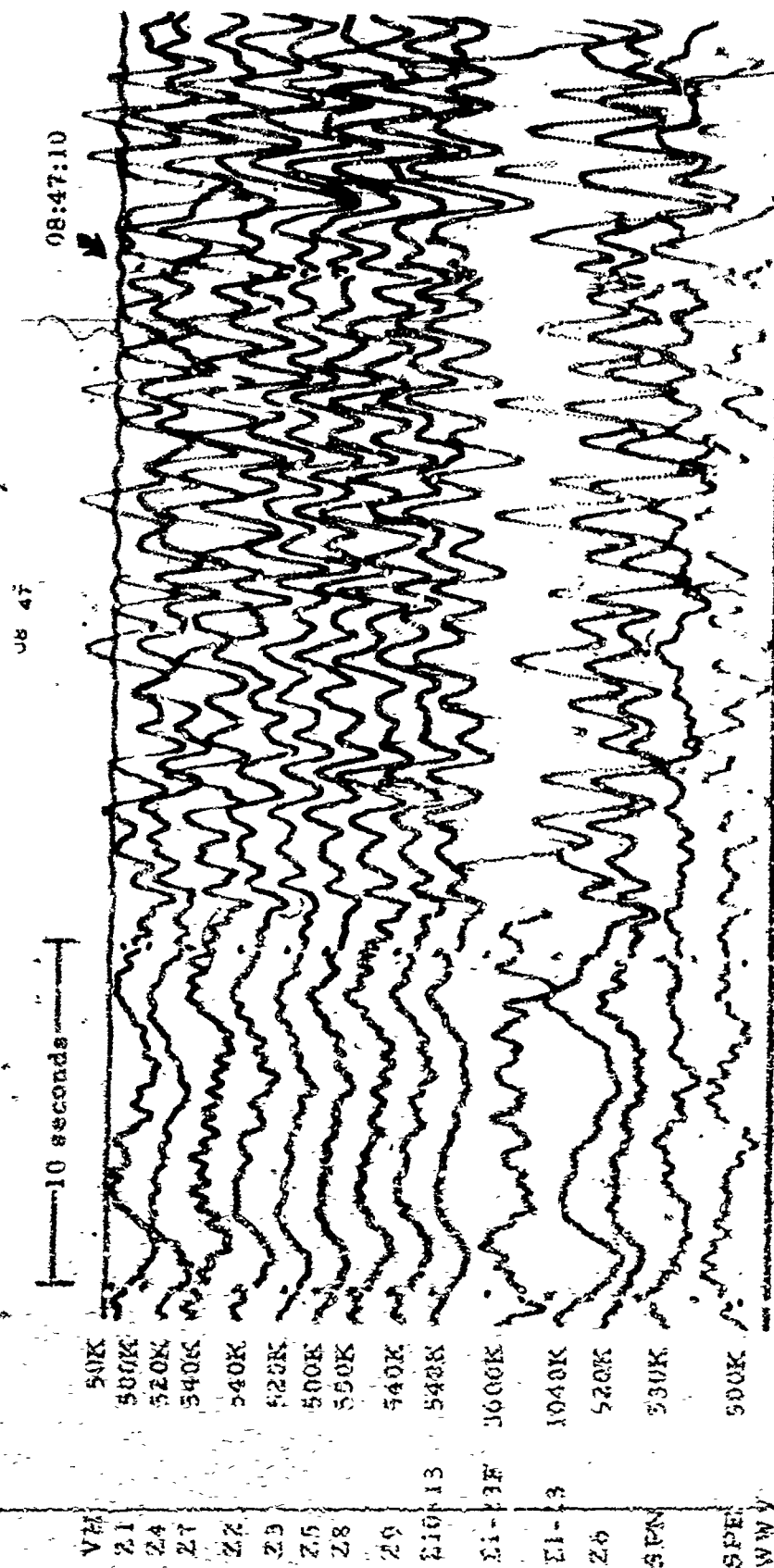


Figure 3-1. WMSO seismogram illustrating a P-phase arrival from the Gulf of California.  
 Epicentral data:  $\Delta \approx 14^\circ$ ,  $h \approx 14$  km, azimuth  $\approx 261^\circ$ , magnitude  $\approx 4.6$   
 (X10 enlargement of 16-mm film)

WMSO  
 Run 034  
 3 Feb 1964  
 Data Group 311

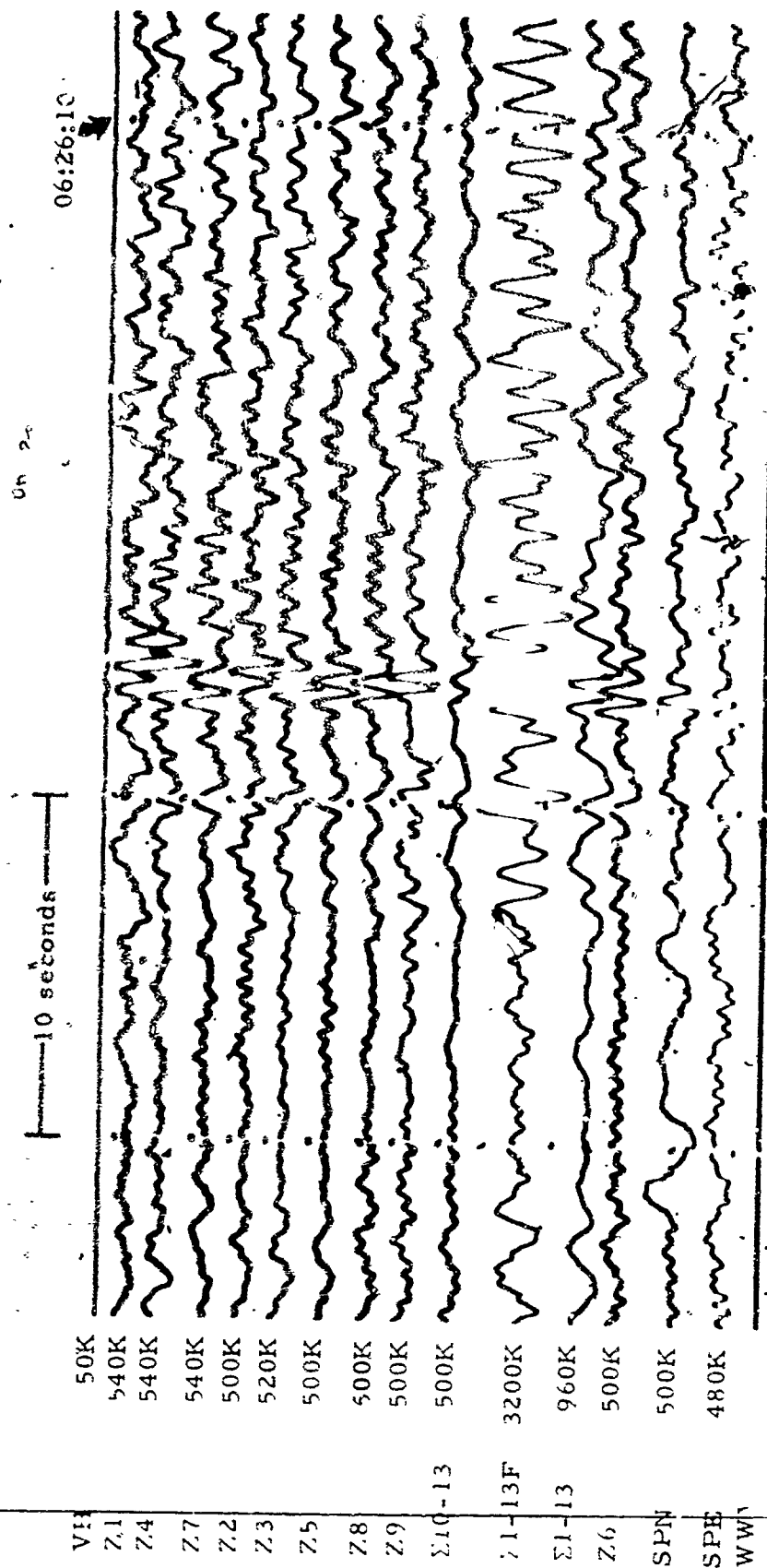


Figure 3-2. WMSO short-period seismogram illustrating a P-phase arrival from Central Idaho. Epicentral data:  $\Delta \approx 16^\circ$ ,  $h \approx 33$  km, azimuth  $\approx 313^\circ$ , magnitude  $\approx 4.3$  (X10 enlargement of 16-mm film)

WMSO  
Run 039  
8 Feb 1964  
Dat Group 311

3.2 DISTANCE =  $17^{\circ}$  to  $40^{\circ}$

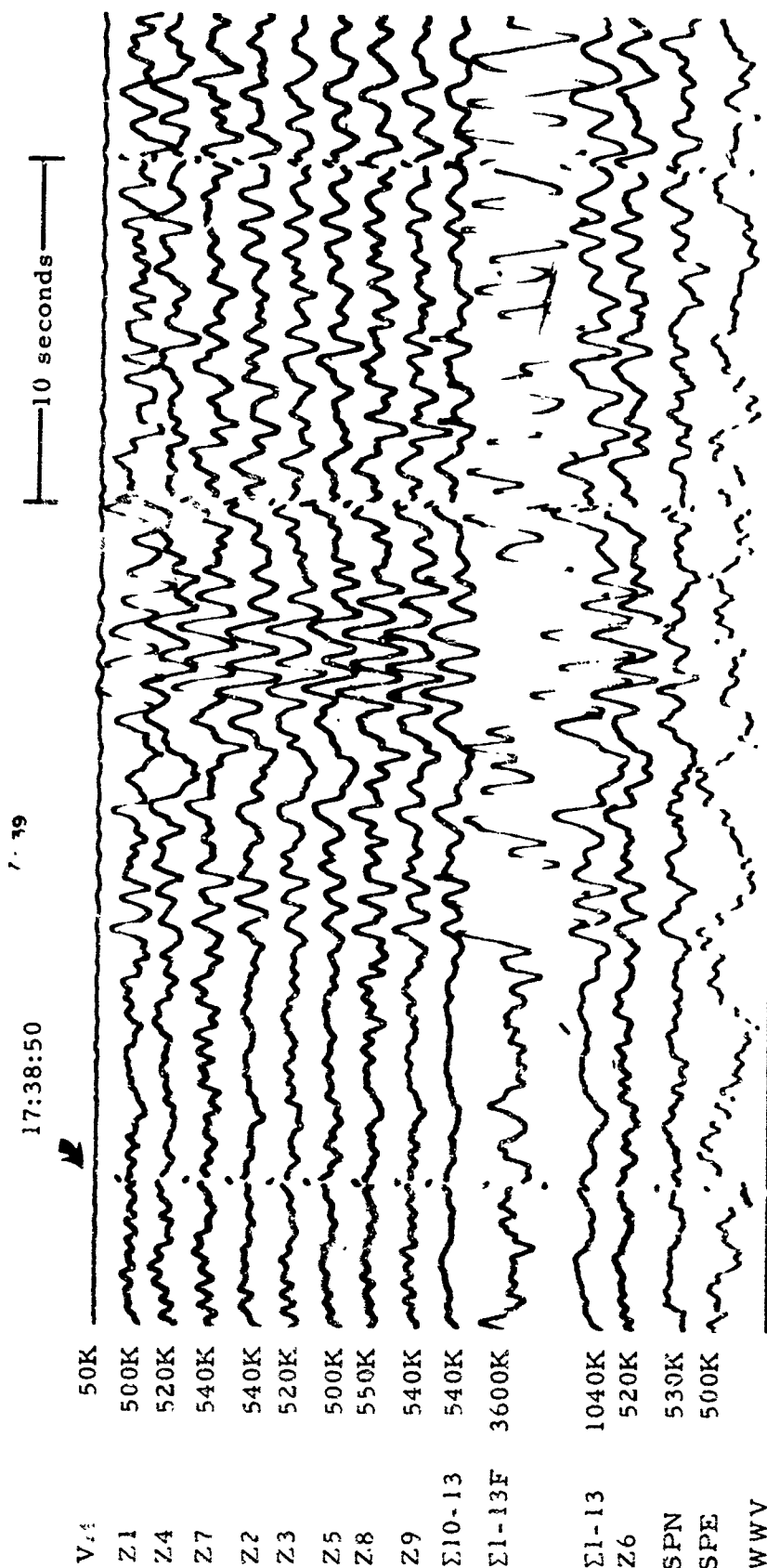


Figure 2-3. WMSO seismogram illustrating a P-phase arrival from Guerrero, Mexico.  
 Epicentral data:  $\Delta \approx 17^\circ$ ,  $h \approx 33$  km, azimuth  $\approx 181^\circ$ , magnitude  $\approx 4.1$   
 (X10 enlargement of 16-mm film)

WMSO  
 Run 034  
 3 Feb 1964  
 Data Group 3003



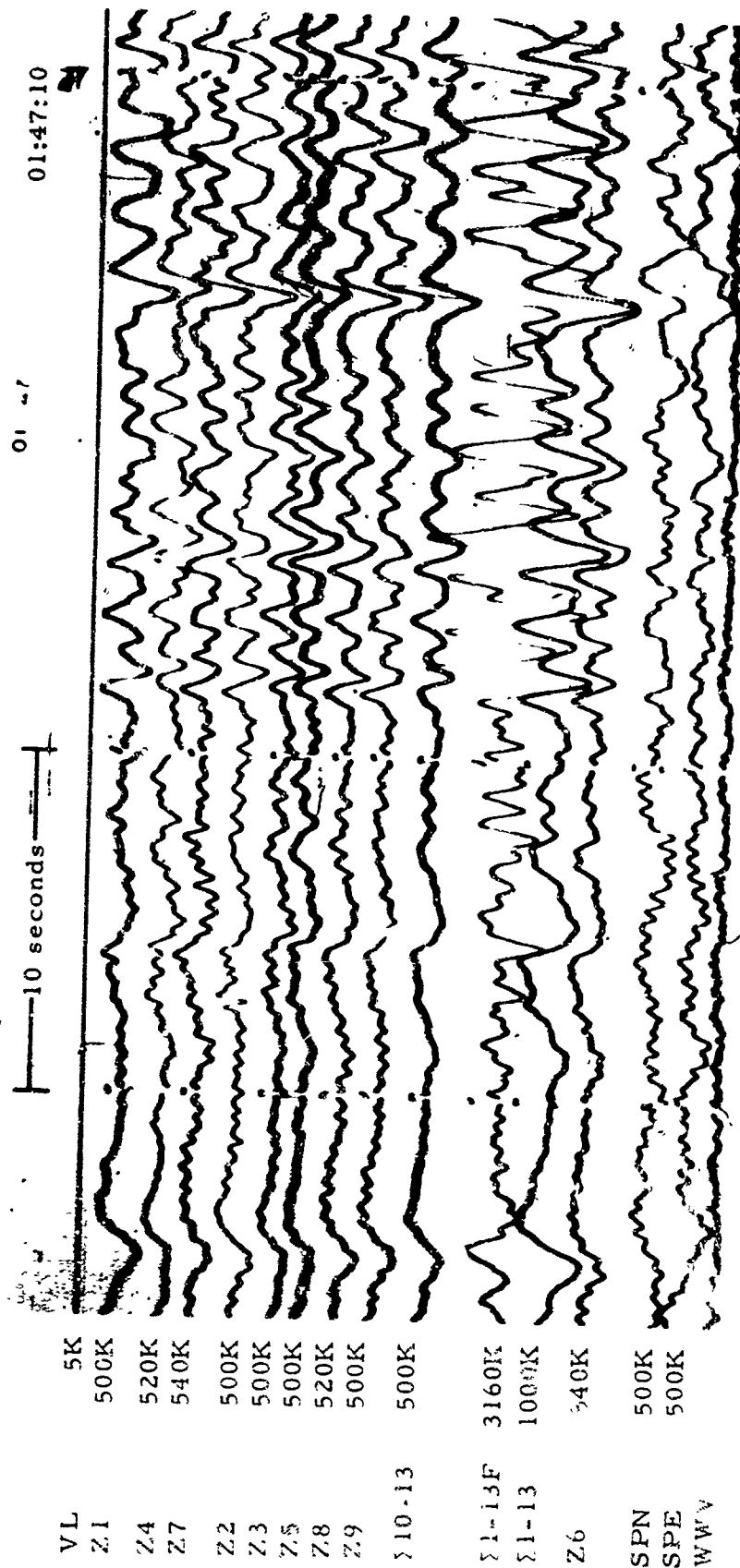


Figure 3-4. WMSO seismogram illustrating a P-phase arrival from the Revilla Gigedo Island region. Epicentral data:  $\Delta \approx 18^\circ$ ,  $h \approx 33$  km, azimuth  $\approx 208^\circ$ , magnitude  $\approx 3.8$  (X10 enlargement of 16-mm film)

WMSO  
Run 023  
23 Jan 1964  
Data Group 311

TR 64-50

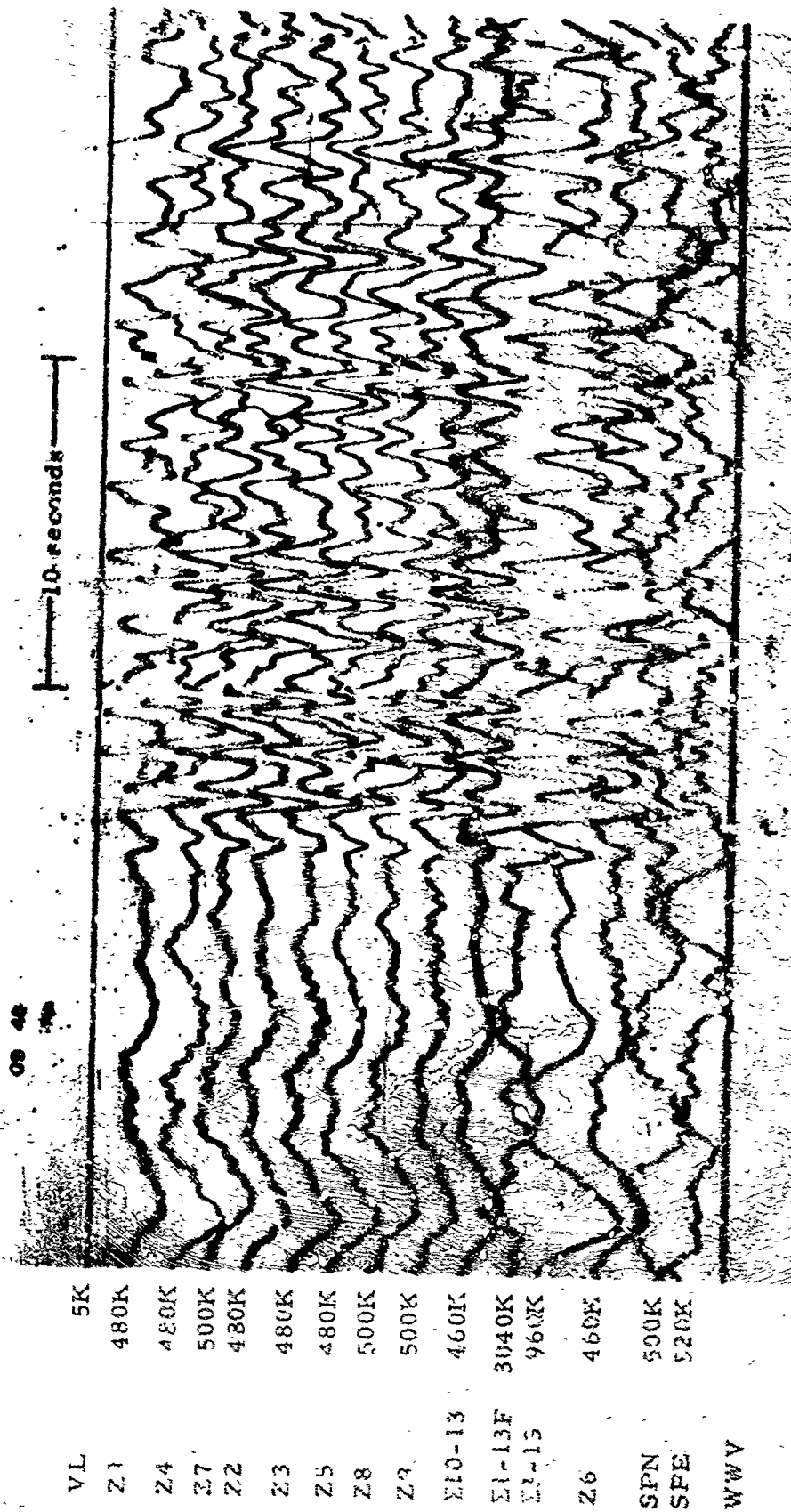


Figure 3-5. WMSO short-period seismogram illustrating a P-phase arrival.  
 Epicenter: Jalisco, Mexico,  $\Delta \approx 18^\circ$ ,  $h \approx 33$  km, azimuth  $\approx 204^\circ$ ,  
 magnitude  $\approx 4.4$  (X10 enlargement of 16-mm film)

WMSO  
 Run 001  
 1 Jan 1964  
 Data Group 311

TR 64-50

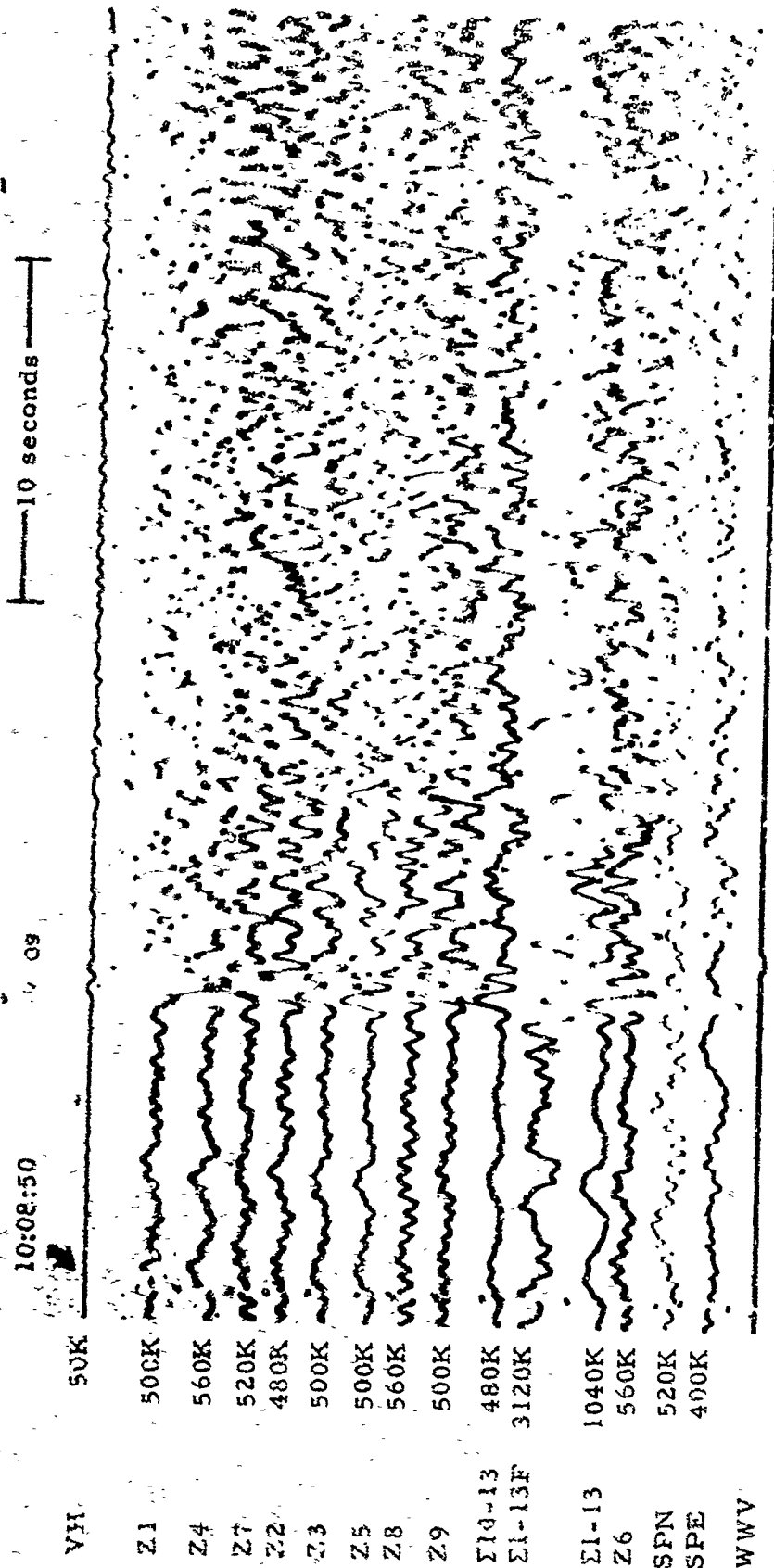


Figure 3-6. WMSO short-period seismogram illustrating a P-phase arrival from the Ontario-Quebec border. Epicentral data:  $\Delta \approx 20^\circ$ ,  $h \approx 33$  km, azimuth  $\approx 48^\circ$ , magnitude  $\approx 3.8$  (X10 enlargement of 16-mm film)

WMSO

Run 008

8 Jan 1964

Data Group 311

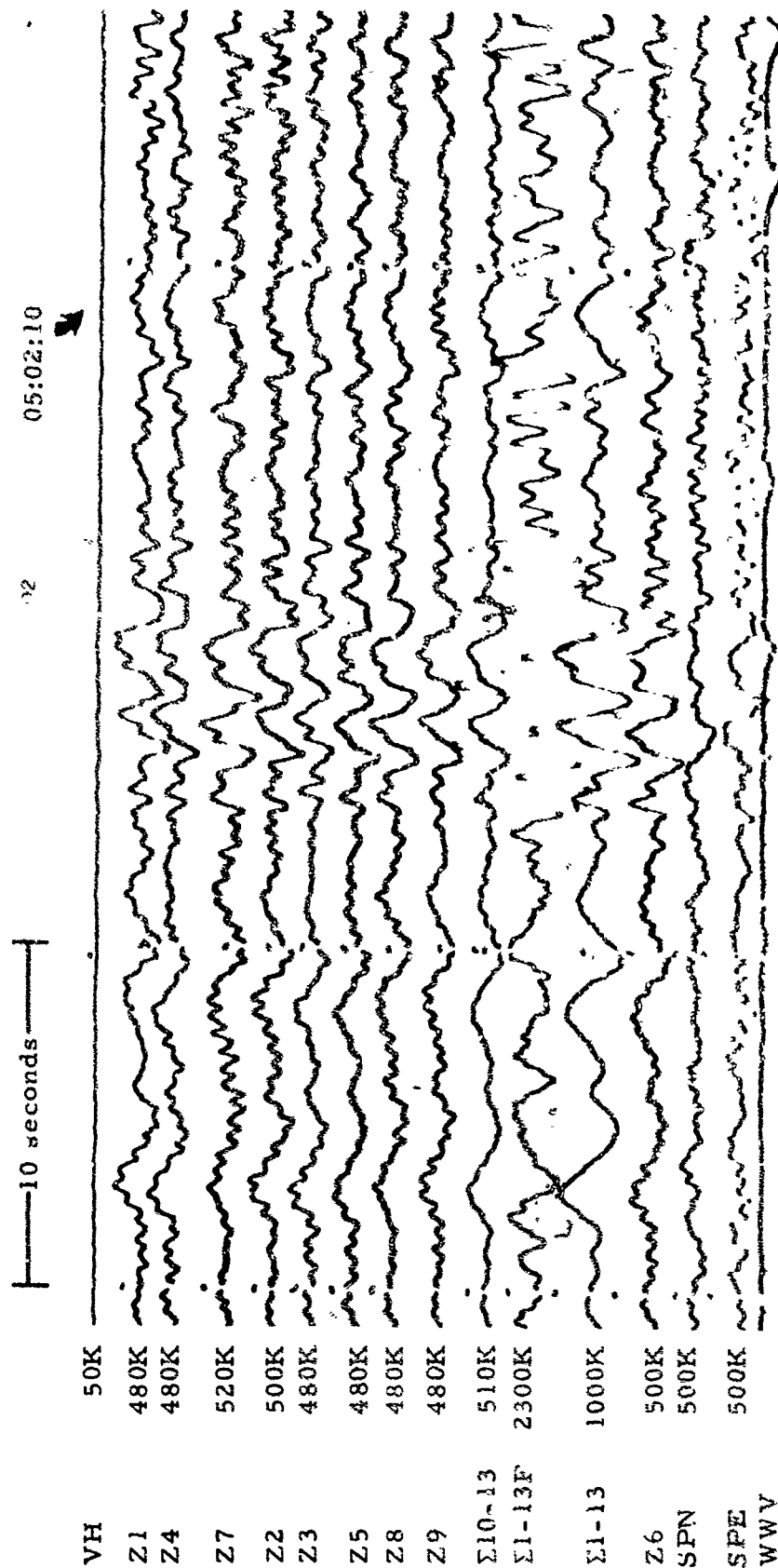


Figure 3-7. WMSO seismogram illustrating a P-phase arrival from off the coast of Oregon. Epicentral data:  $\Delta \approx 230^\circ$ ,  $h \approx 17$  km, azimuth  $\approx 309^\circ$ , magnitude  $\approx 4.5$   
(X10 enlargement of 16-mm film)

WMSO  
Run 028  
28 Jan 1964  
Data Group 311

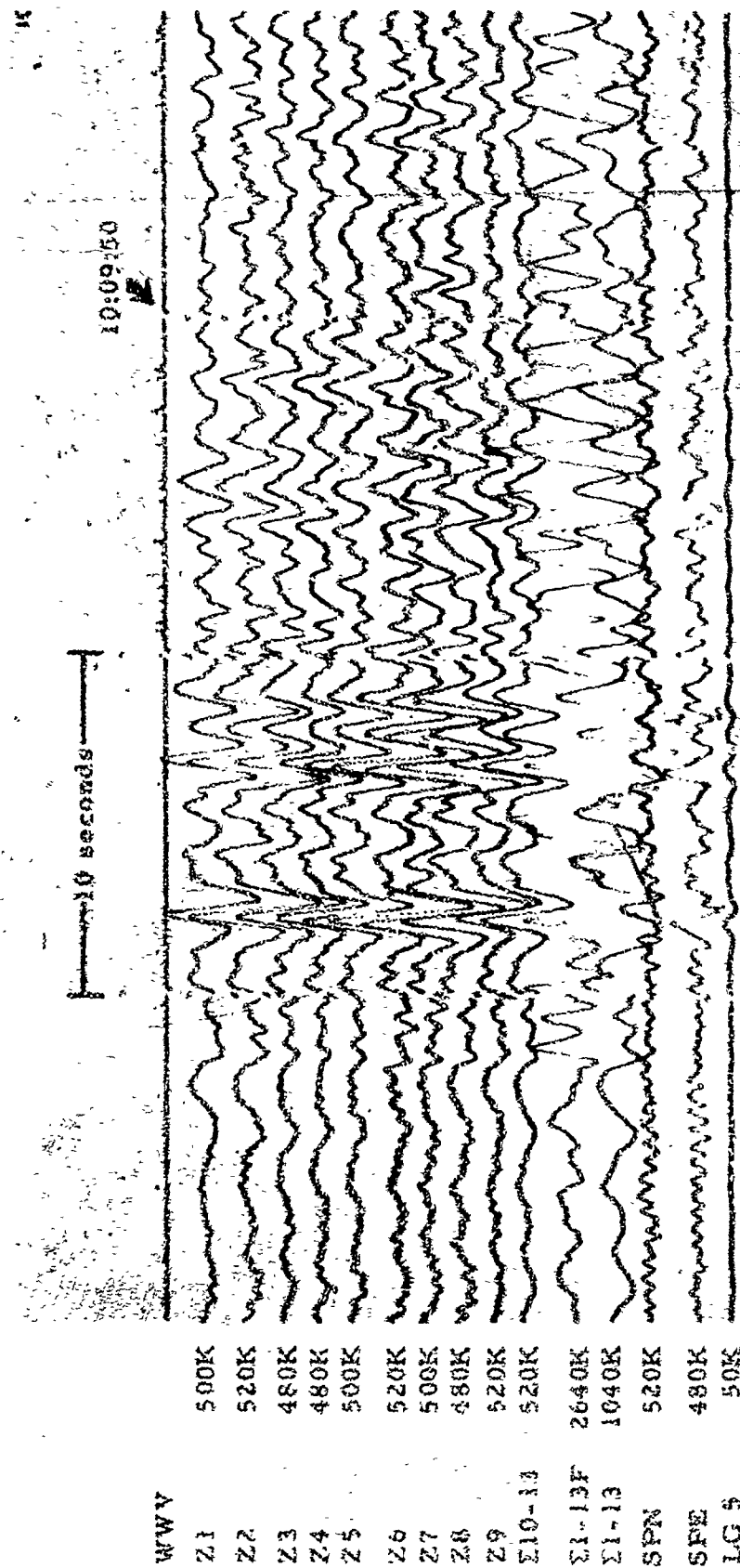


Figure 3-8. WMSO seismogram illustrating a P-phase arrival from off the coast of Oregon. Epicentral data:  $\Delta \approx 26^\circ$ ,  $h \approx 33$  km, azimuth  $\approx 302^\circ$ , magnitude  $\approx 3.7$   
(X10 enlargement of 16-mm film)

WMSO  
Run 271  
28 Sep 1963

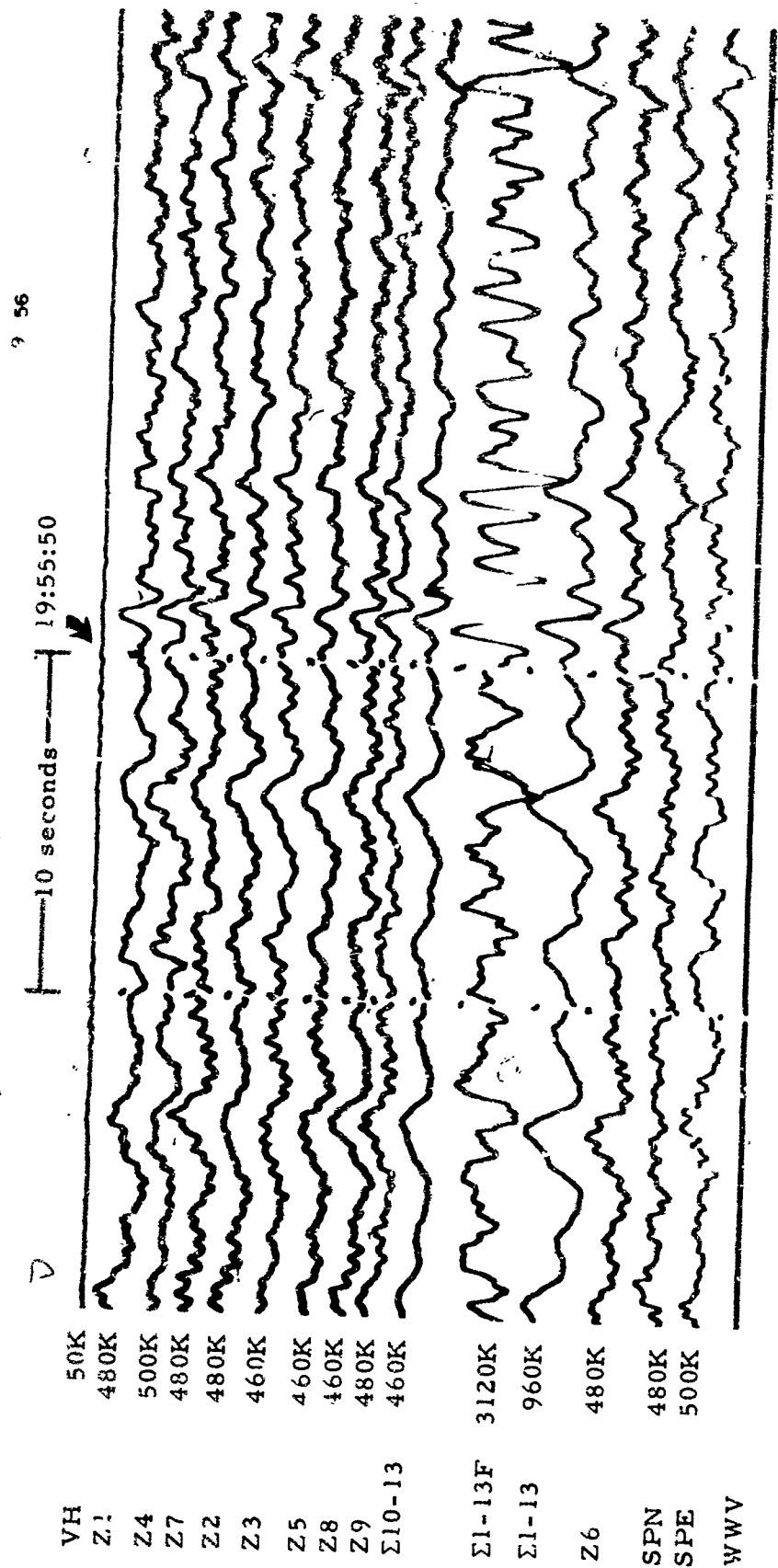


Figure 3-9. WMSO short-period seismogram illustrating a P-phase arrival.  
 Epicenter: near the north coast of Venezuela,  $\Delta \approx 36^\circ$ ,  $h \approx 41$  km,  
 azimuth  $\approx 126^\circ$ , magnitude  $\approx 4.5$  (X10 enlargement of  
 16-mm film)

WMSO  
 Run 025  
 25 Jan 1964  
 Data Group 311

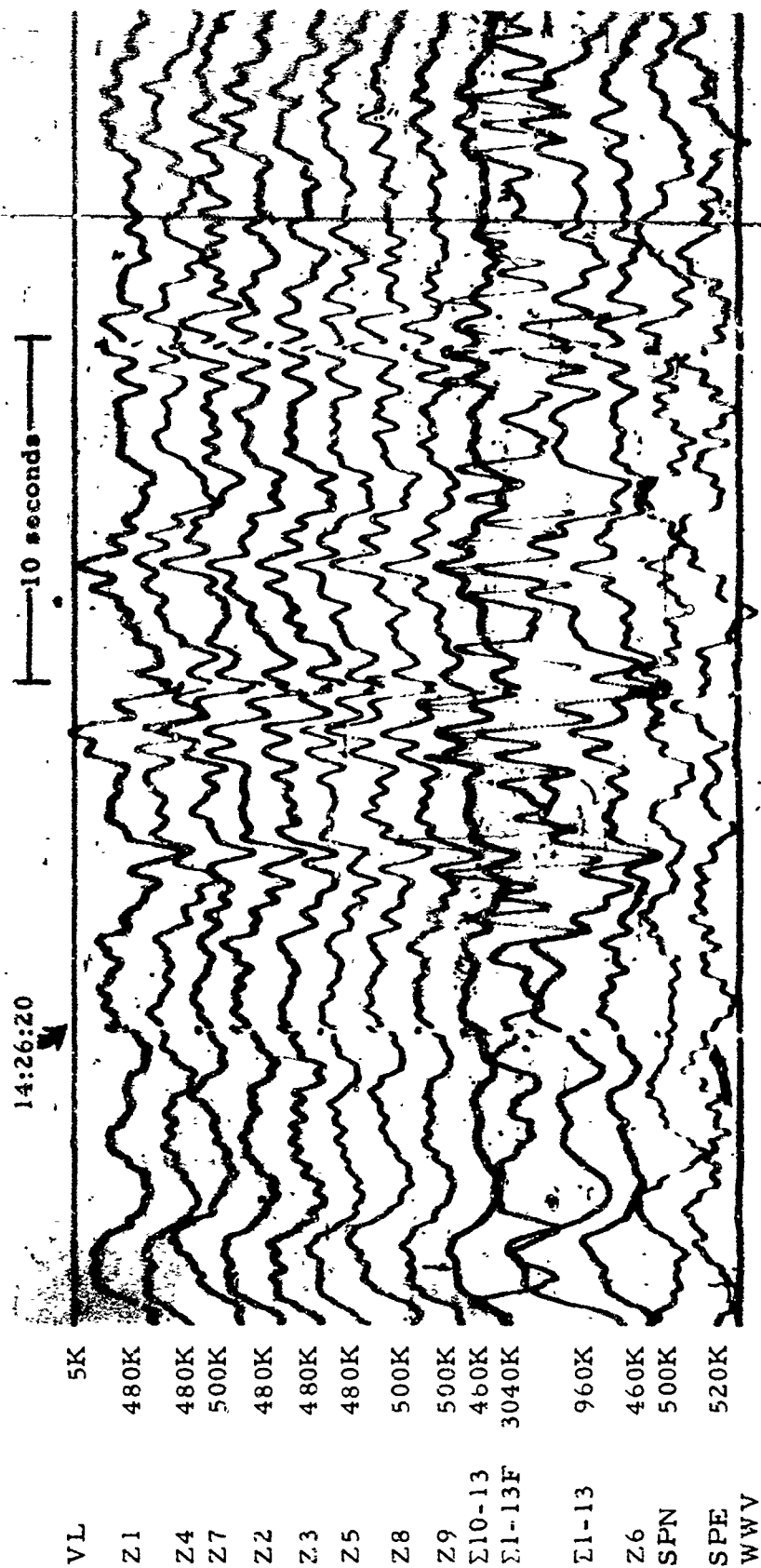


Figure 3-10. WMSO seismogram illustrating a P-phase arrival from the Galapagos Islands. Epicentral data:  $\Delta \approx 39^\circ$ ,  $h \approx 33$  km, azimuth  $\approx 192^\circ$ , magnitude  $\approx 4.6$  (X10 enlargement of 16-mm film)

WMSO  
Run 001  
1 Jan 1964  
Data Group 311

TR 64-50

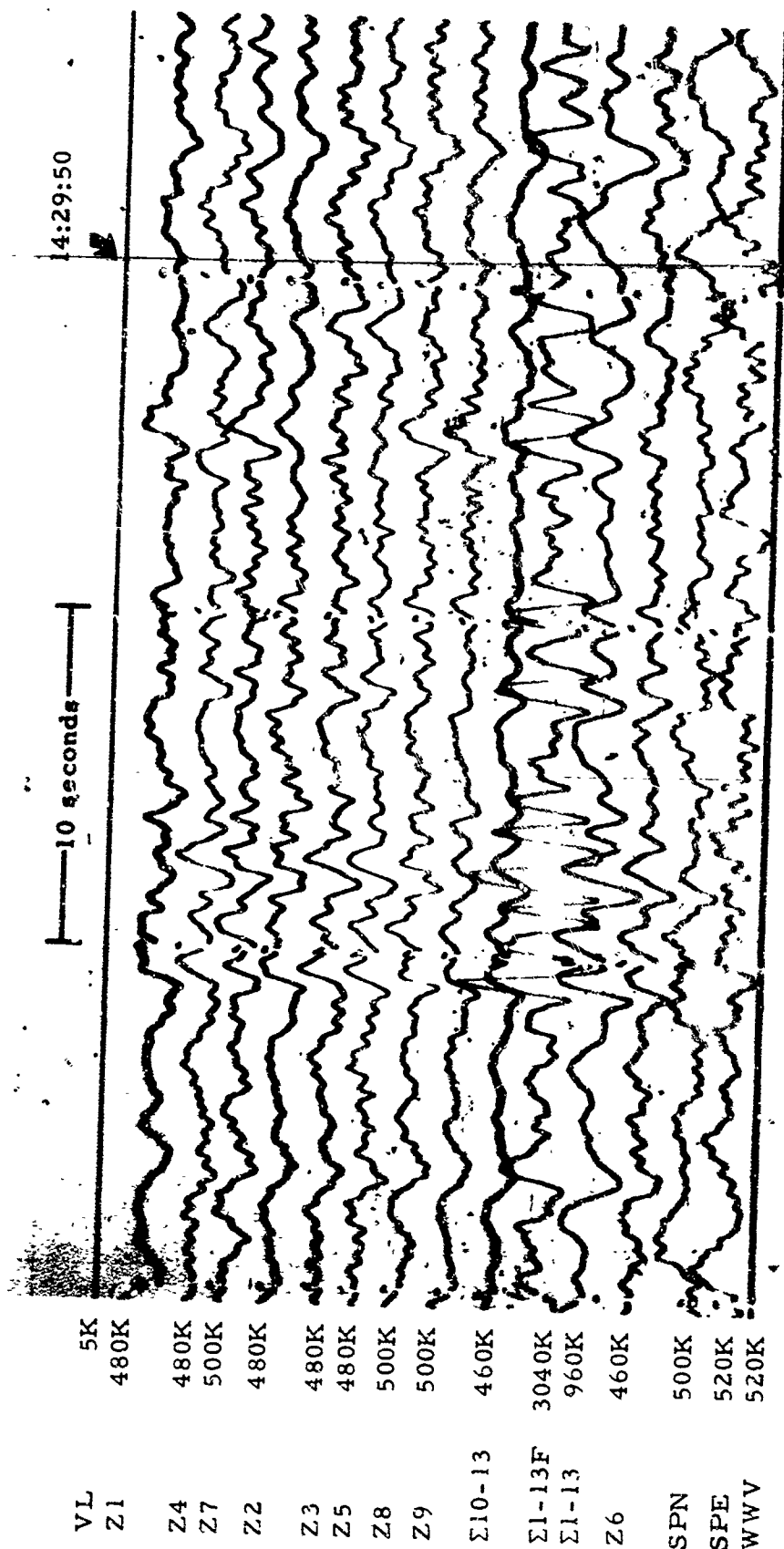


Figure 3-11. WMSO seismogram illustrating a P-phase arrival. Epicenter: near the coast of Southern Chile,  $\Delta \approx 39^\circ$ ,  $h \approx 33$  km, azimuth  $\approx 162^\circ$ , magnitude  $\approx 4.7$  (X10 enlargement of 16-mm film)

WMSO

Run 001

1 Jan 1964

Data Group 311



21 50

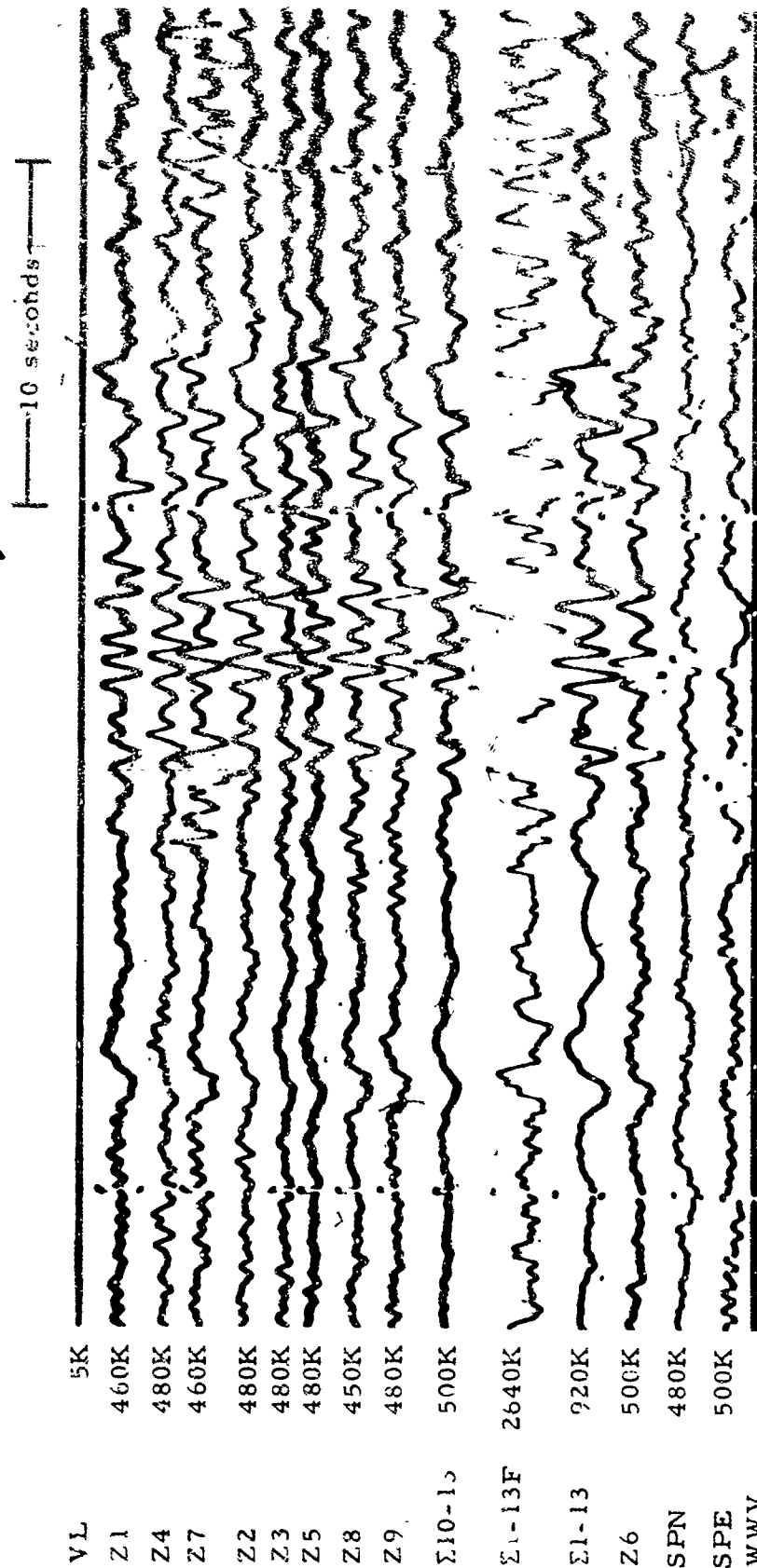


Figure 3-12. WMSO short-period seismogram illustrating a P-phase arrival from Ecuador. Epicentral data:  $\Delta \approx 40^\circ$ ,  $h \approx 33$  km, azimuth  $\approx 147^\circ$ , magnitude  $\approx 4.6$  (X10 enlargement of 16-mm film)

WMSO  
Run 031  
31 Jan 1964  
Data Group 311

3.3 DISTANCE =  $41^{\circ}$  to  $60^{\circ}$

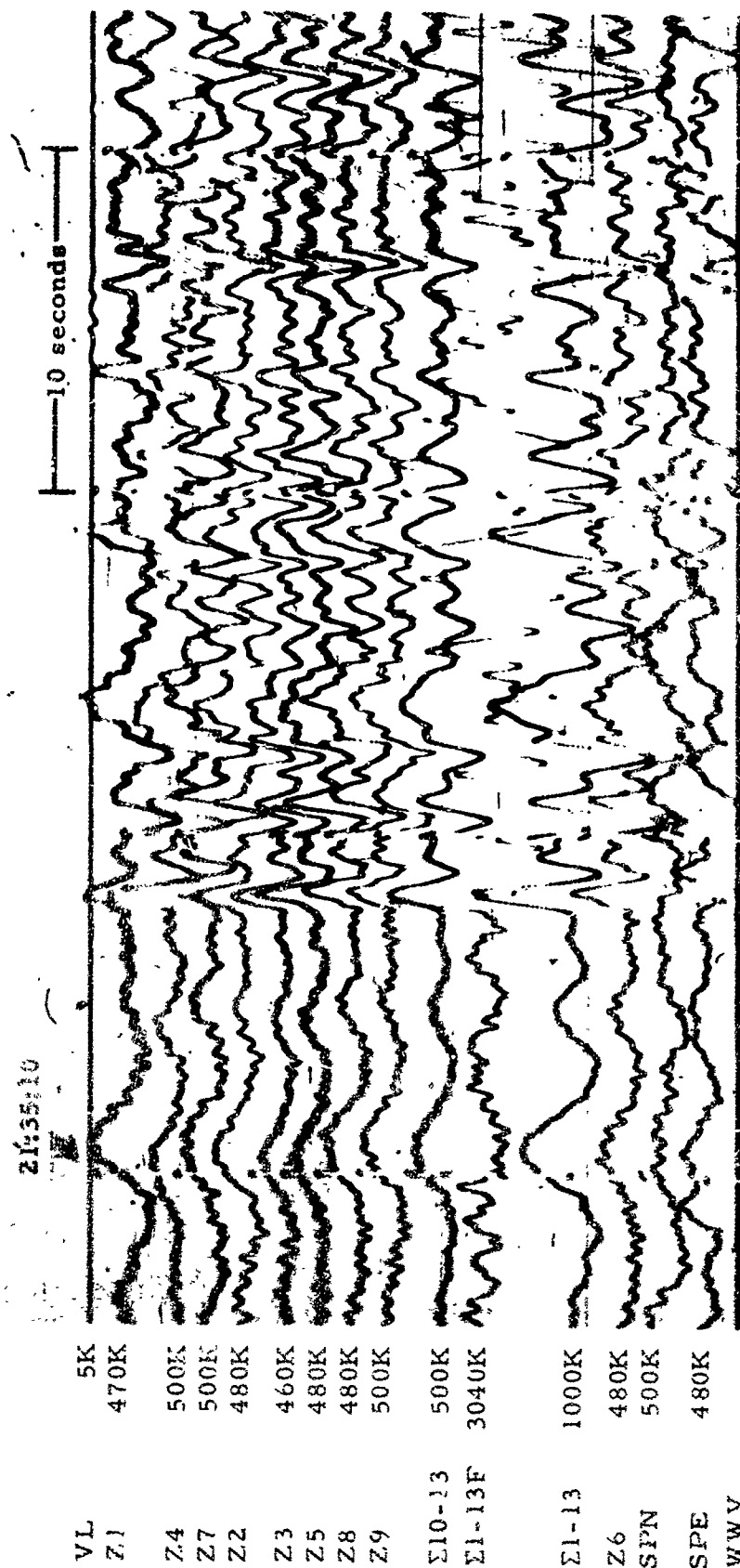


Figure 3-13. WMSO seismogram illustrating a P-phase arrival from the North Atlantic Ocean. Epicentral data:  $\Delta \approx 48^\circ$ ,  $h \approx 33$  km, azimuth  $\approx 88^\circ$ , magnitude  $\approx 4.7$  (X10 enlargement of 16-mm film)

WMSO  
Run 015  
15 Jan 1964  
Data Group 311

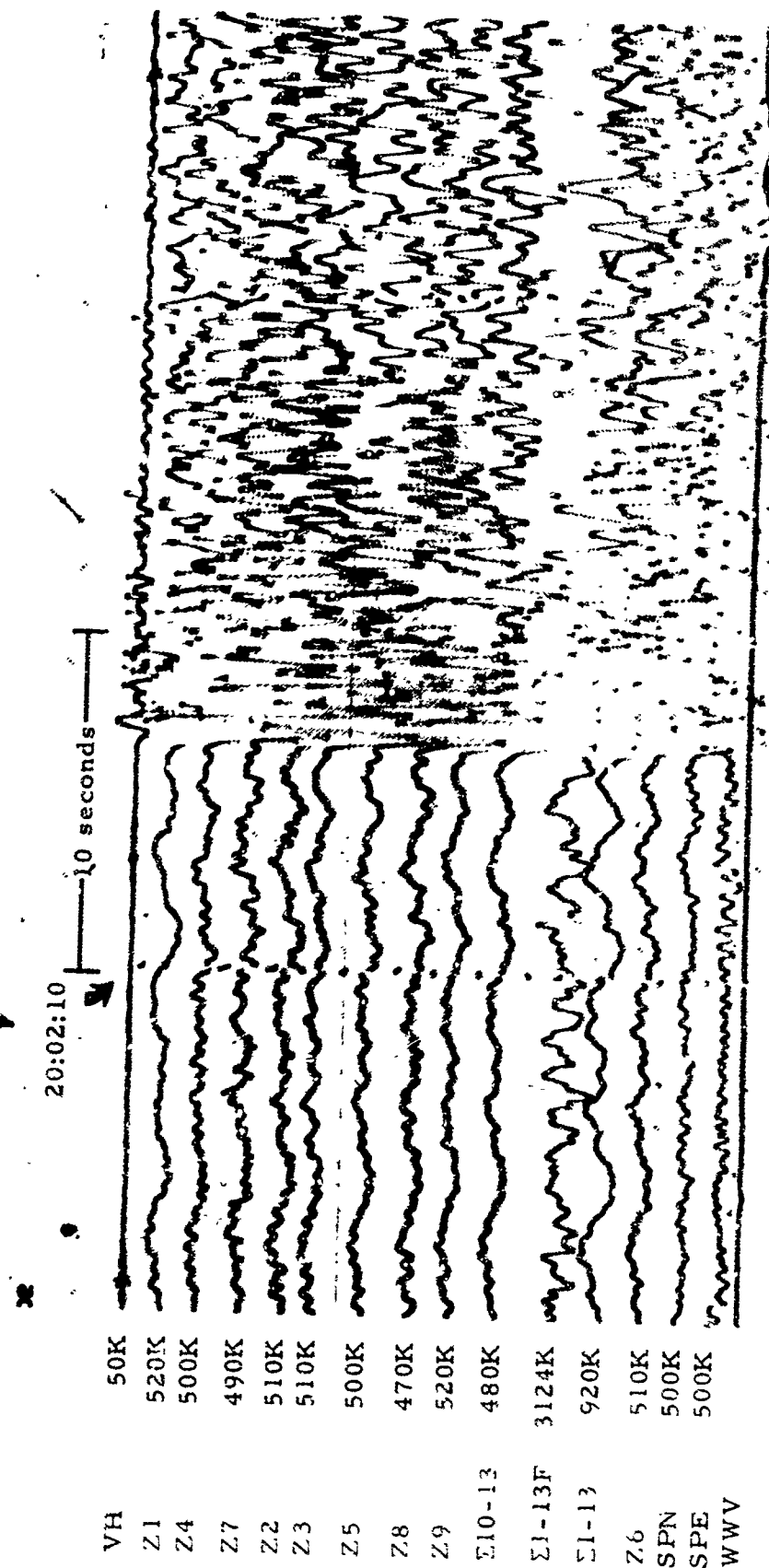


Figure 3-14. An event from Western Brazil as recorded at WMSO. Epicentral data:  
 $\Delta \approx 51^\circ$ ,  $h \approx 585$  km, azimuth  $\approx 144^\circ$ , magnitude  $\approx 4.9$   
 (X10 enlargement of 16-mm film)

WMSO  
 Run 315  
 1 Nov 1963  
 Data Group 302

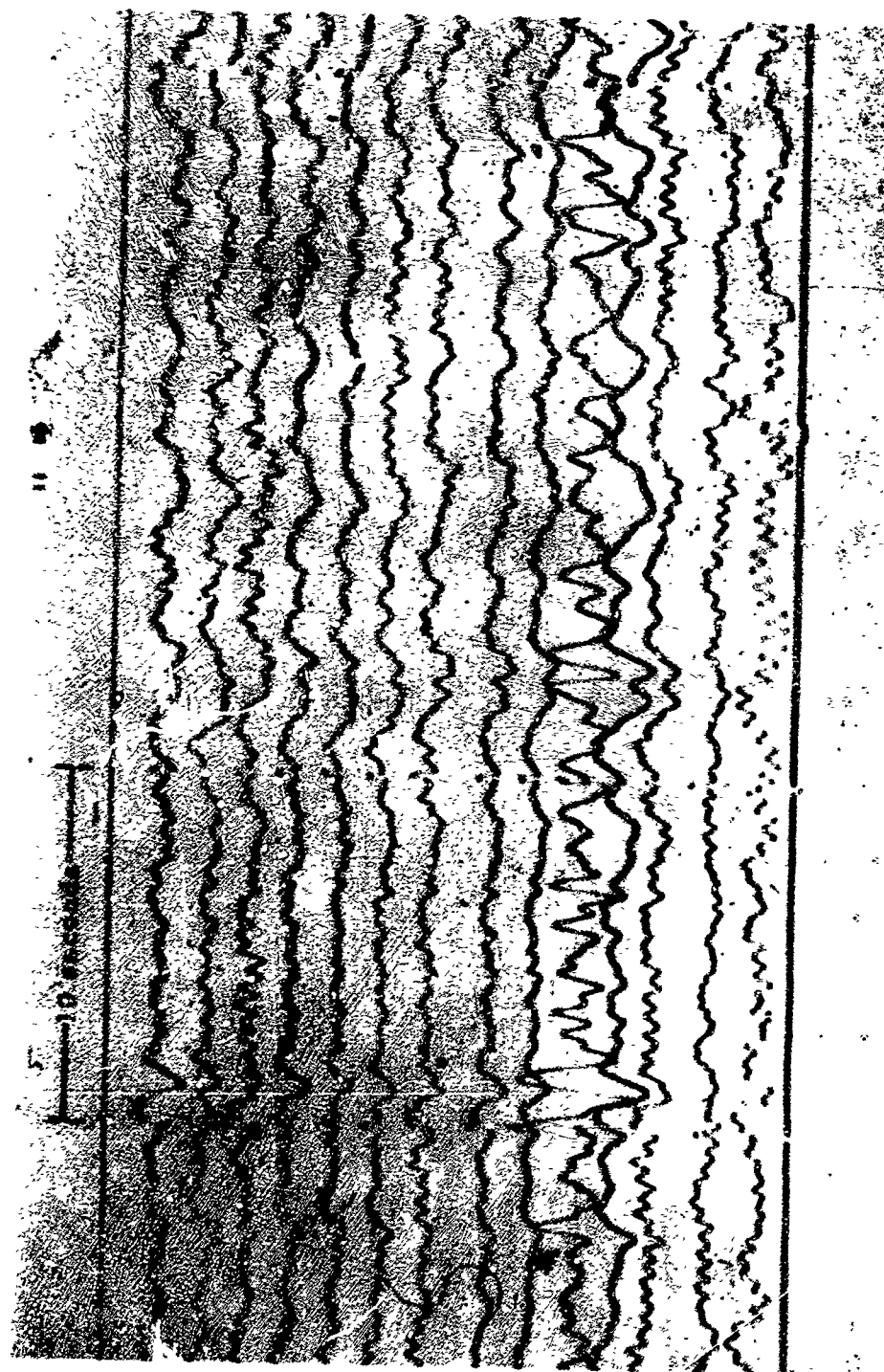


Figure 3-15. WMSO seismogram illustrating a P-phase arrival. Epicenter: south of Hawaii Island,  $\Delta \approx 53^\circ$ ,  $h \approx 33$  km, azimuth  $\approx 268^\circ$ , magnitude  $\approx 4.4$   
(X10 enlargement of 16-mm film)

WMSO

Run 007

7 Jan 1964

Data Group 311

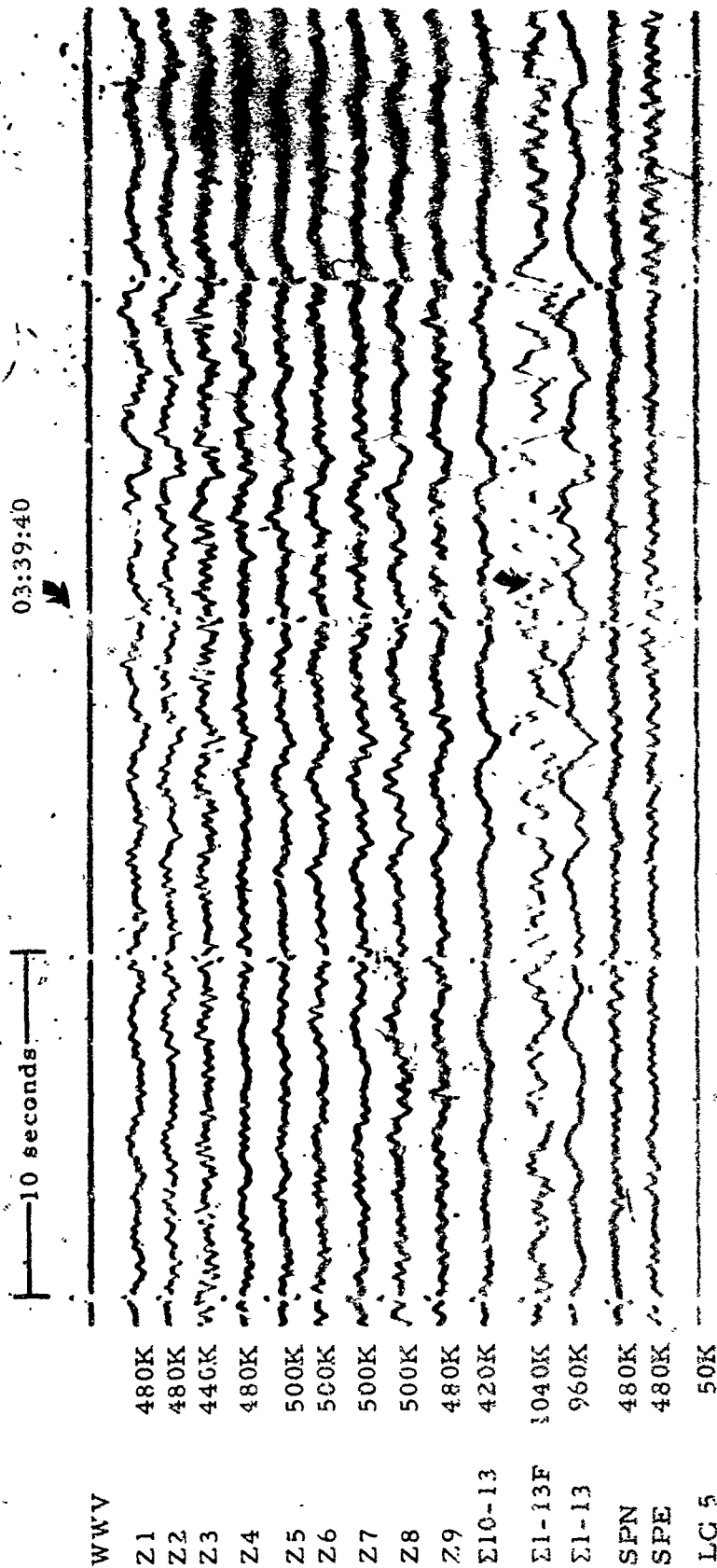


Figure 3-16. WMSO seismogram illustrating a P-phase arrival from the Andreanof Island region. Epicentral data:  $\Delta \approx 56^\circ$ ,  $h \approx 33$  km, azimuth  $\approx 213^\circ$ , magnitude  $\approx 4.1$  (X10 enlargement of 16-mm film)

WMSO  
Run 247  
4 Sep 1963

TR 64-50

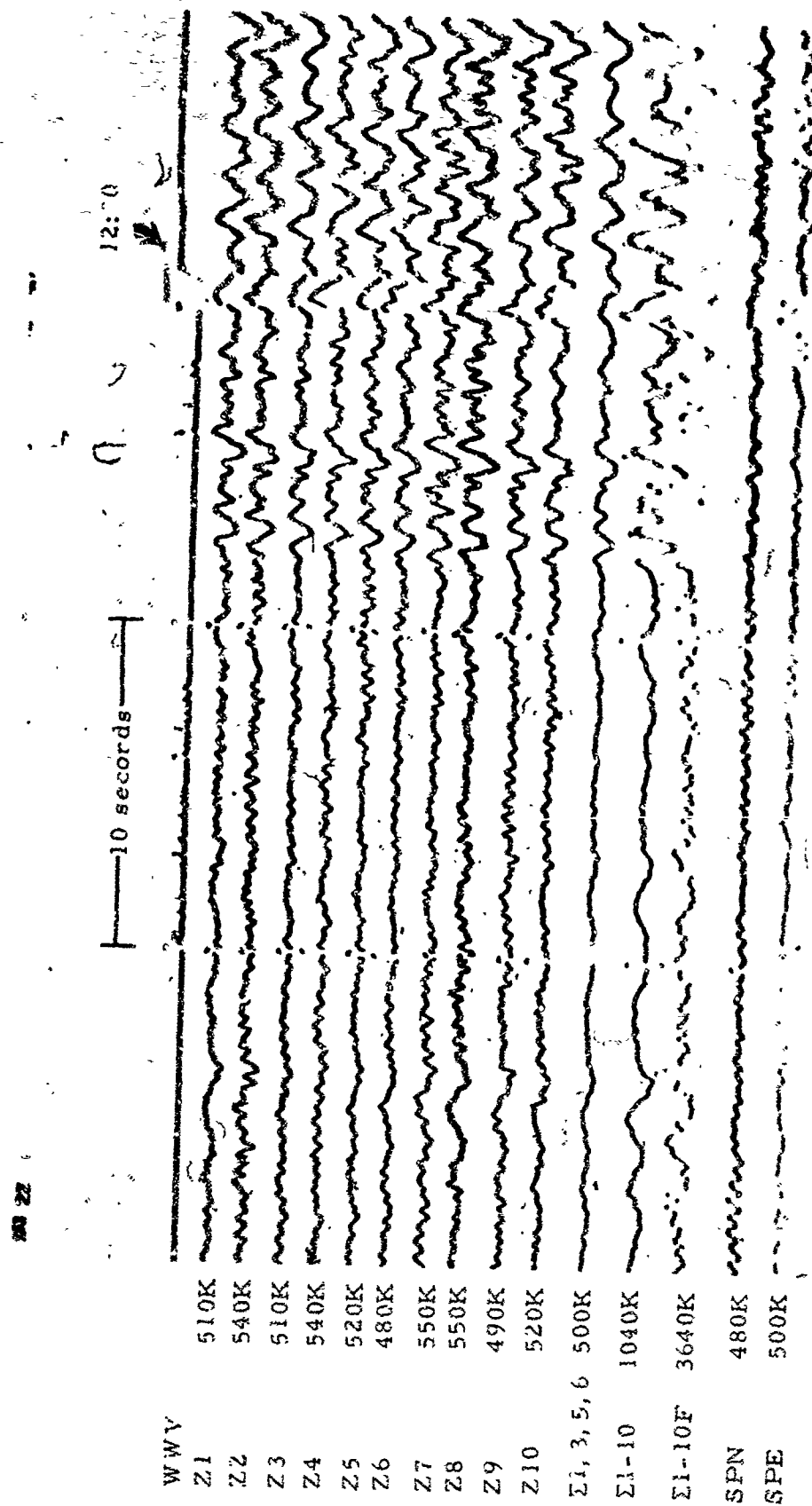


Figure 3-17. WMSO seismogram illustrating a P-phase arrival from the Andreanof Islands region. Epicentral data:  $\Delta \approx 58^\circ$ ,  $h \approx 33$  km, azimuth  $\approx 314^\circ$ , magnitude  $\approx 4.5$  (X10 enlargement of 16-mm film)

WMSO  
Run 221  
9 Aug 1963

10 seconds

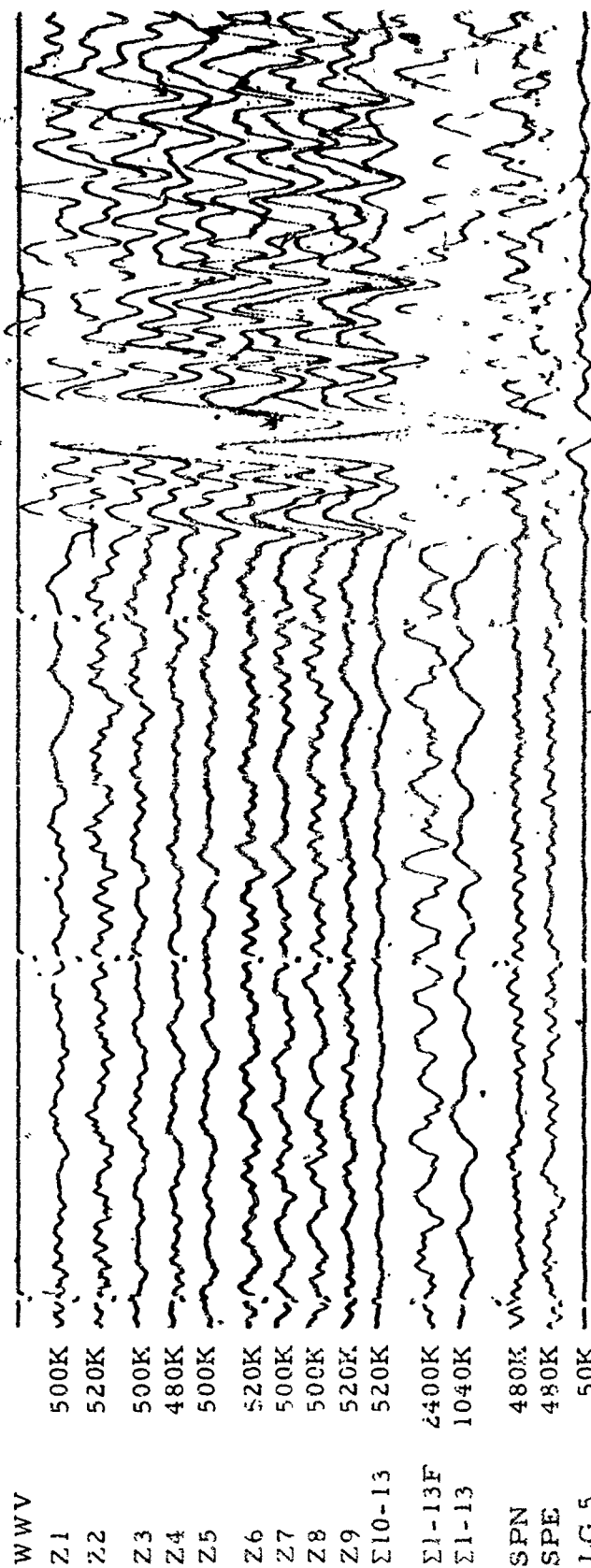


Figure 3-18. WMSO primary short-period seismogram illustrating a P-phase arrival from the Andean of Islands region. Epicentral data:  $\Delta \approx 57^\circ$ ,  $h \approx 33$  km, azimuth  $\approx 312^\circ$ , magnitude  $\approx 5.3$  (X10 enlargement of 16-mm film)

WMSO  
Run 269  
26 Sep 1963



3.4 DISTANCE =  $61^{\circ}$  to  $80^{\circ}$

15 36

10 seconds

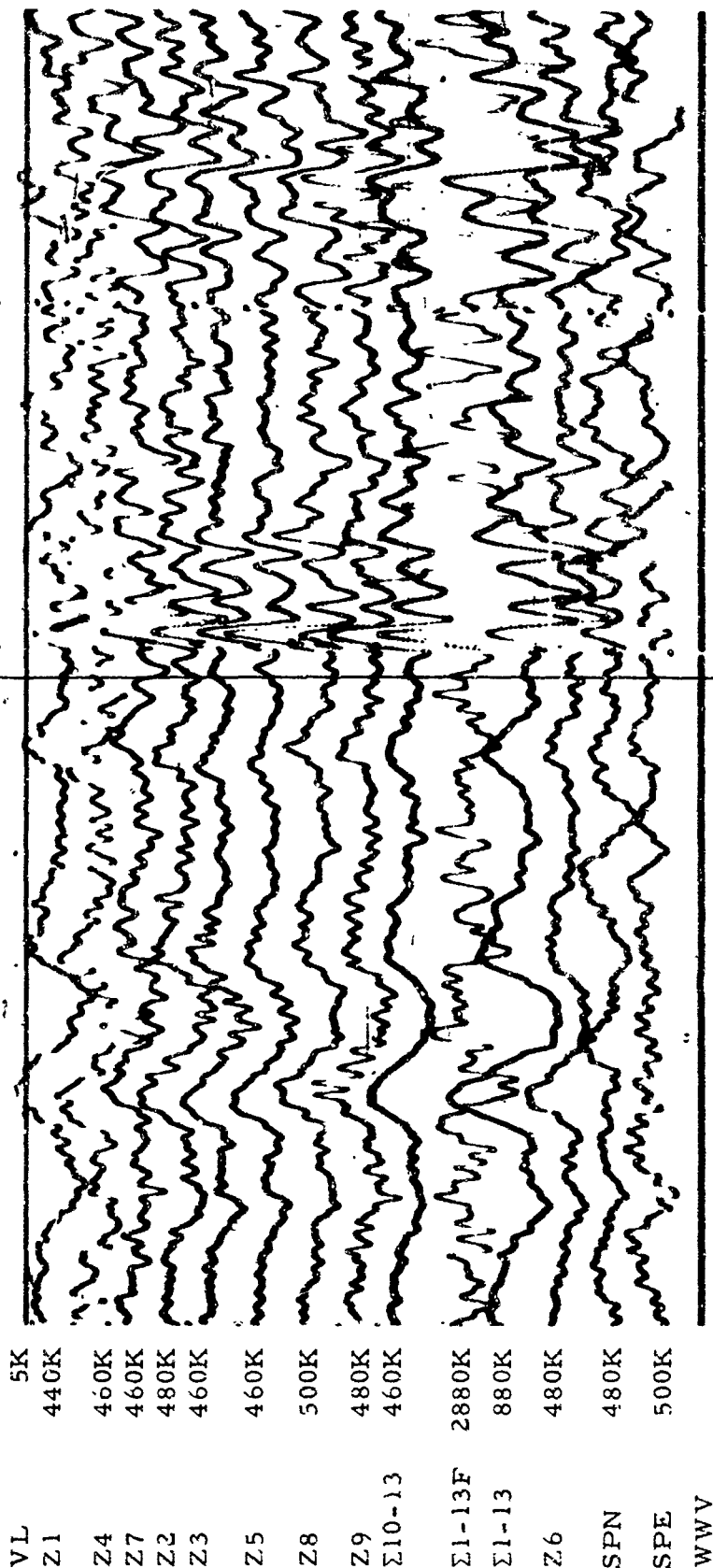


Figure 3-19. WMSO seismogram illustrating a P-phase arrival. Epicenter: near the coast of Northern Chile,  $\Delta \approx 62^\circ$ ,  $h \approx 80$  km, azimuth  $\approx 150^\circ$ , magnitude  $\approx 5.2$   
(X10 enlargement of 16-mm film)

WMSO  
Run 050  
19 Feb 1964  
Data Group 3003

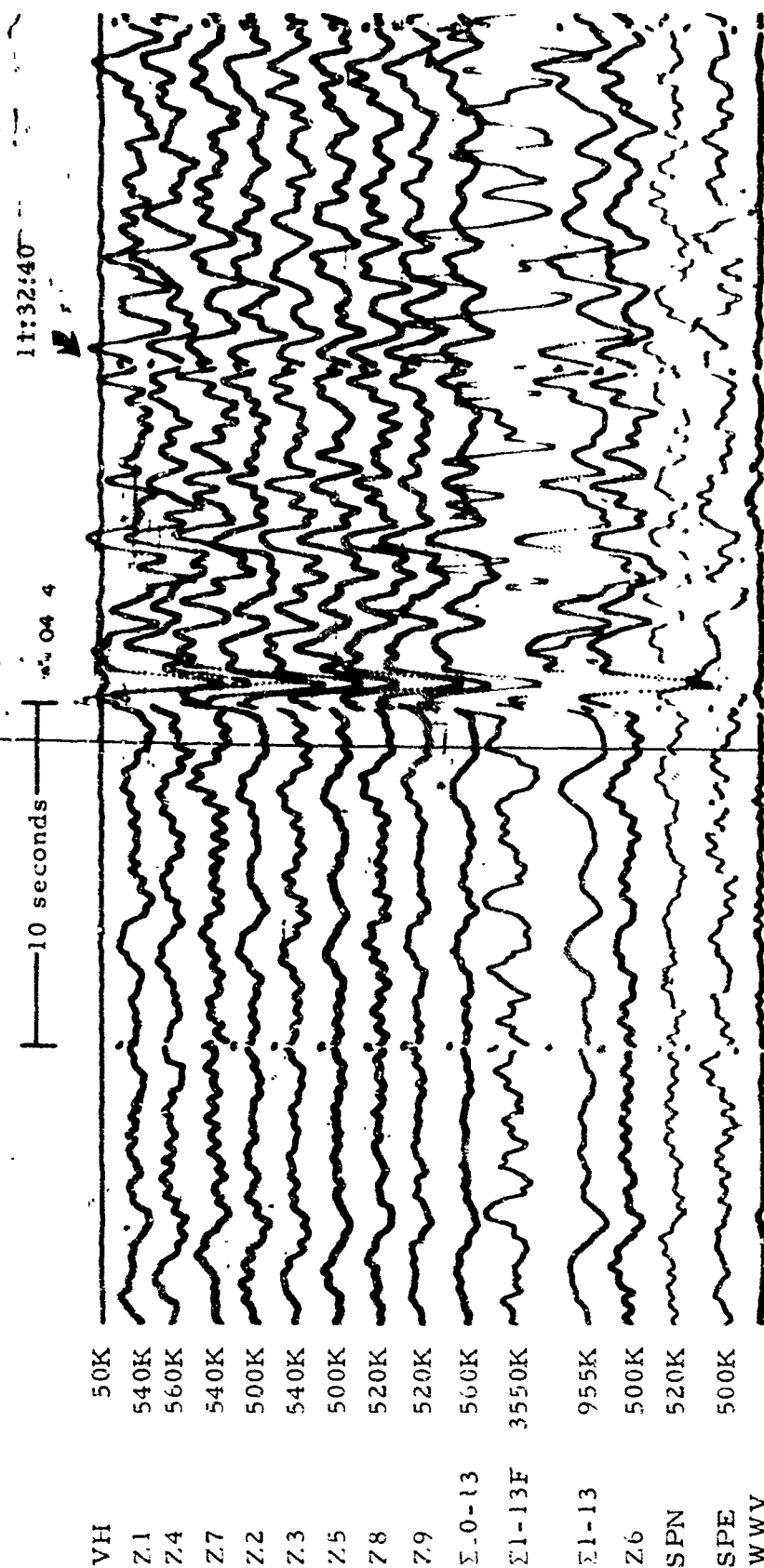


Figure 3-20. WMSO seismogram illustrating a P-wave arrival from the Bolivia-Brazil border. Epicentral data:  $\Delta \approx 66^\circ$ ,  $h \approx 32$  km, azimuth  $\approx 136^\circ$ , magnitude  $\approx 5.3$  (X10 enlargement of 16-mm film)

WMSO  
Run 044  
13 Feb 1964  
Data Group 3003

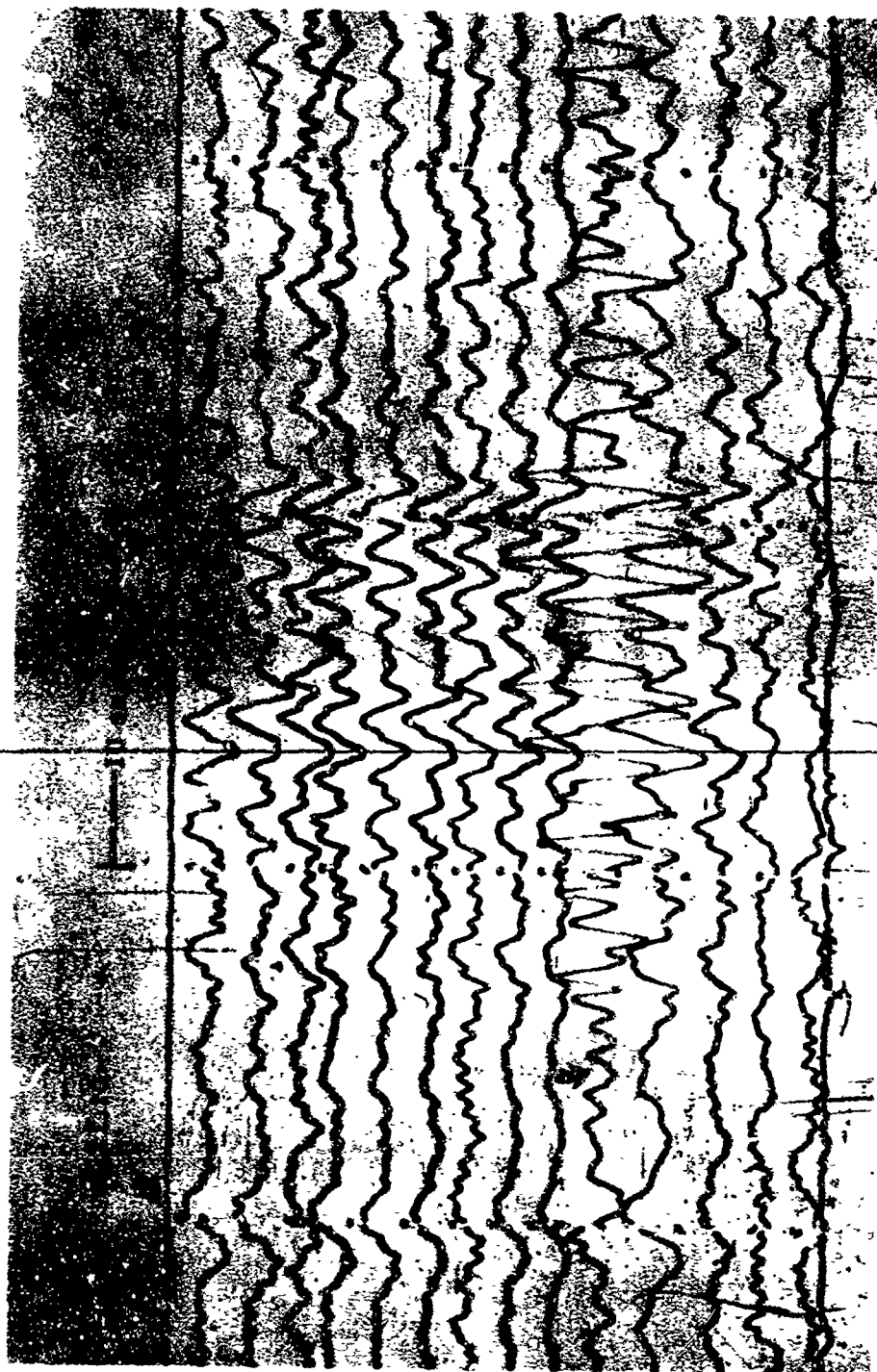


Figure 3-21. WMSO seismogram illustrating a P-phase arrival from the Easter Island region. Epicentral data:  $\Delta \approx 67^\circ$ ,  $h \approx 33$  km, azimuth  $\approx 186^\circ$ , magnitude  $\approx 4.5$   
(X10 enlargement of 16-mm film)

VH	50K
Z1	480K
Z4	540K
Z7	540K
Z2	480K
Z3	500K
Z5	500K
Z8	500K
Z9	500K
$\Sigma 10-13$	500K
$\Sigma 1-13F$	2880K
$\Sigma 1-13$	1000K
Z6	480K
SPN	500K
SPE	500K
WWV	

WMSO  
Run 018  
18 Jan 1964  
Data Group 311

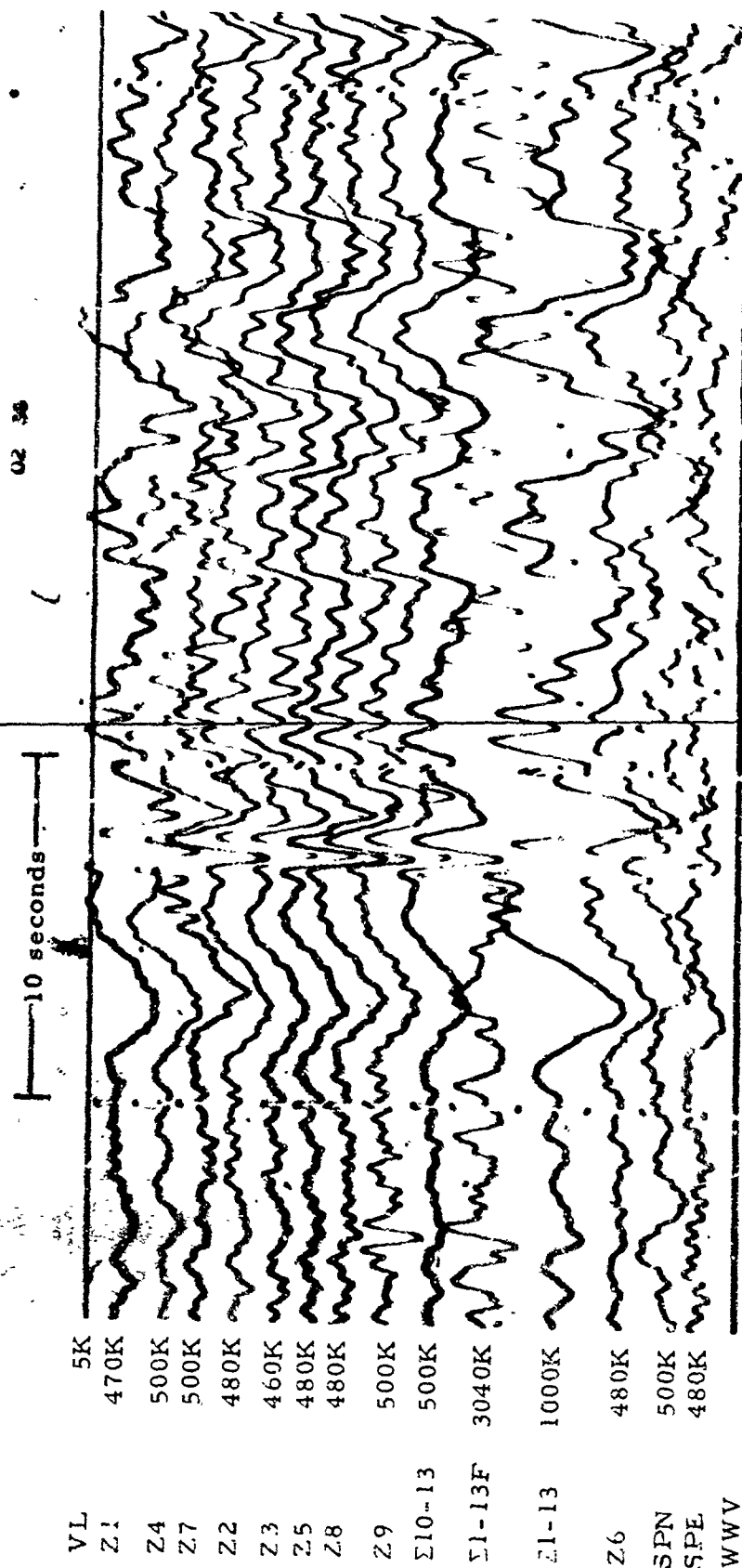


Figure 3-22. WMSO seismogram illustrating a P-phase arrival from the Kurile Islands.  
Epicentral data:  $\Delta \approx 79^\circ$ ,  $h \approx 45$  km, azimuth  $\approx 318^\circ$ , magnitude  $\approx 5.3$   
(X10 enlargement of 16-mm film)

WMSO  
Run 015  
'5 Jan 1964  
Data Group 311

3.5 DISTANCE =  $81^{\circ}$  to  $100^{\circ}$

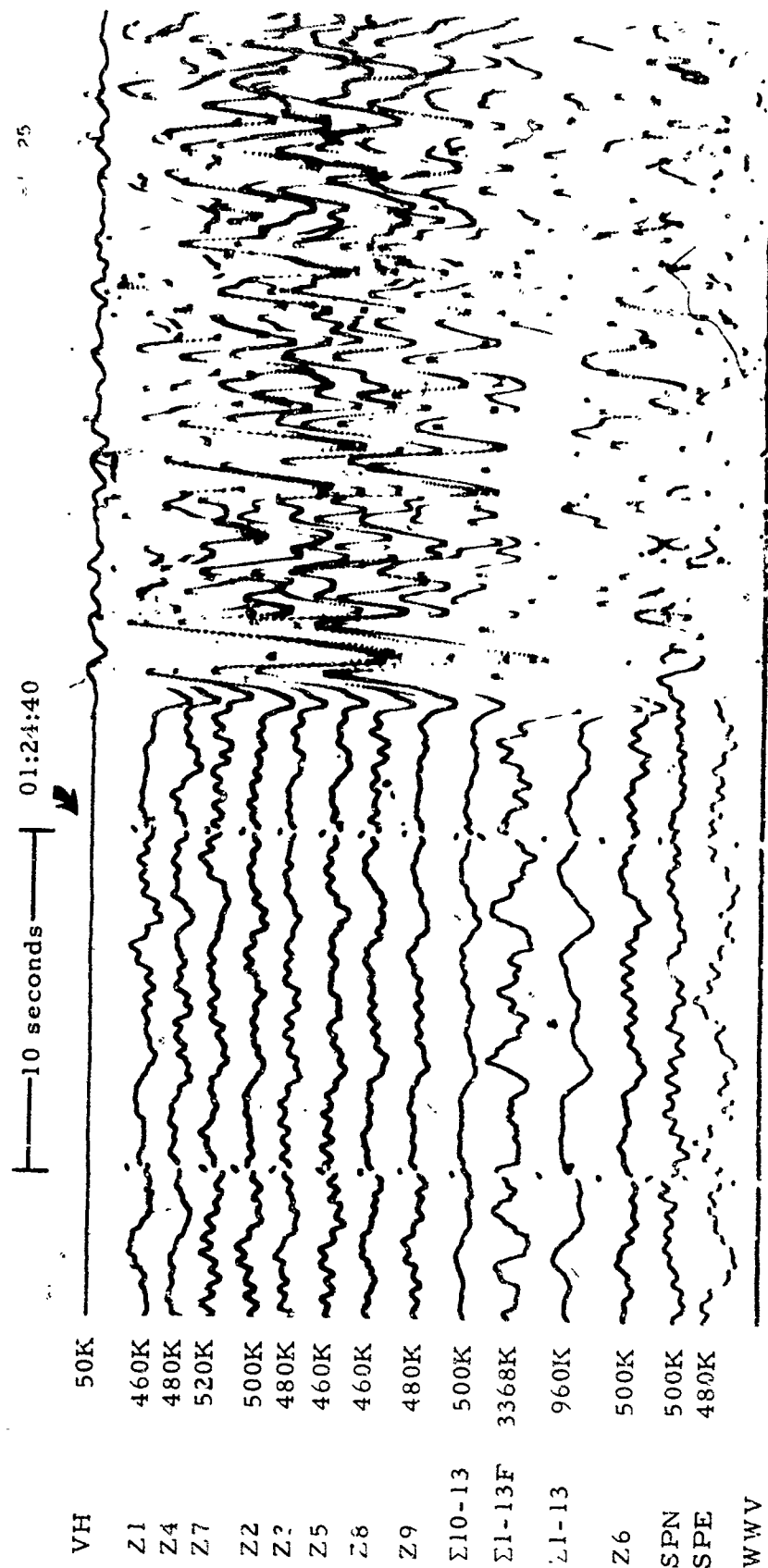


Figure 3-23. WMSO seismogram illustrating a P-phase arrival from the mid-Atlantic Ocean. Epicentral data:  $\Delta \approx 82^\circ$ ,  $h \approx 33$  km, azimuth  $\approx 95^\circ$ , magnitude  $\approx 5.3$   
(X10 enlargement of 16-mm film)

WMSO  
Run 027  
27 Jan 1964  
Data Group 311

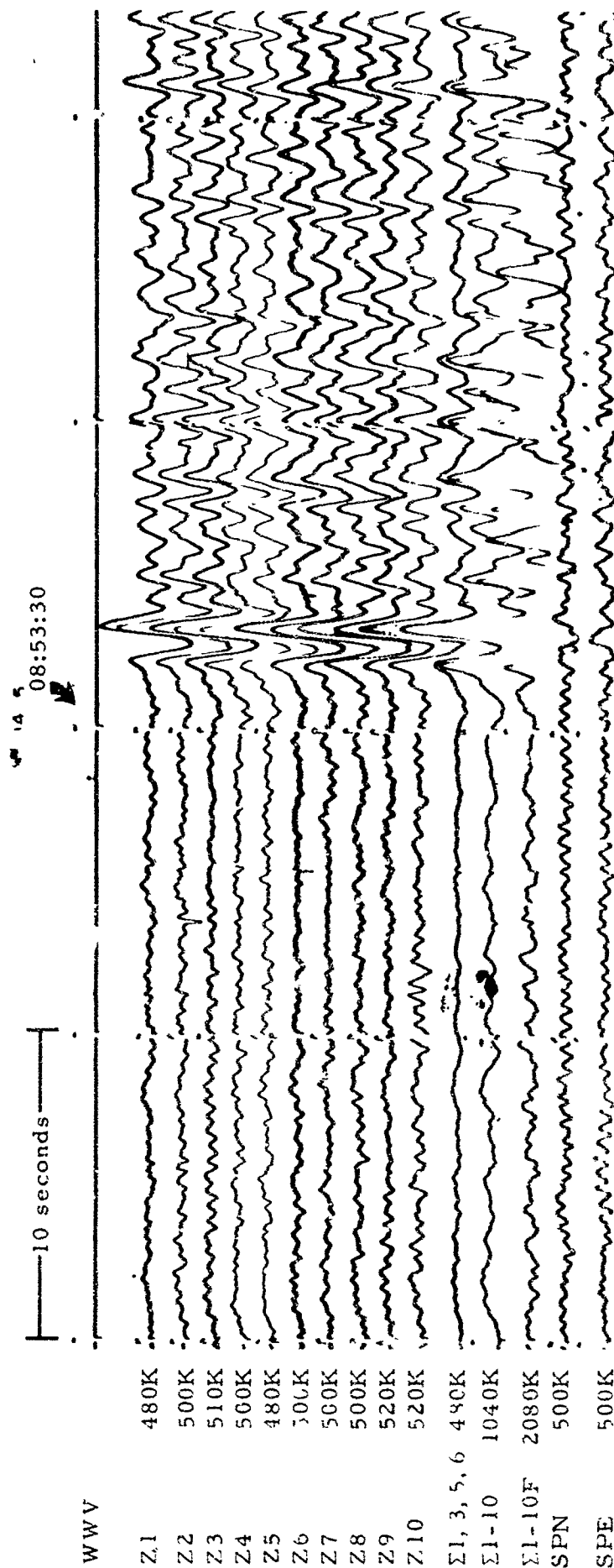


Figure 3-24. WMSO seismogram illustrating a P-phase arrival. Epicenter: near the east coast of Hokkaido,  $\Delta \approx 84^\circ$ ,  $h \approx 80$  km, azimuth  $\approx 319^\circ$ , magnitude  $\approx 5.4$   
(X10 enlargement of 16-mm film)

WMSO  
Run 145  
25 May 1963



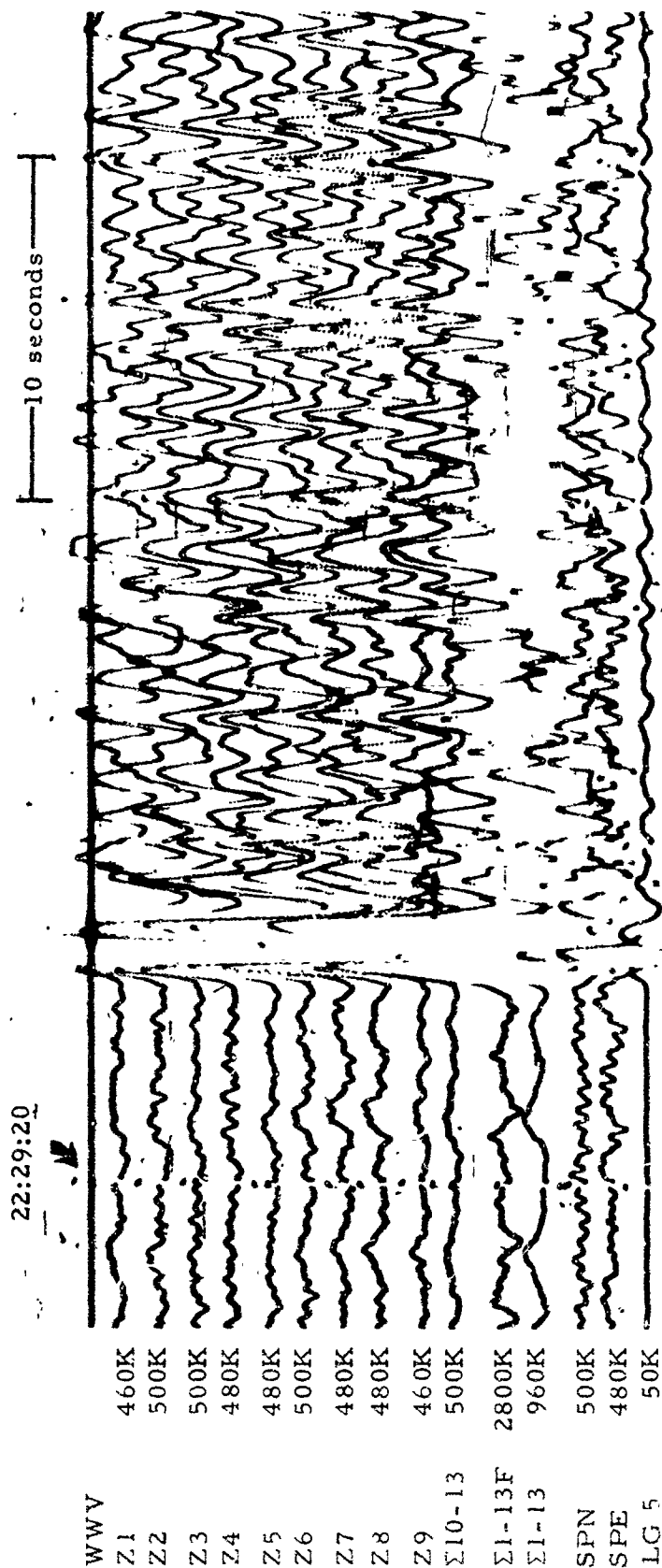


Figure 3-25. WMSO short-period seismogram illustrating a P-phase arrival from the Ionian Sea. Epicentral data:  $\Delta \approx 88^\circ$ ,  $h \approx 47$  km, azimuth  $\approx 46^\circ$ , magnitude  $\approx 5.3$  (X10 enlargement of 16-mm film)

WMSO  
Run 274  
29 Sep 1963

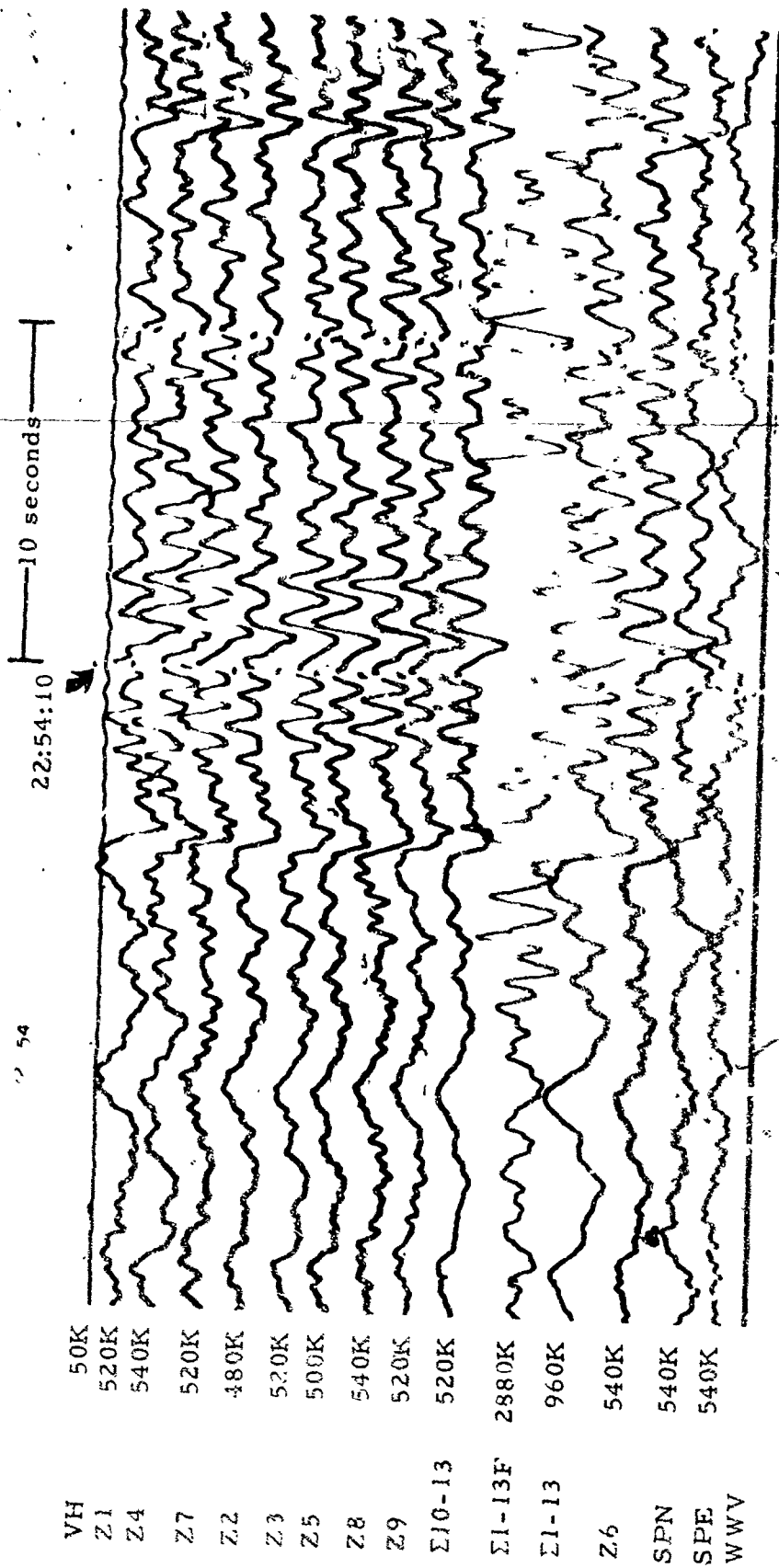


Figure 3-26. WMSO short-period seismogram illustrating a P-phase arrival from the Aegean Sea. Epicentral data:  $\Delta \approx 890$ ,  $h \approx 33$  km, azimuth  $\approx 41^\circ$ , magnitude  $\approx 4.5$  (X10 enlargement of 16-mm film)

WMSO  
Run 054  
23 Feb 1964  
Data Group 3003

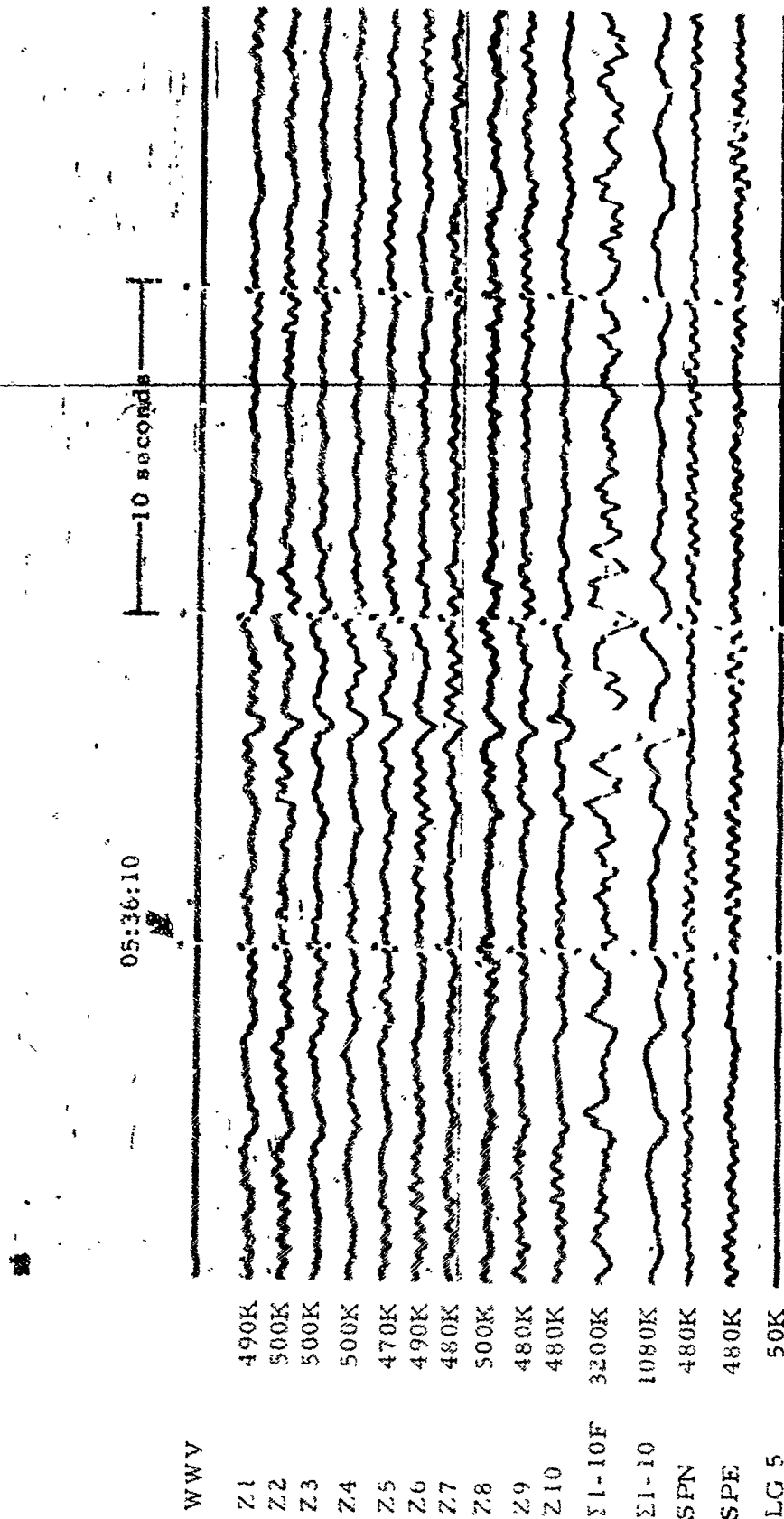


Figure 3-27. WMSO seismogram illustrating a P-phase arrival from the Fiji Islands.  
 Epicentral data:  $\Delta \approx 92^\circ$ ,  $h \approx 509$  km, azimuth  $\approx 250^\circ$ , magnitude  $\approx 4.1$   
 (X10 enlargement of 16-mm film)

WMSO  
 Run 223  
 11 Aug 1963

TR 64-50

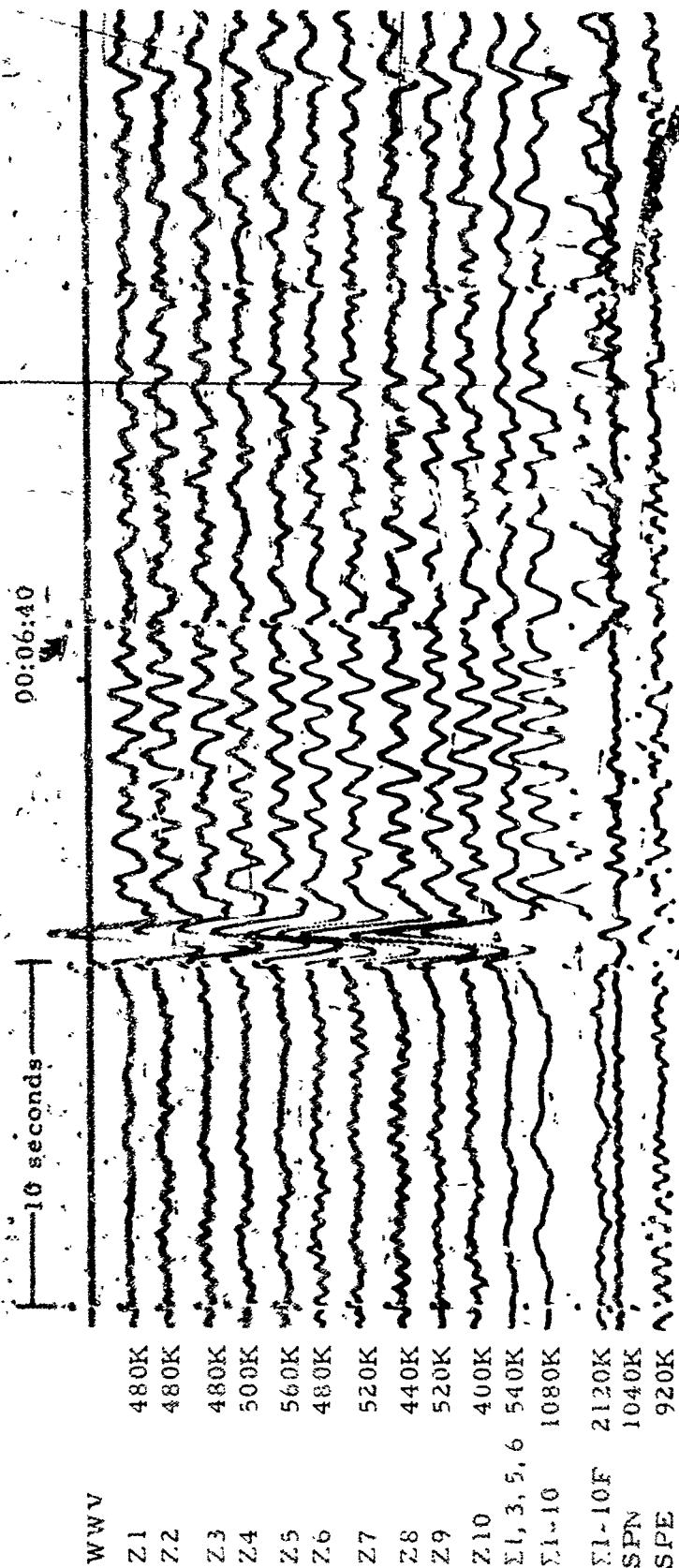


Figure 3-28. WMSO seismogram illustrating a P-phase arrival from the Fiji Islands.  
Epicentral data:  $\Delta \approx 92^\circ$ ,  $h \approx 515$  km, azimuth  $\approx 250^\circ$ , magnitude  $\approx 5.2$   
(X10 enlargement of 16-mm film)

WMSO  
Run 217  
5 Aug 1963

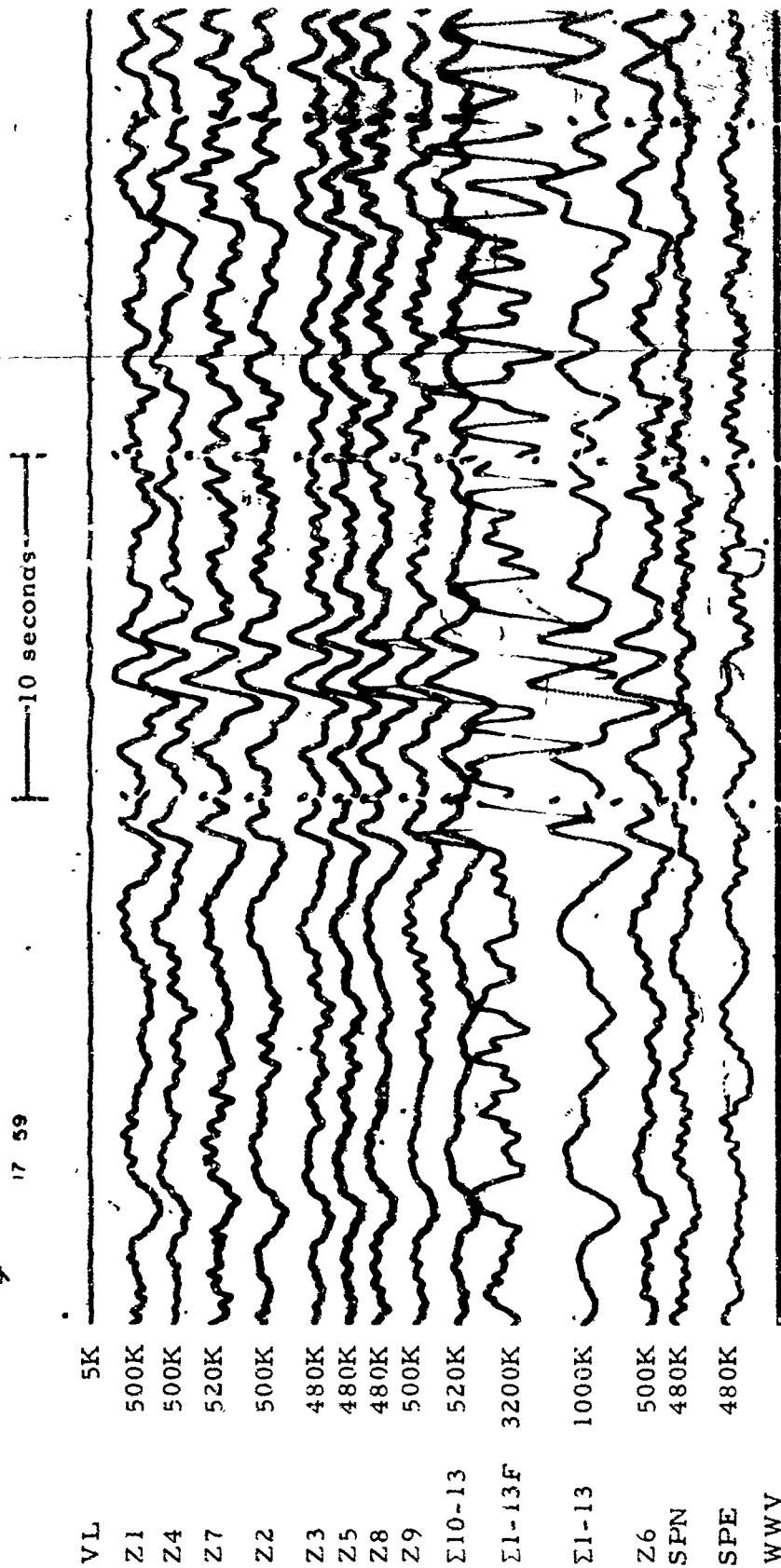


Figure 3-29. WMSO seismogram illustrating a P-phase arrival from off the coast of Turkey. Epicentral data:  $\Delta \approx 94^\circ$ ,  $h \approx 41$  km, azimuth  $\approx 39^\circ$ , magnitude  $\approx 5.3$   
(X10 enlargement of 16-mm film)

WMSO  
Run 030  
30 Jan 1964  
Data Group 311

3.6 DISTANCE = 101° to 120°

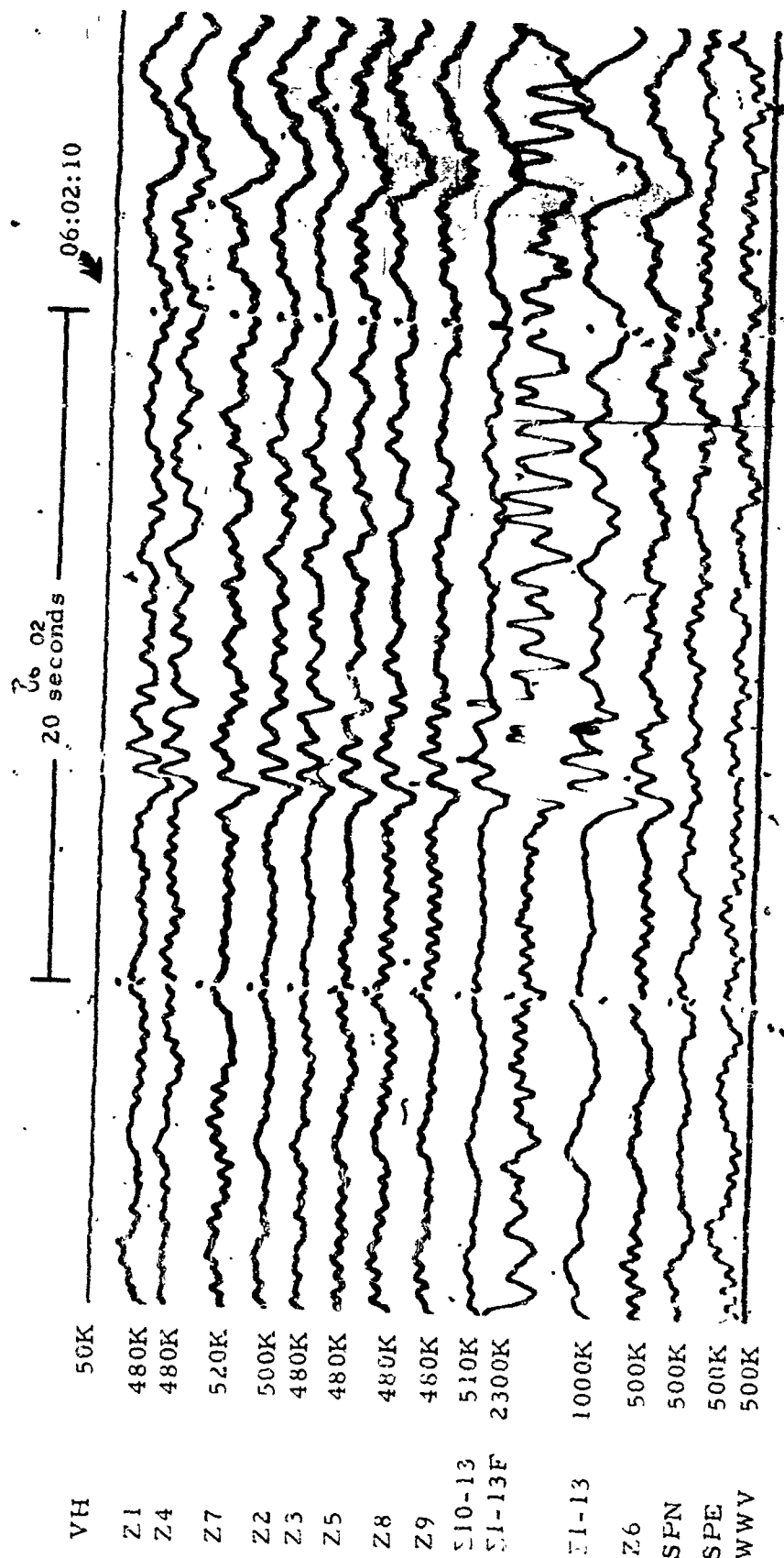


Figure 3-30. WMSO seismogram illustrating a PKP phase arrival from New Britain.  
 Epicentral data:  $\Delta \approx 112^\circ$ ,  $h \approx 33$  km, azimuth  $\approx 278^\circ$ , magnitude  $\approx 5.1$   
 (X10 enlargement of 16-mm film)

WMSO  
 Kun 028  
 28 Jan 1964  
 Data Group 311

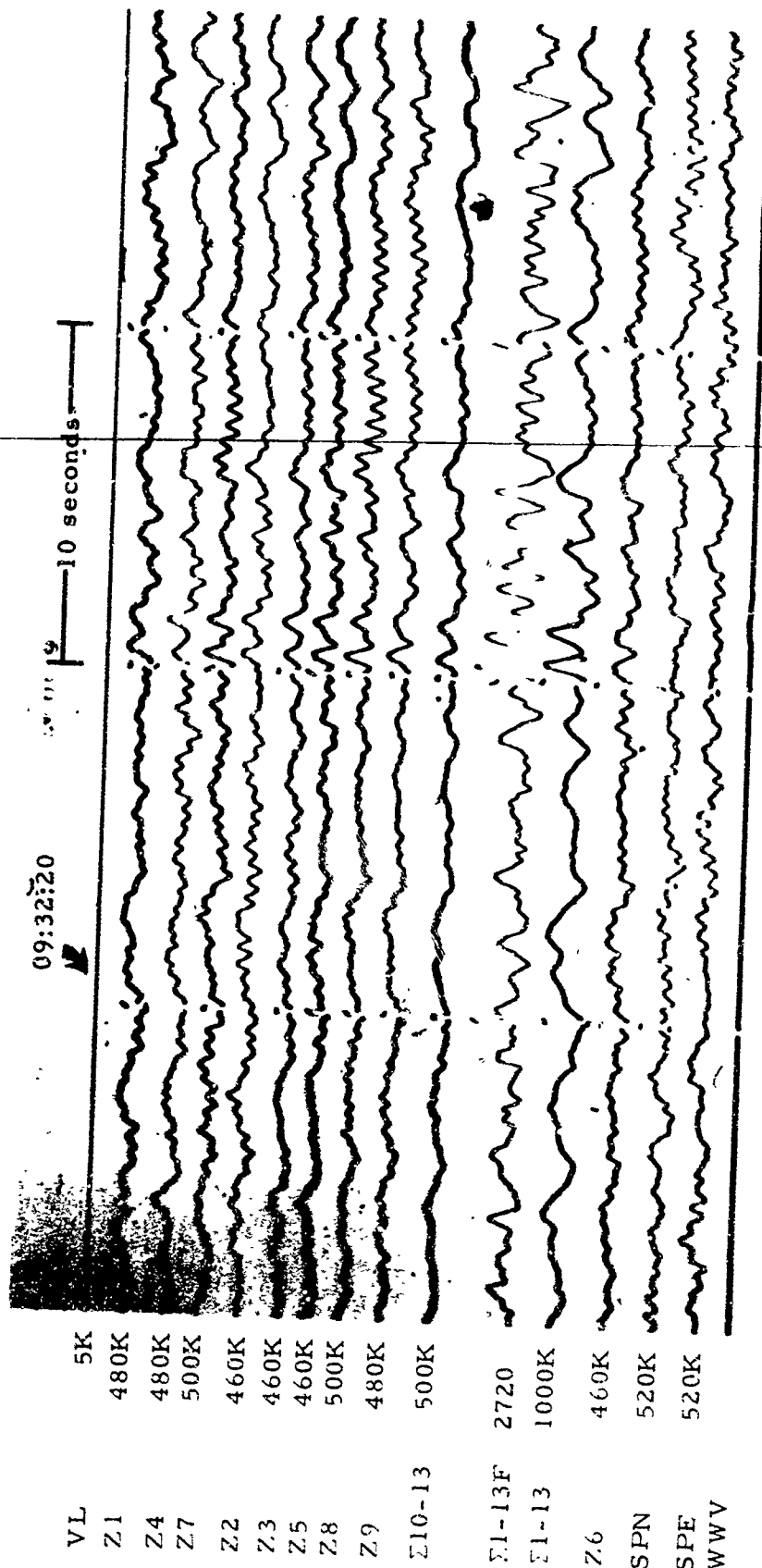


Figure 3-31. WMSO seismogram illustrating a PKP phase arrival. Epicenter: near the coast of Southern Iran,  $\Delta \approx 114^\circ$ ,  $h \approx 33$  km, azimuth  $\approx 27^\circ$ , magnitude  $\approx 5.6$   
(X10 enlargement of 16-mm film)

WMSO  
Run 019  
19 Jan 1964  
Data Group 311



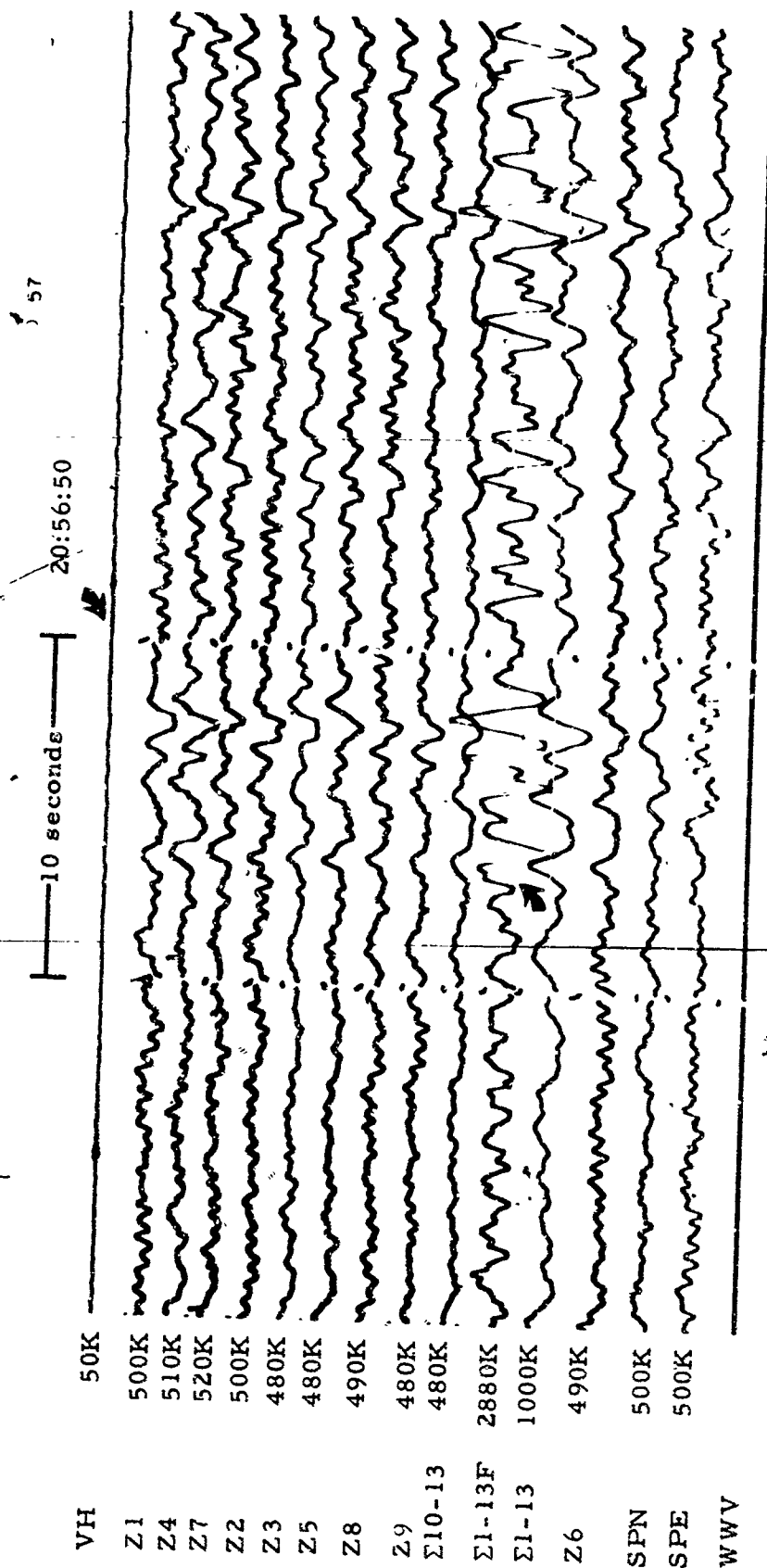


Figure 3-32. WMSO short-period seismogram illustrating a PKP phase arrival.  
 Epicenter: near the north coast of Luzon,  $\Delta \approx 115^\circ$ ,  $h \approx 53$  km, azimuth  $\approx 319^\circ$ ,  
 magnitude  $\approx 4.8$  (X10 enlargement of 16-mm film)

WMSO  
 Run 020  
 20 Jan 1964  
 Data Group 311

3.7 DISTANCE =  $121^{\circ}$  to  $140^{\circ}$

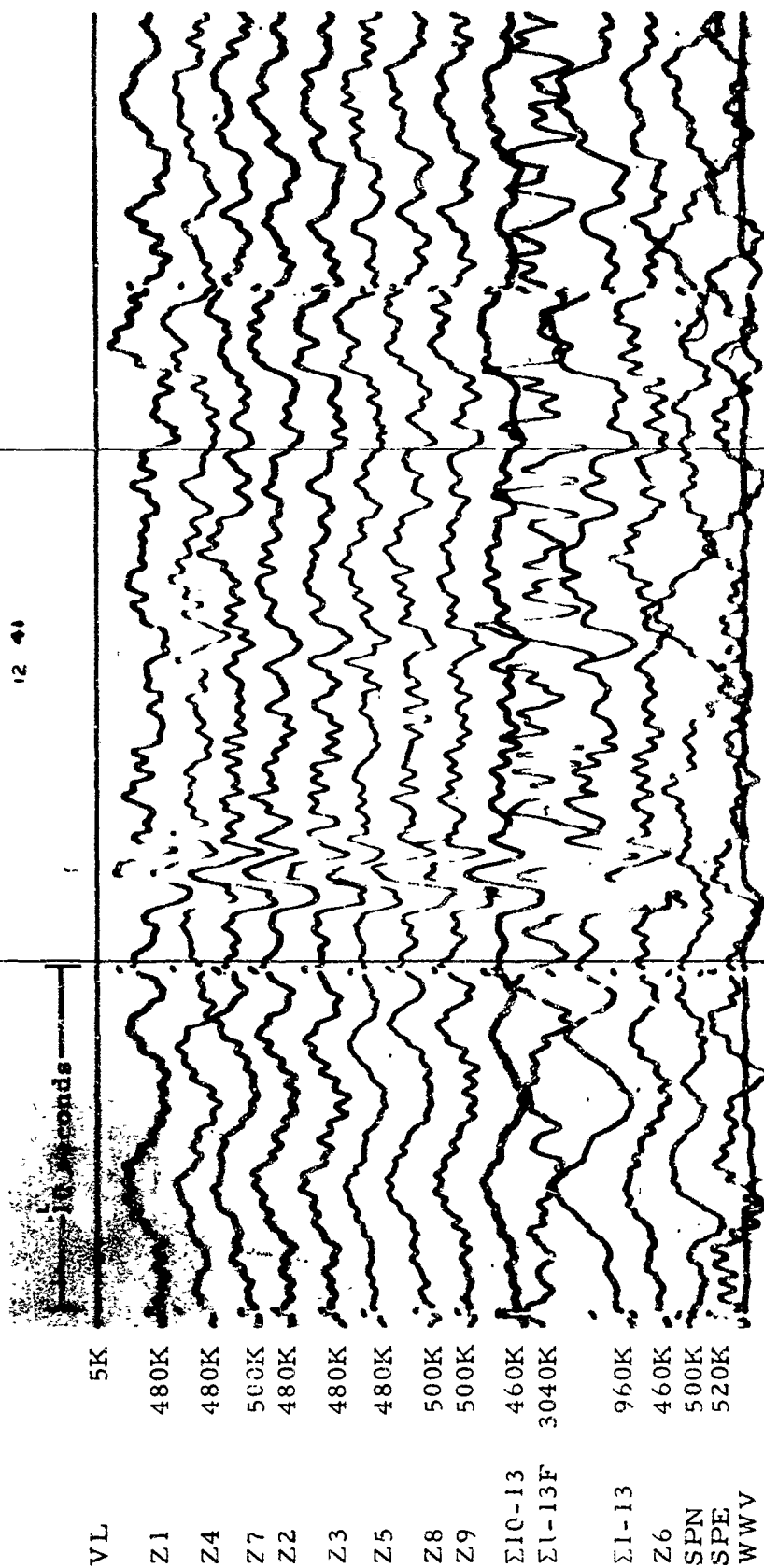
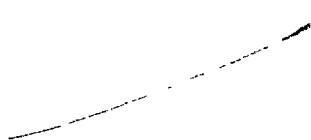


Figure 3-32. WMSO short-period seismogram illustrating a PKP phase arrival from the Banda Sea. Epicentral data:  $\Delta \approx 127^\circ$ ,  $h \approx 96$  km, azimuth  $\approx 291^\circ$ , magnitude  $\approx 5.7$  (X10 enlargement of 16-mm film)

WMSO  
Run 001  
1 Jan 1964  
Data Group 311



3.8 DISTANCE =  $141^{\circ}$  to  $160^{\circ}$

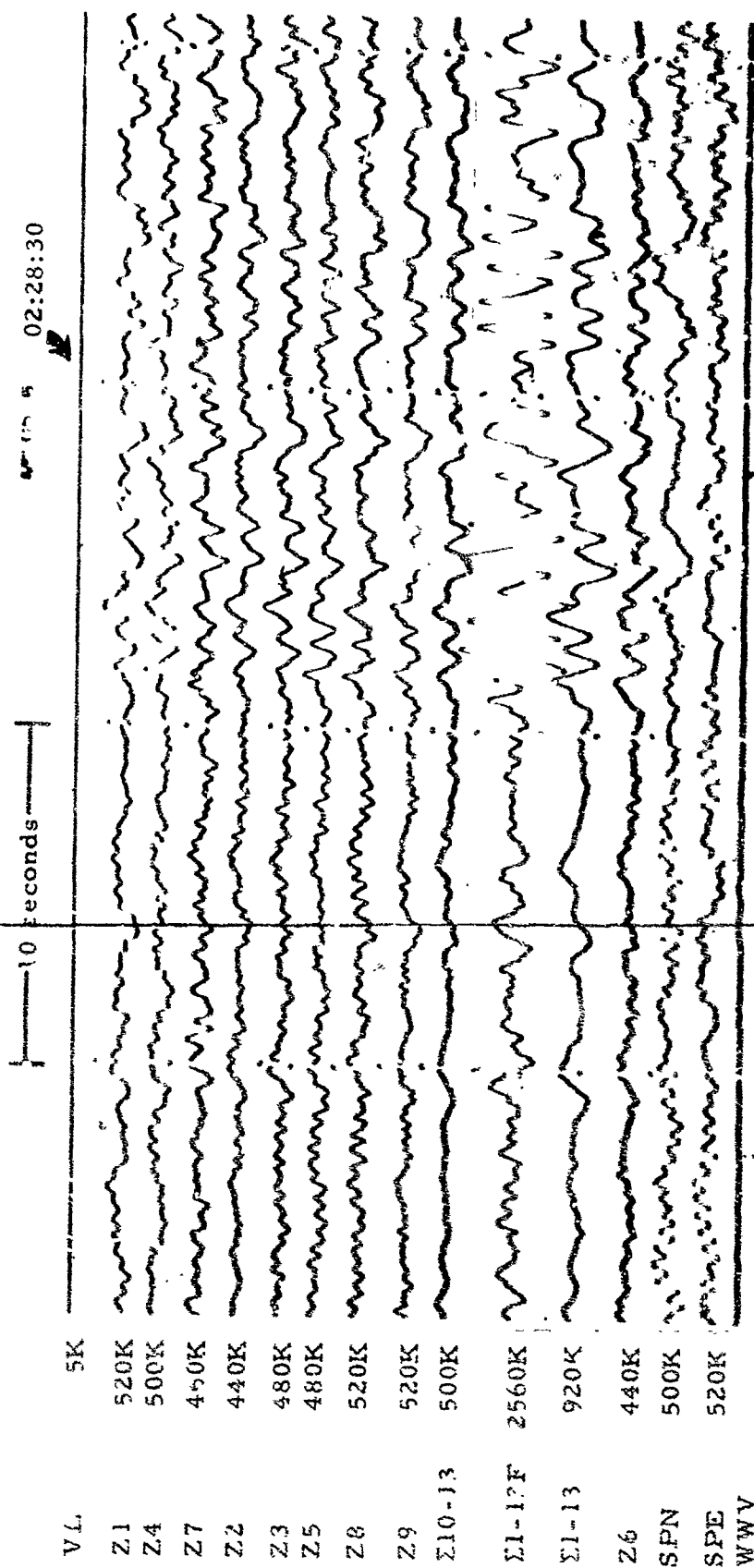


Figure 3-34. WMSO short-period seismogram illustrating a PKP phase arrival.  
 Epicenter: off the southern coast of Java,  $\Delta \approx 143^\circ$ ,  $h \approx 81$  km, azimuth  $\approx 307^\circ$ ,  
 no magnitude data available. (X10 enlargement of 16-mm film)

WMSO  
 Run 056  
 25 Feb 1964  
 Data Group 3003

WWV	
Z1	480K
Z2	510K
Z3	500K
Z4	490K
Z5	510K
Z6	520K
Z7	510K
Z8	520K
Z9	500K
$\Sigma 10-13$	540K
$\Sigma 1-13F$	540K
$\Sigma 1-13$	866K
N	550K
E	510K
LG 5	50K

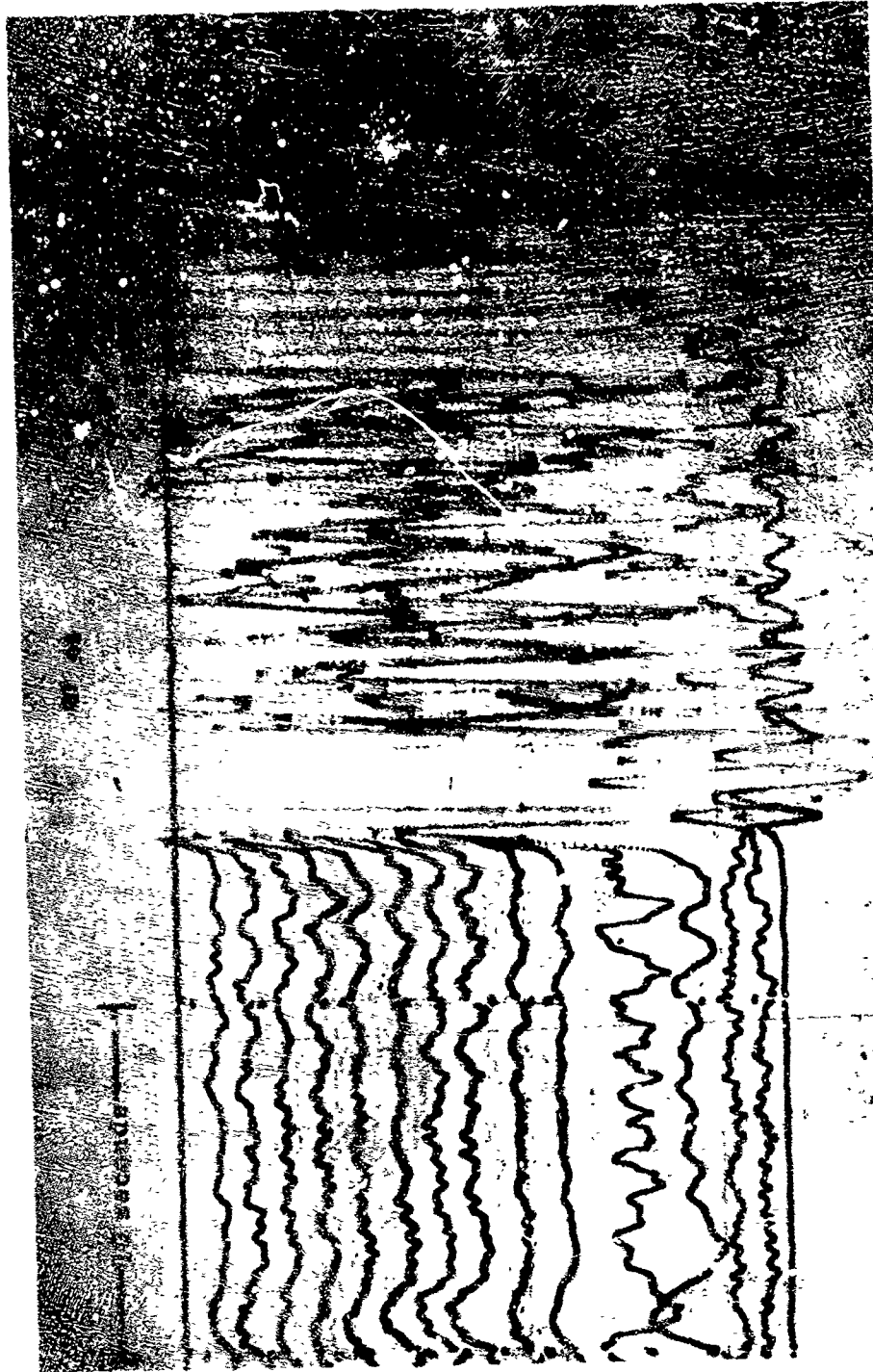


Figure 3-35. WMSO seismogram illustrating a PKP phase arrival. Epicenter: off the southern coast of Sumatra,  $\Delta \approx 144^\circ$ ,  $h \approx 50$  km, azimuth  $\approx 321^\circ$ , magnitude  $\approx 6.1$  (X10 enlargement of 16-mm film)

$v_1$  MSO  
Run 297  
24 Oct 1964

TR 64-50

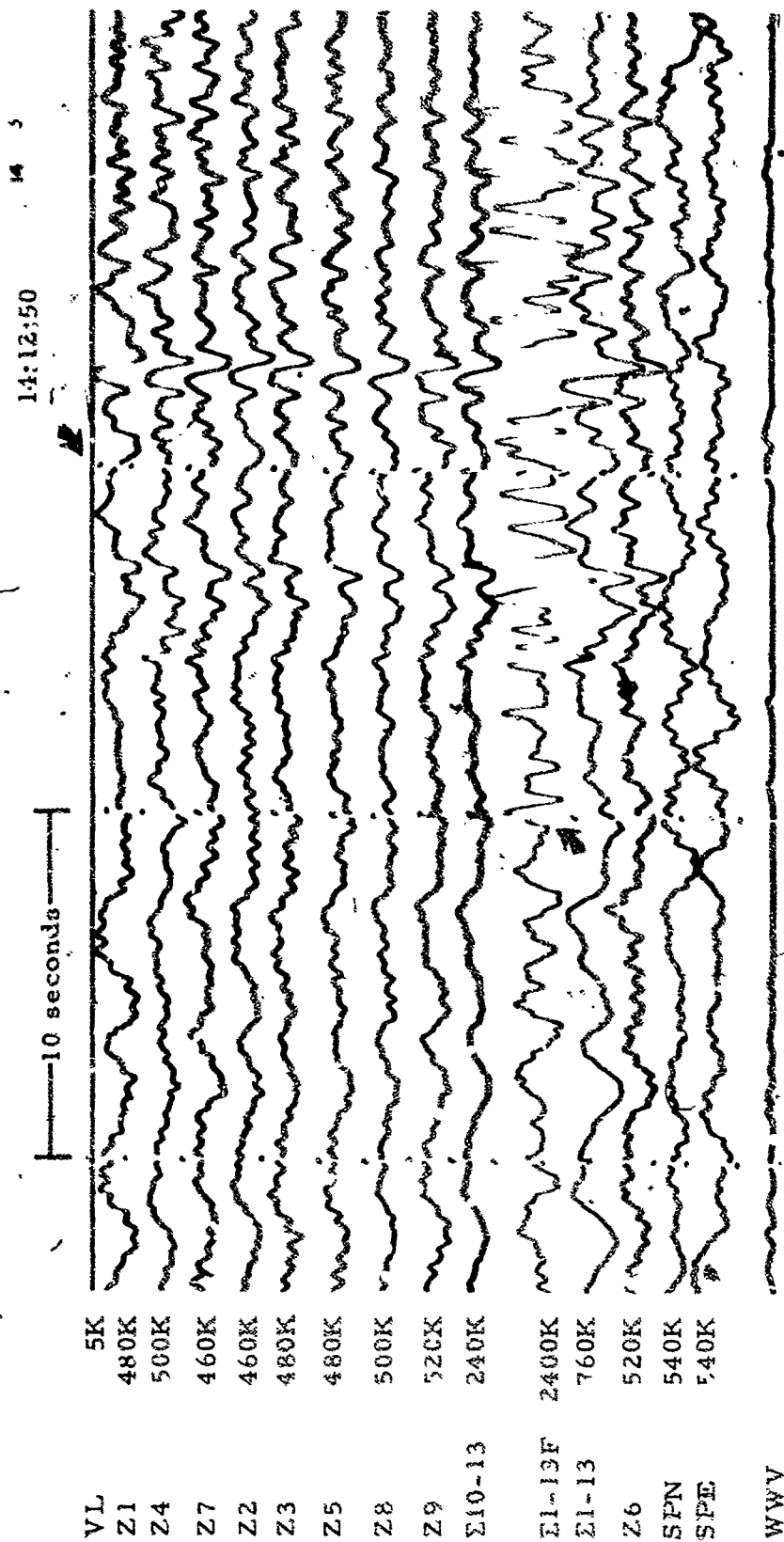


Figure 3-36. WMSO seismogram illustrating a PKP phase arrival from the Sunda Strait.  
Epical data:  $\Delta \approx 144^\circ$ ,  $h \approx 33$  km, azimuth  $\approx 316^\circ$ , magnitude  $\approx 5.2$   
(X10 enlargement of 16-mm film)

WMSO  
Run 052  
21 Feb 1964  
Data Group 3003

TR 64-50

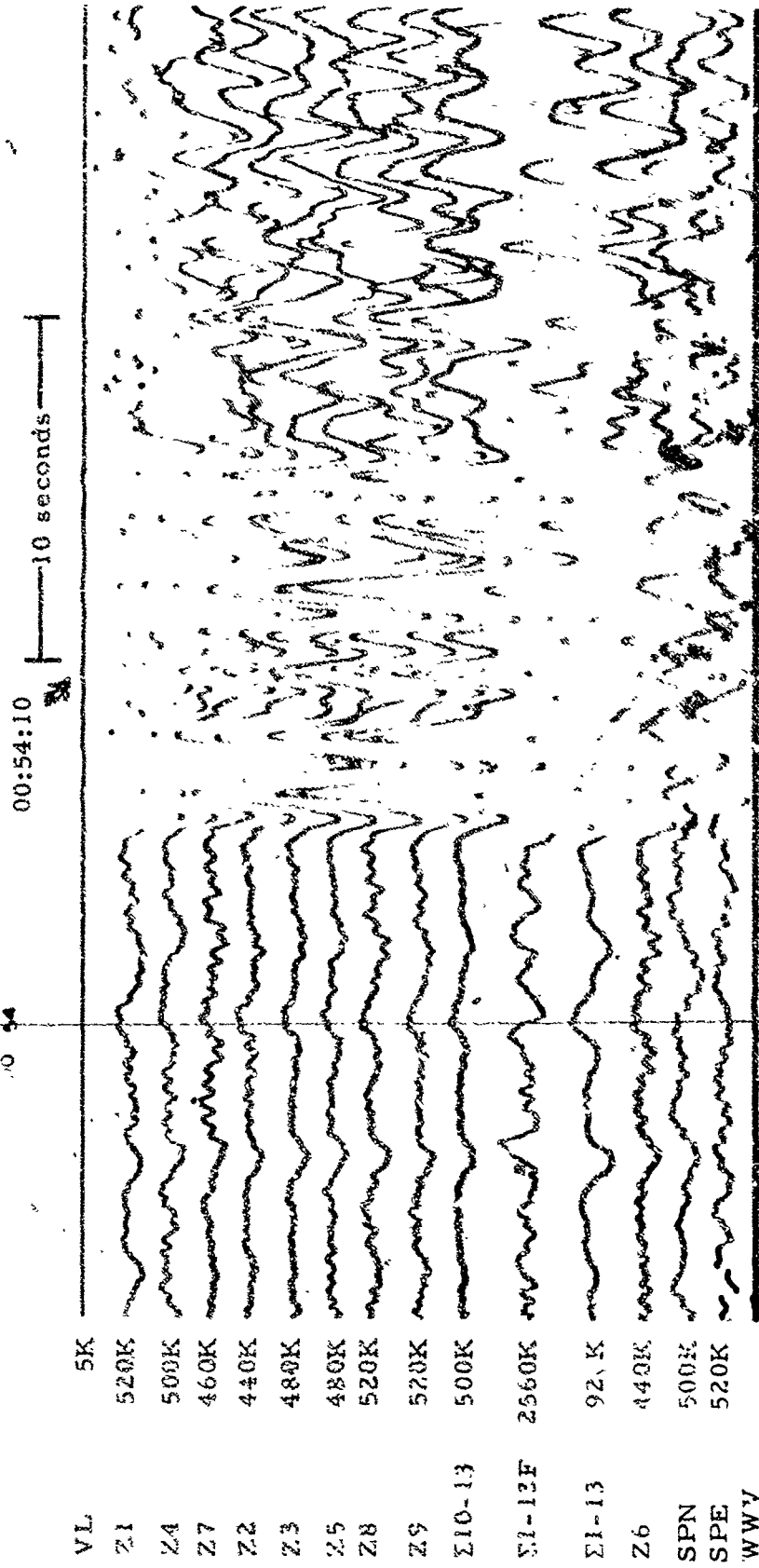


Figure 3-37. WMSO seismogram illustrating a PKP phase arrival from the Prince Edward Island region. Epicentral data:  $\Delta \approx 145^\circ$ ,  $h \approx 33$  km, azimuth  $\approx 120^\circ$ , magnitude  $\approx 6.7$  (X10 enlargement of 16-mm film)

WMSO  
Run 056  
25 Feb 1964  
Data Group 3003



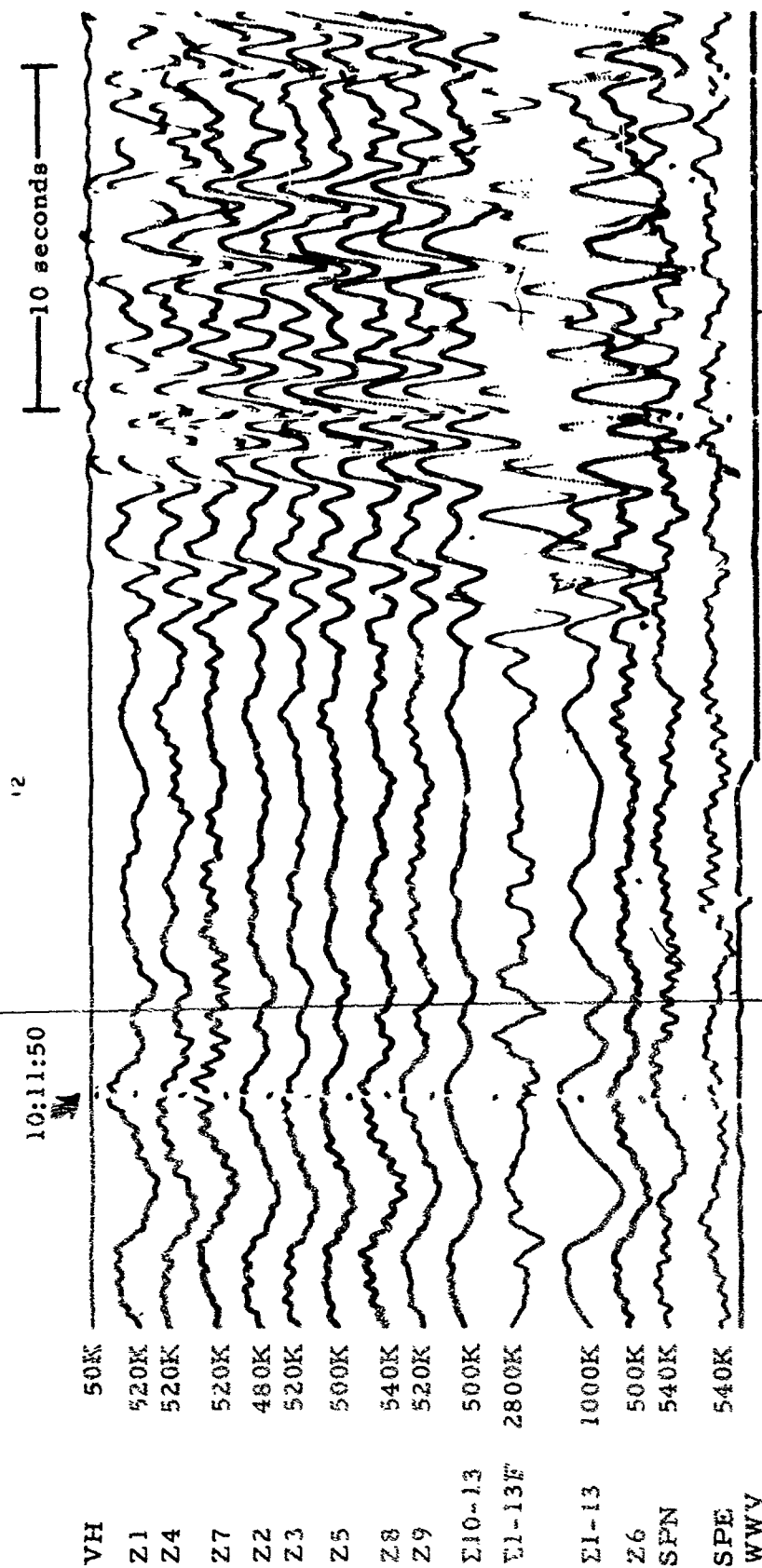


Figure 3-38. WMSO seismogram illustrating a PKP phase arrival from the Chagay Archipelago region. Epicentral data:  $\Delta \approx 150^\circ$ ,  $h \approx 33$  km, azimuth  $\approx 28^\circ$ , magnitude  $\approx 5.2$  (X10 enlargement of 16-mm film)

WMSO  
 Run 055  
 24 Feb 1964  
 Data Group 3003

TR 64-50

03:28:30

10 seconds

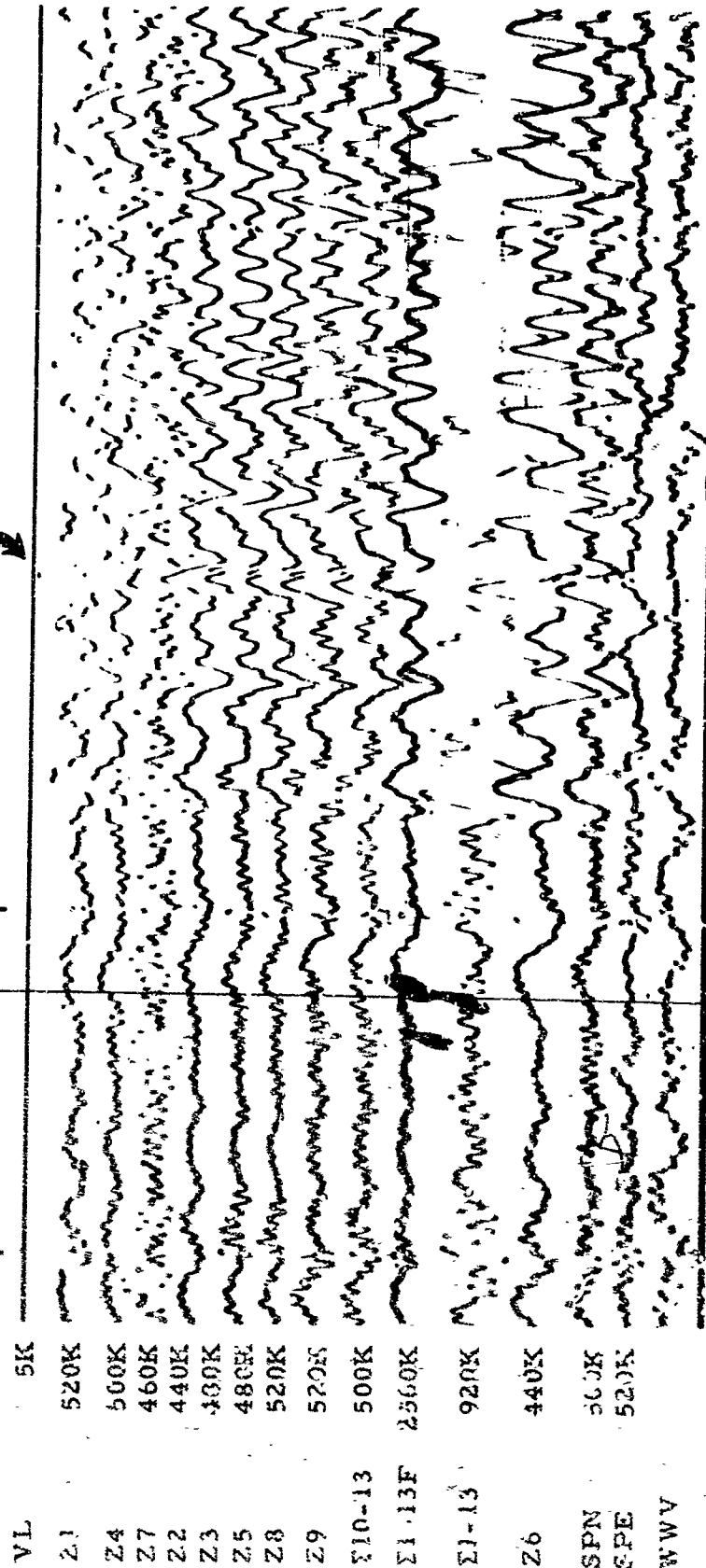


Figure 3-39. WMSO seismogram illustrating a PKP phase arrival. Epicenter: south of Australia,  $\Delta \approx 153^\circ$ ,  $h \approx 33$  km, azimuth  $\approx 227^\circ$ , no magnitude data available. (X10 enlargement of 16-mm film)

WMSO

Run 05b

25 Feb 1964

Data Group 3003

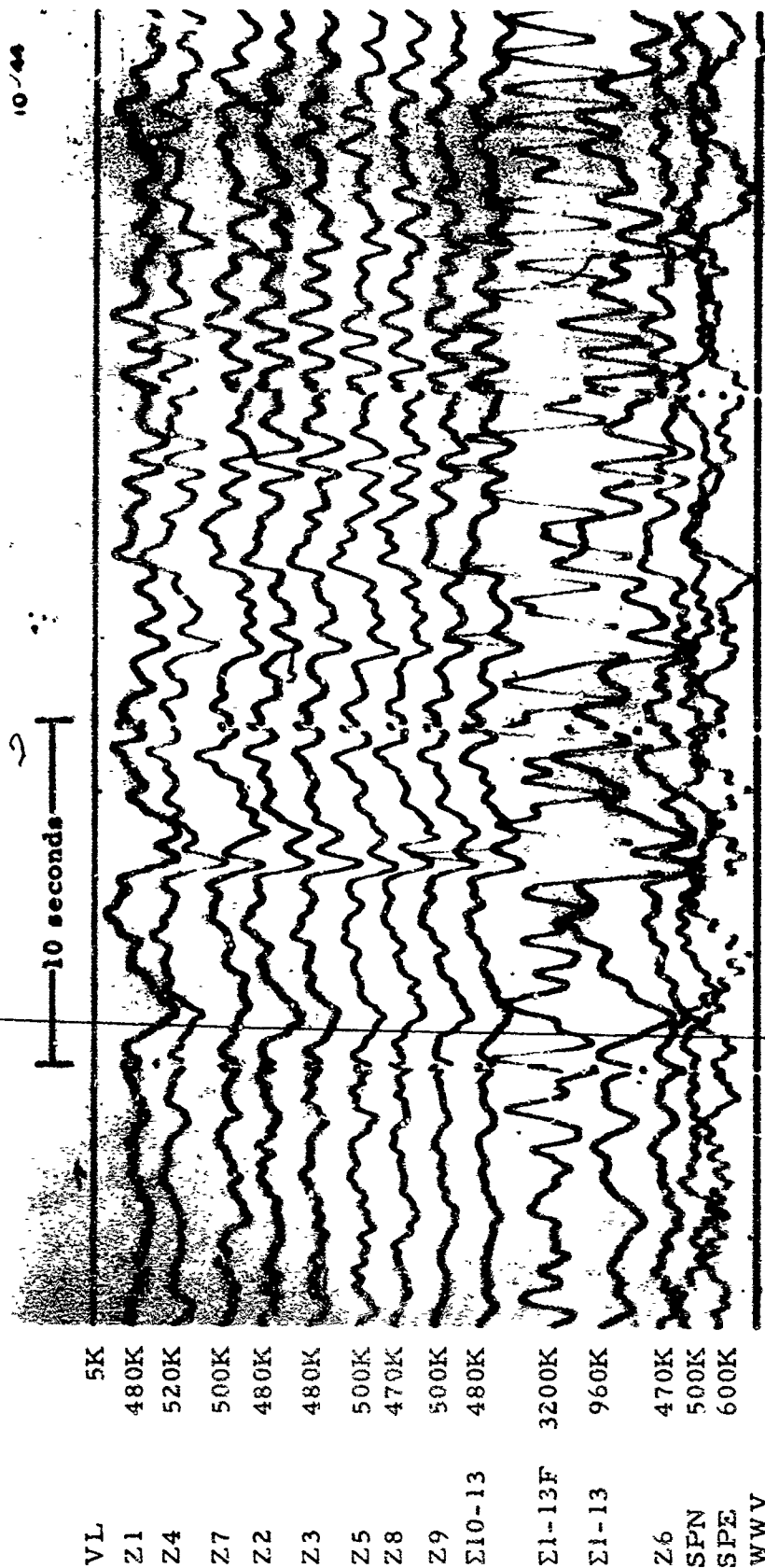


Figure 3-40. WMSO short-period seismogram illustrating a PKP phase arrival from the Indian Ocean. Epicentral data:  $\Delta \approx 155^\circ$ ,  $h \approx 33$  km, azimuth  $\approx 337^\circ$ , no magnitude data available (X10 enlargement of 16-mm film)

WMSO  
Run 011  
11 Jan 1964  
Data Group 311

4. NOISE SAMPLES

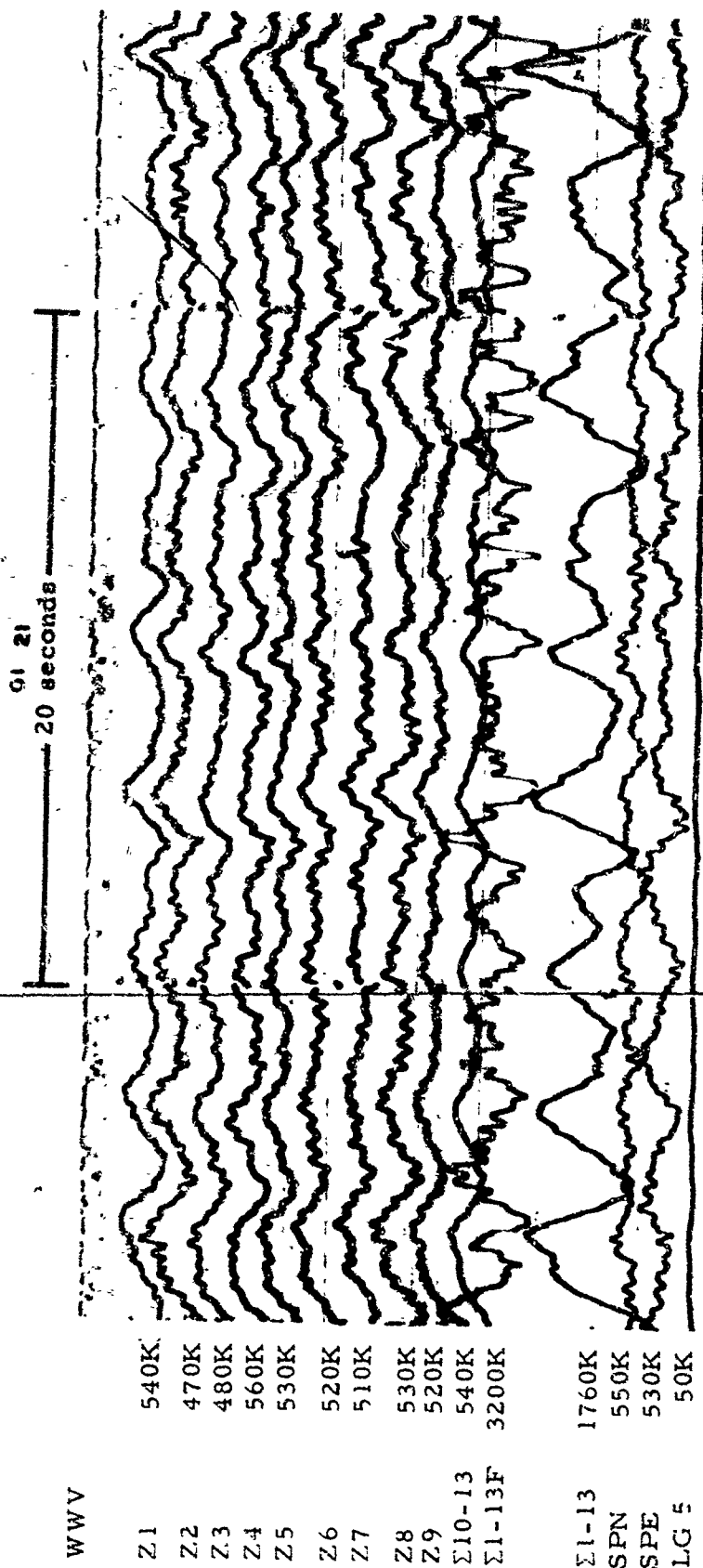


Figure 4-1. WMSO short-period seismogram illustrating 1/2-second microseisms  
(X10 enlargement of 16-mm film)

WMSO  
Run 303  
30 Oct 1963

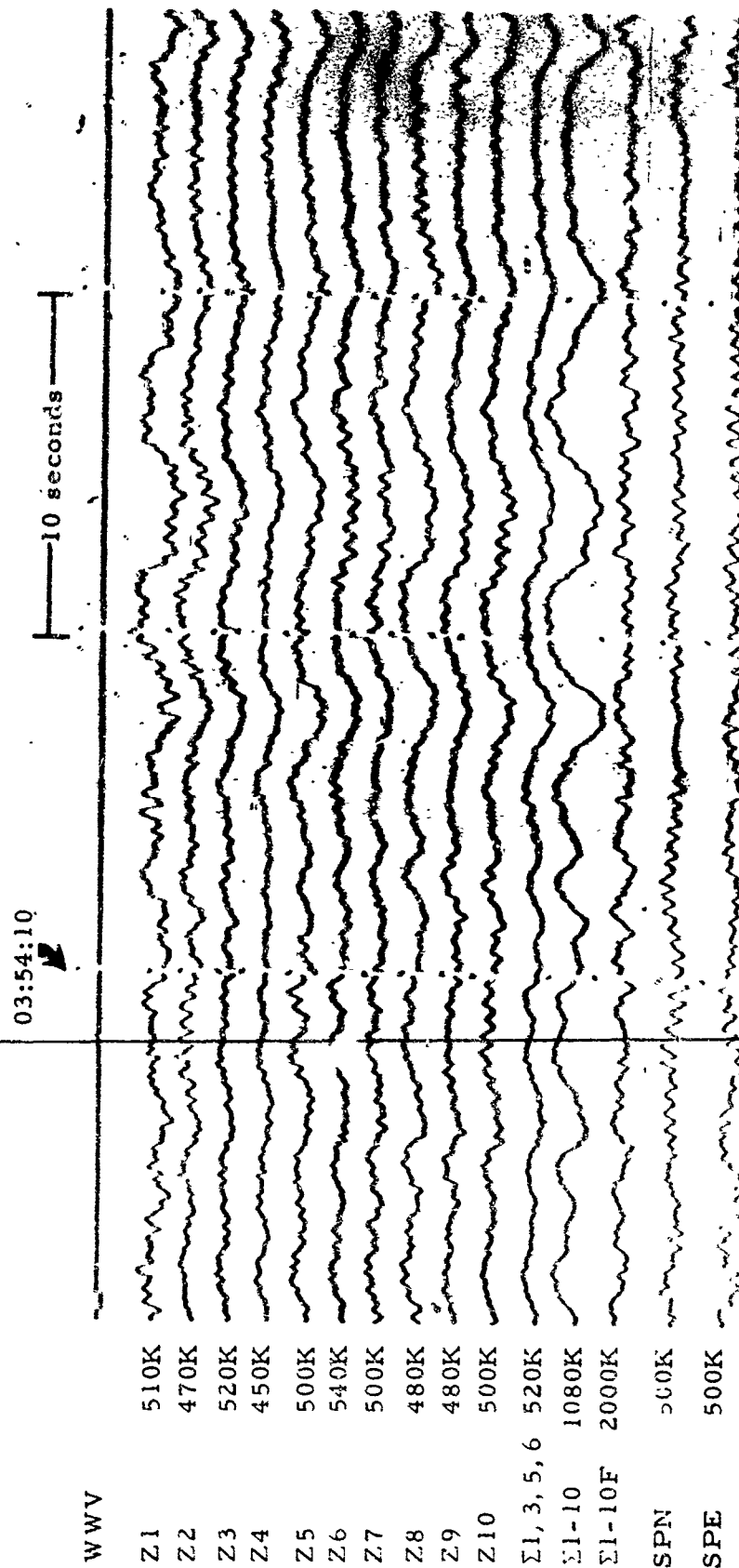


Figure 4-2. WMSO seismogram illustrating the occurrence of 4- to 6-second microseisms at a low level on the short-period system (X10 enlargement of 16-mm film)

WMSO  
Run 161  
10 Jun 1963

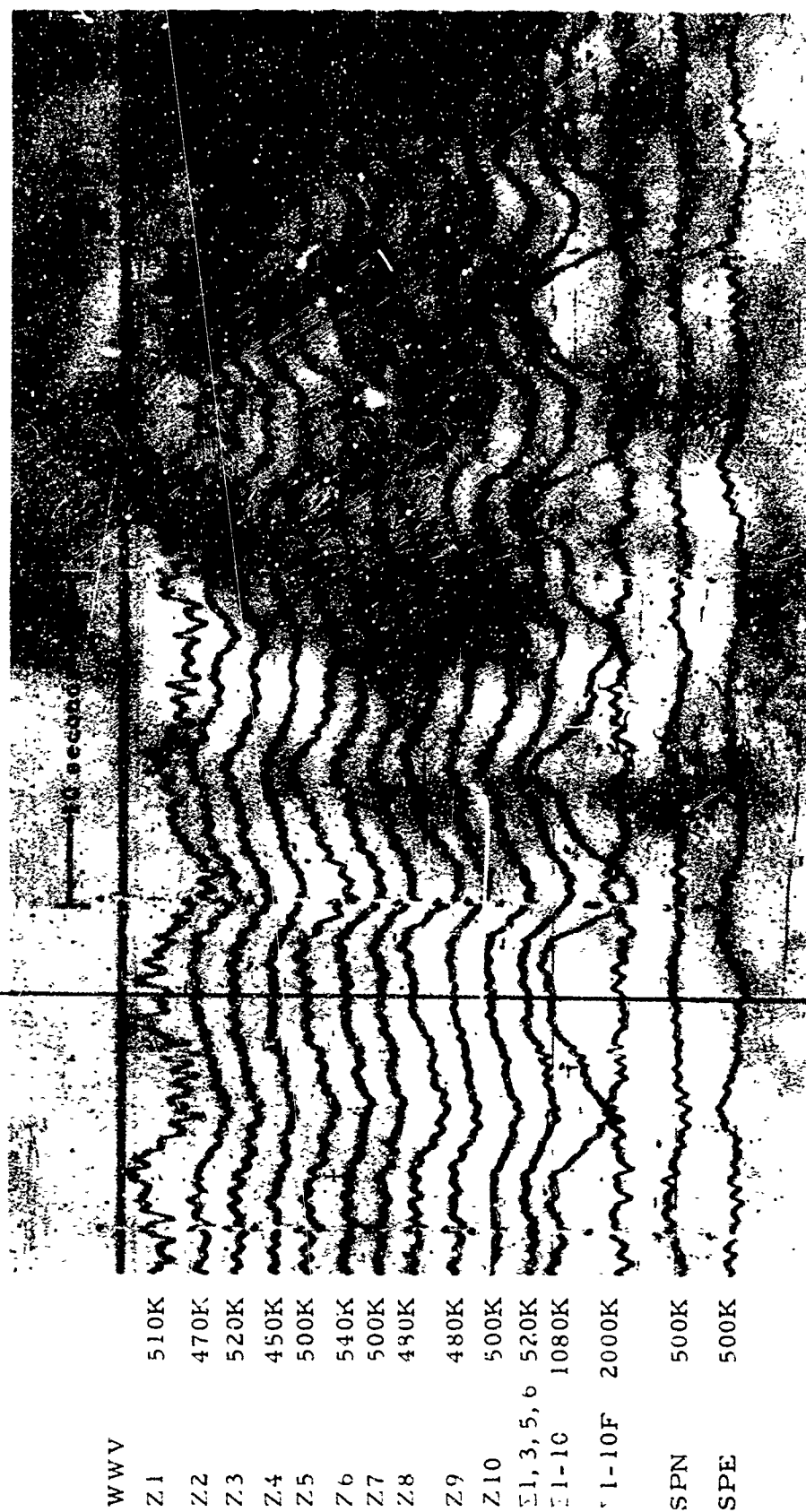


Figure 4-3. WMSO seismogram illustrating the occurrence of 4- to 6-second microseisms at a moderate level on the short-period system (X10 enlargement of 16-mm film)

WMSO

Run 161

10 Jun 1963

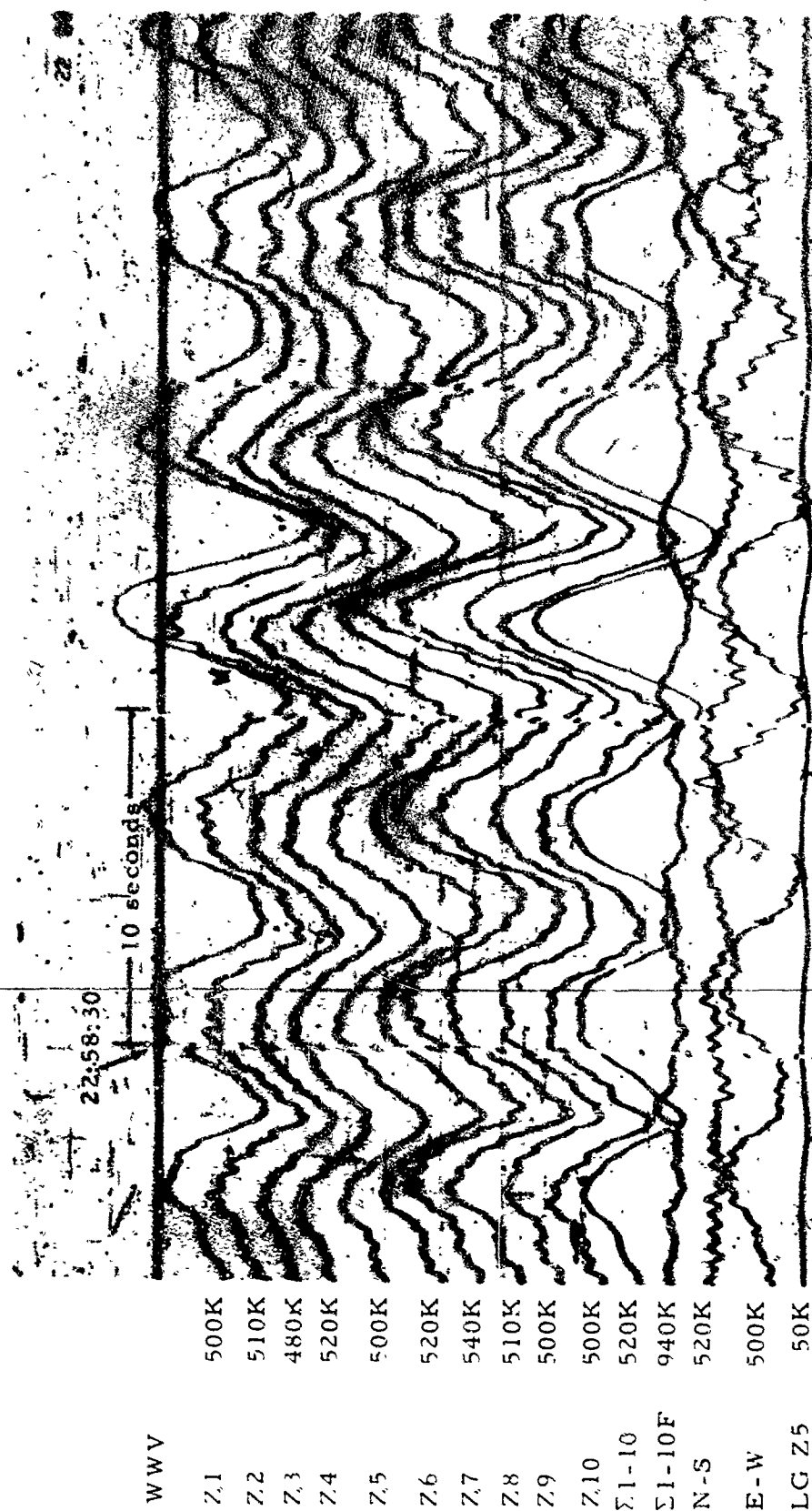


Figure 4-4. WMSO seismogram illustrating the occurrence of 4- to 6-second microseisms at a high level on the short-period system (X10 enlargement of 16-mm film)

WMSO

Run 364

30 Dec 1962



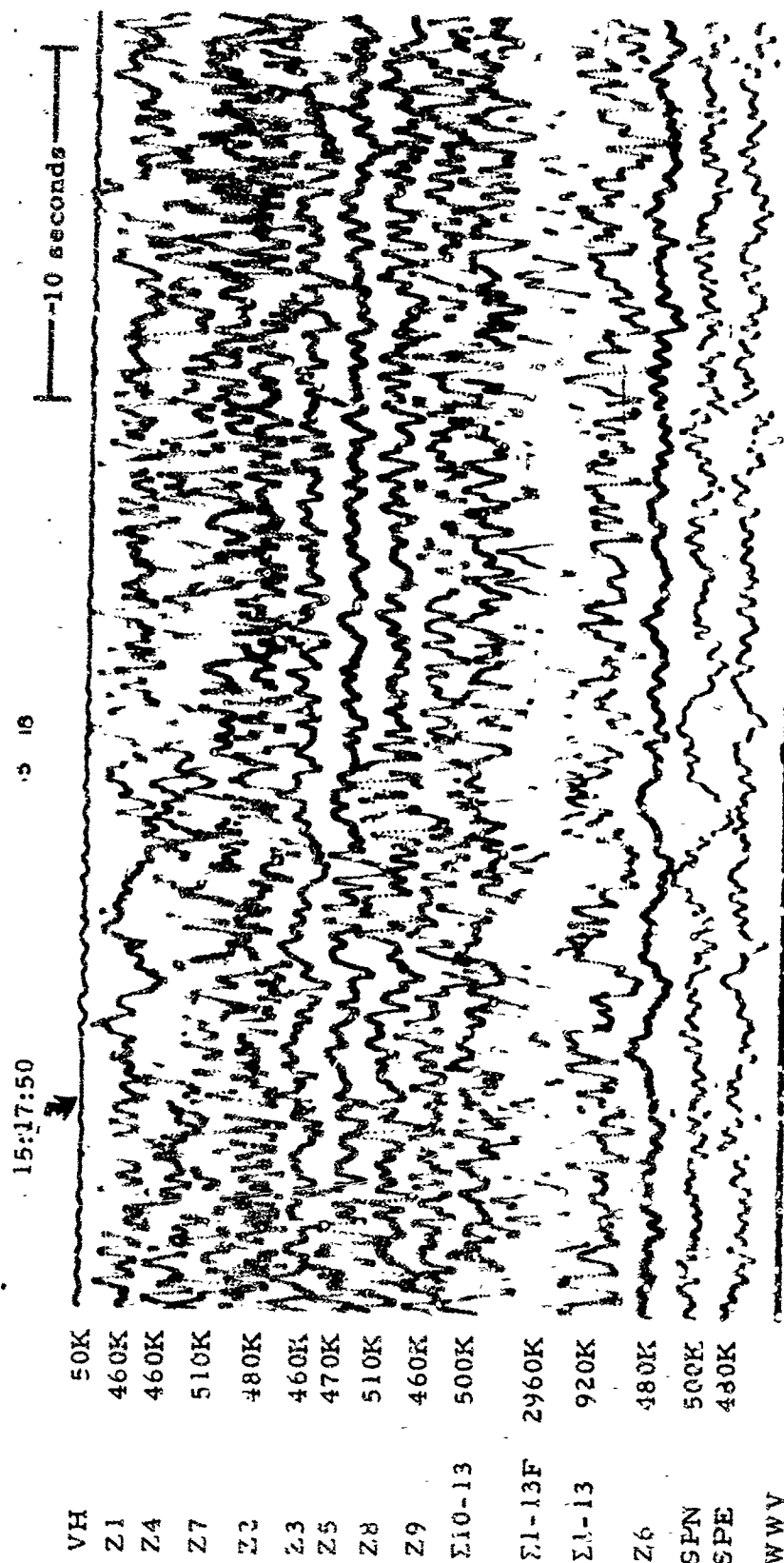


Figure 4-5. WMSO seismogram illustrating wind generated noise on the short-period system. Wind speed is approximately 38 mph (X10 enlargement of 16-mm film)

WMSO  
Run 046  
15 Feb 1964  
Data Group 5003

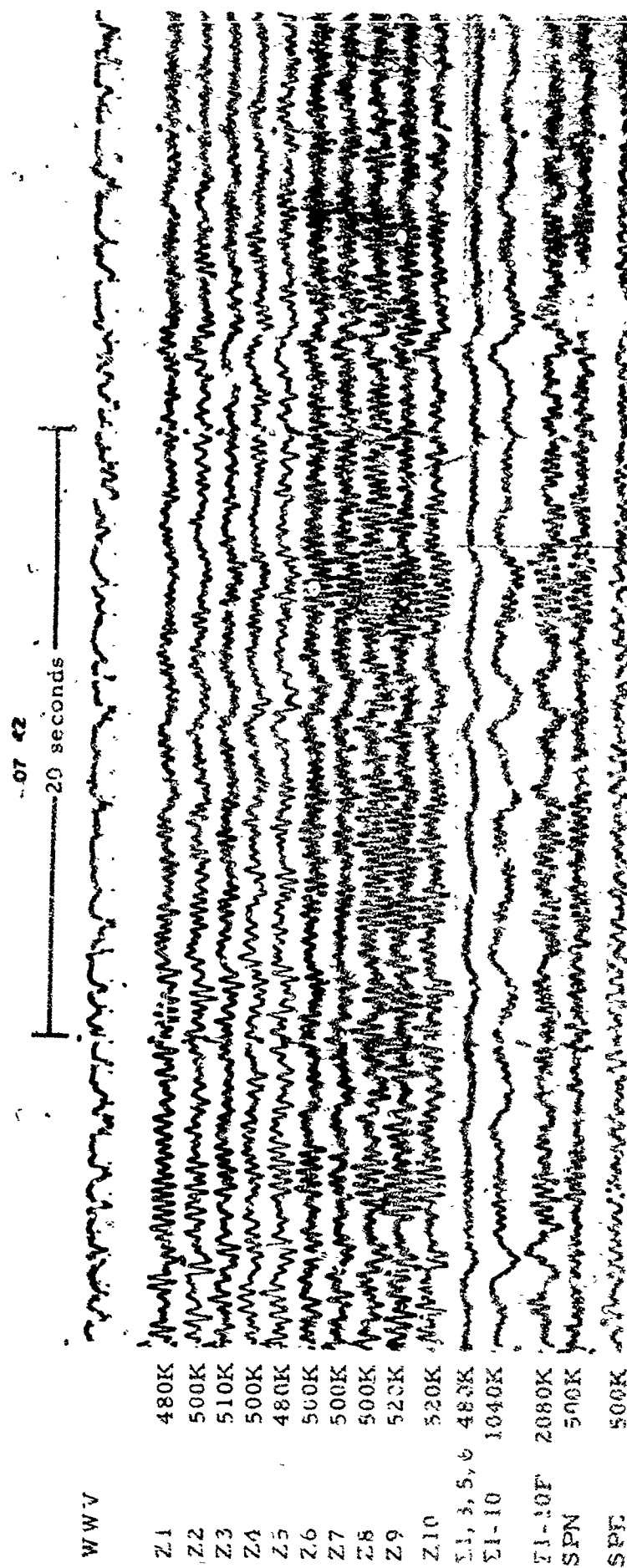


Figure 4-6. WMSO seismogram illustrating the short-period system response to train noise.  
(X10 enlargement of 16-mm film)

TR 64-50

WWV	
Z1	1020K
Z2	540K
Z3	480K
Z4	520K
Z5	540K
Z6	540K
Z7	540K
Z8	540K
Z9	580K
Z10	520K
$\Sigma 1, 3, 5, 6$	620K
$\Sigma 1-10$	1200K
$\Sigma 1-10F$	2320K
SPN	440K
SPE	440K



Figure 4-7. WMSO seismogram illustrating lightning spikes on the short-period system  
(X10 enlargement of 16-mm film)

WMSO  
Run 154  
3 Jun 1963

TR 64-50

WWV	
BPE	3K
BBN	10.2K
BBE	Incip
SLZ	9.2K
SLN	12.1K
SLE	17.7K
SLZ 10w	0.9K
SLN 10w	1.0K
SLE 10w	1.8K
GLZ	19.7K
GLN	16.4K
GLE	13.4K
SI-10	200K
M	
A	



Figure 4-8. WMSO seismogram illustrating overlineup and a generally noisy condition caused by barometric pressure changes (X10 enlargement of 16-mm film)

WMSO  
Run 147  
27 May 1963

TR 64-50

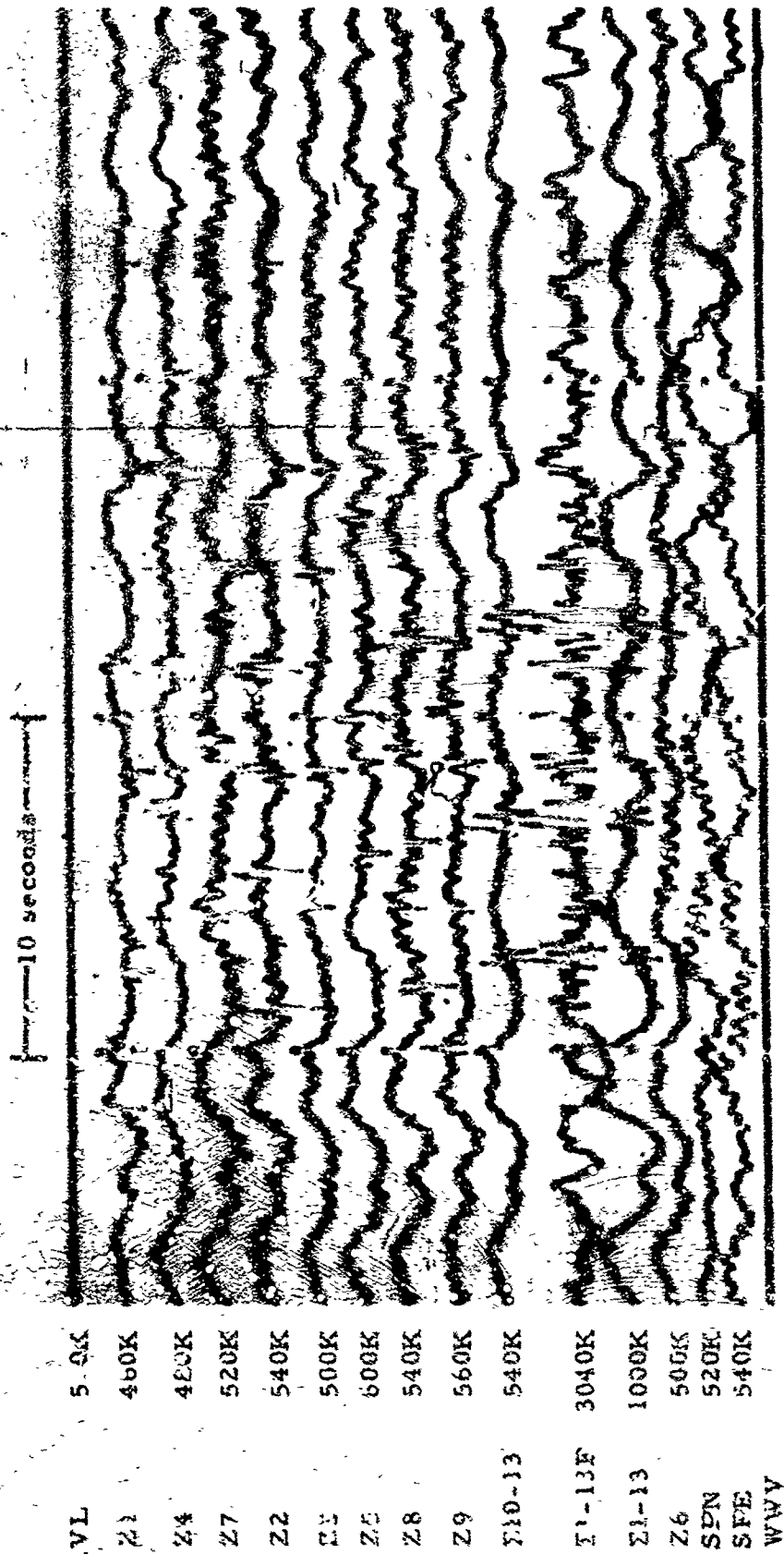


Figure 4-9. WMSO seismicgram illustrating artillery generated acoustic signals. No corresponding seismic signals were recorded. (X10 enlargement of 16-mm film)

WMSO  
Run 340  
6 Dec 1963  
Data Group 341

72 64-50

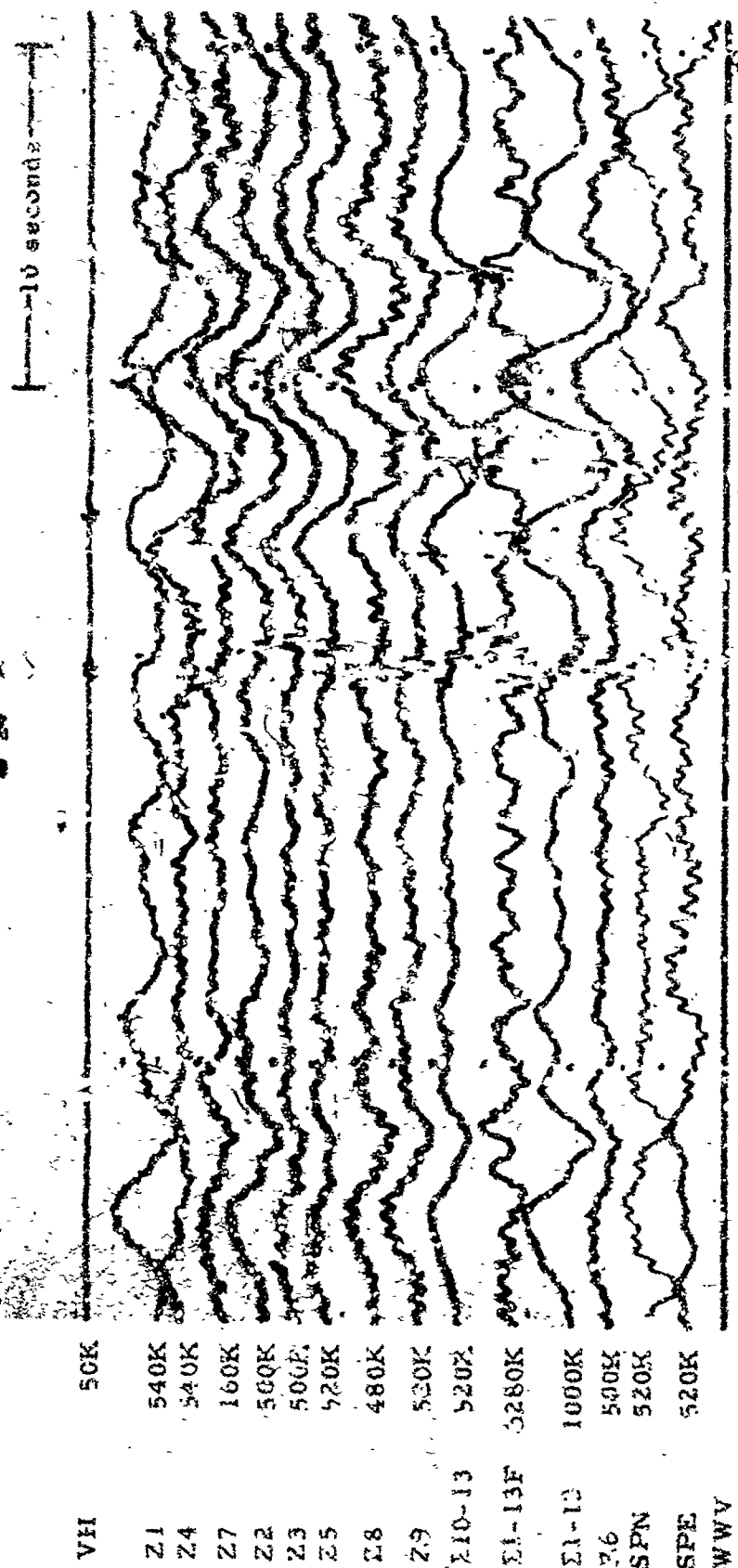


Figure 4-10. Seismic signal and corresponding acoustics from artillery fire as recorded on the WMSO short-period seismogram. (X10 enlargement of 16-mm film)

WMSO  
Run 339  
5 Dec 1963  
Data Group 311

TR 64-30

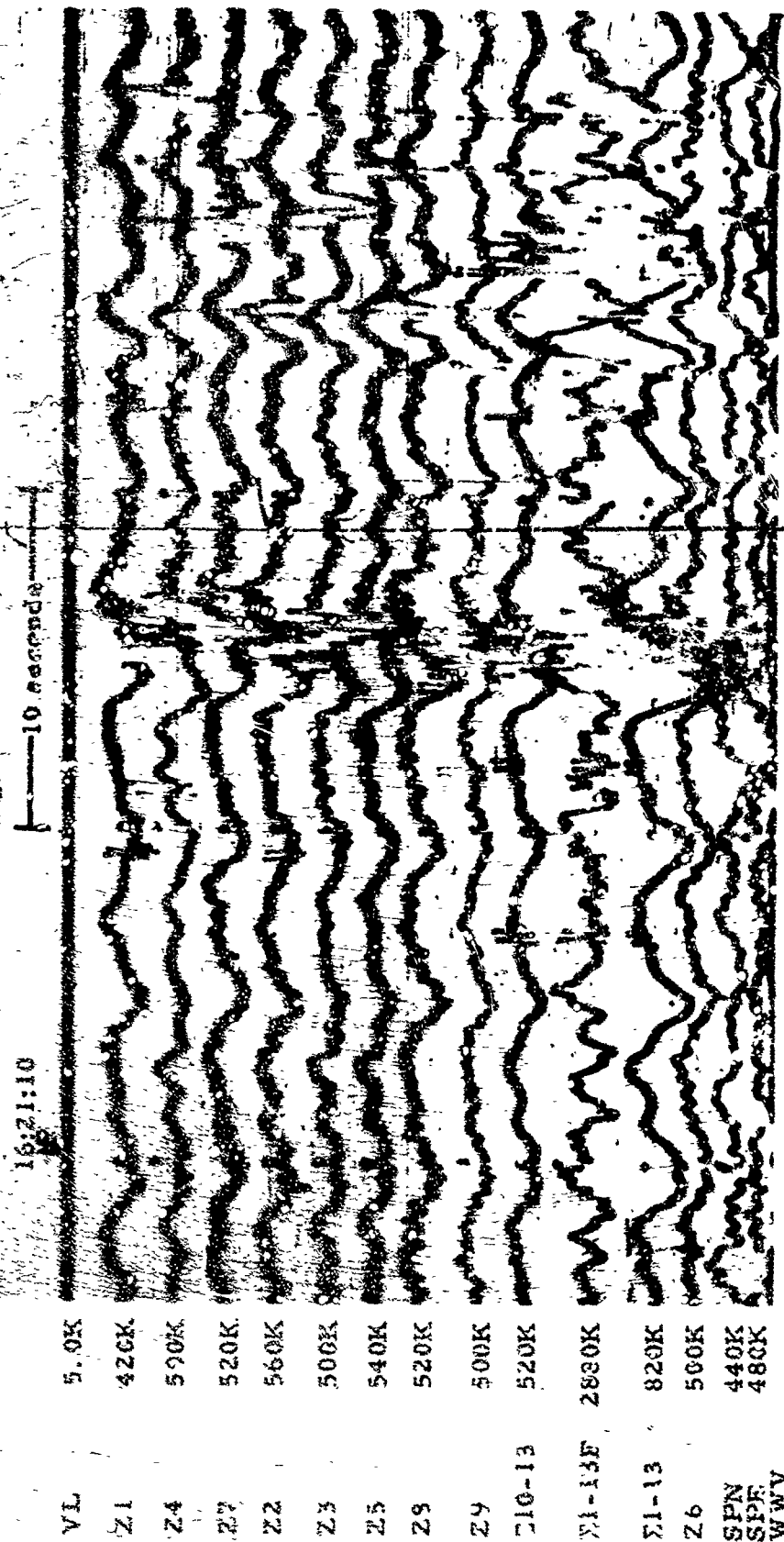


Figure 4-11. WMSO seismogram illustrating the seismic signal and acoustics generated by the demolition of outdated ammunition and artillery duds on Fort Sill. (X10 enlargement of 16-mm film)

WMSO  
Run 314  
10 Dec 1963  
Data Group 311



TR 54-56

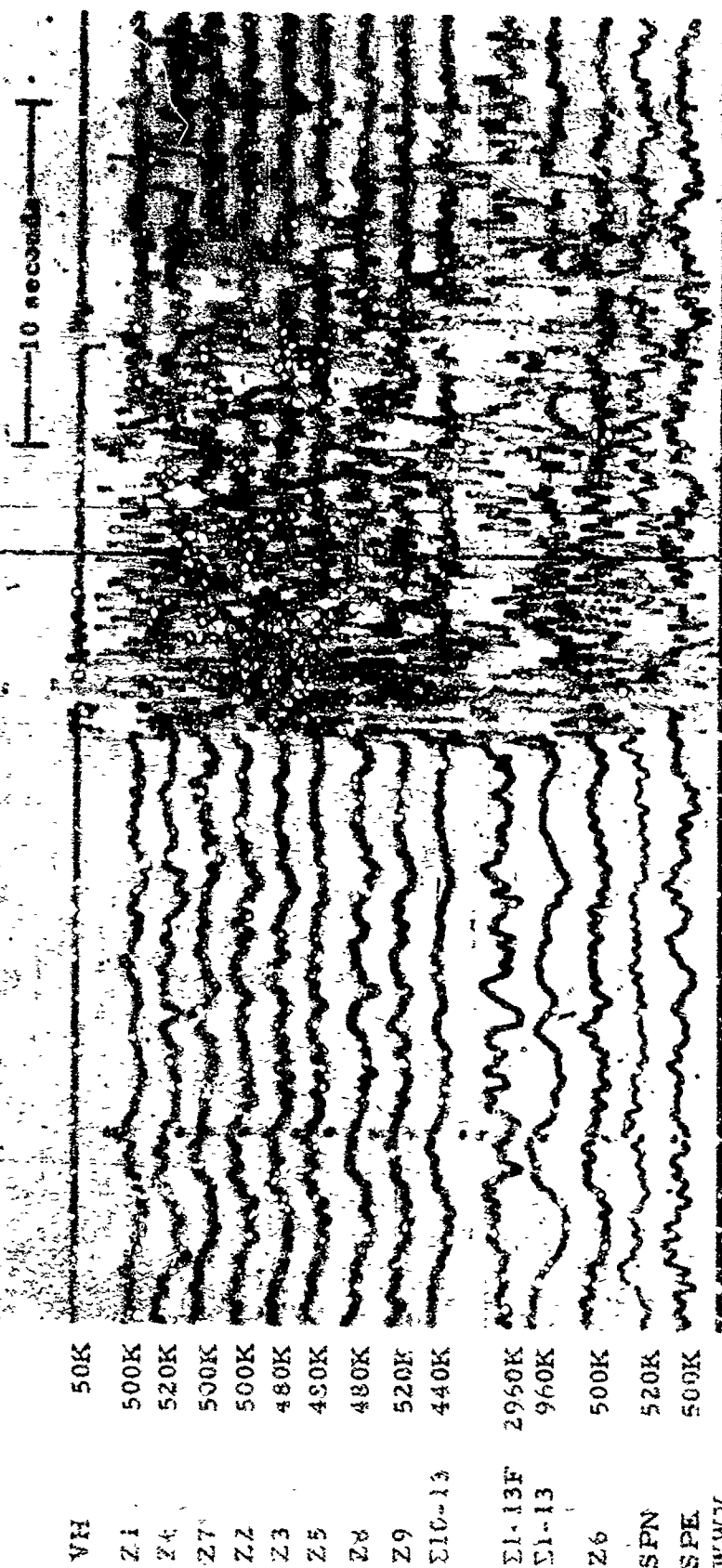


Figure 4-12. WMSO seismogram illustrating a 2500-pound detonation of TNT on Fort Sill. (X10 enlargement of 16-mm film)

WMSO  
Run 337  
3 Dec 1963  
Data Group 311



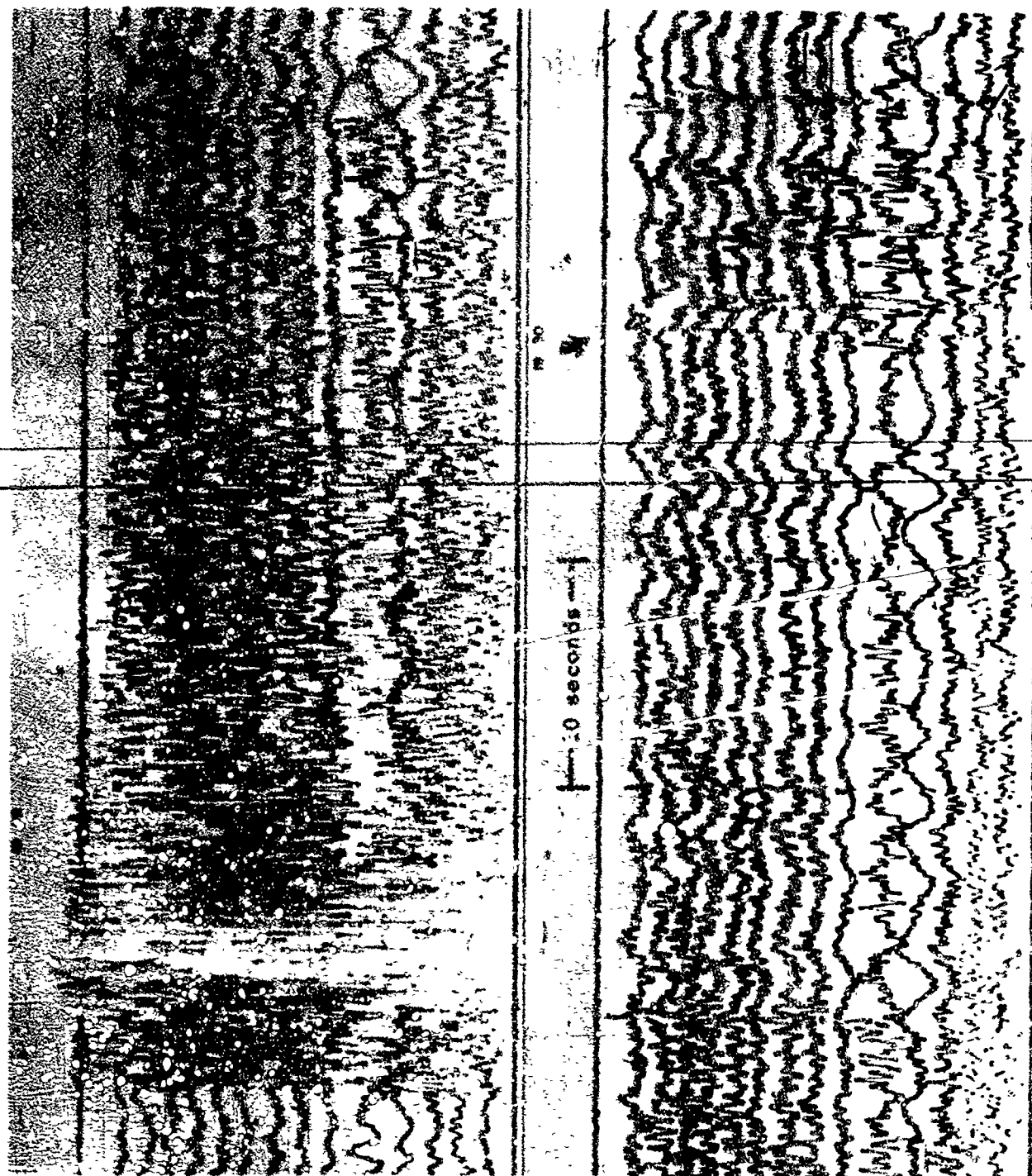


Figure 4-13. WMSO seismogram illustrating an acoustic signal generated by a blast at Richard's Smu Quarry. Epicentral data:  $\Delta = 18.1$  km, azimuth =  $73.9^\circ$   
(X7.4 enlargement of 16-mm film)

TR 64-50

VTR 50K  
 Z1 500K  
 Z4 520K  
 Z7 500K  
 Z2 500K  
 Z3 480K  
 Z5 480K  
 Z8 480K  
 Z9 520K  
 Z10-13 440K  
 Z1-13F 2960K  
 Z1-13 960K  
 Z6 500K  
 SPN 520K  
 SPE 500K  
 WWV

WMSO  
 Run 337  
 3 Dec 1963  
 Data Group 311

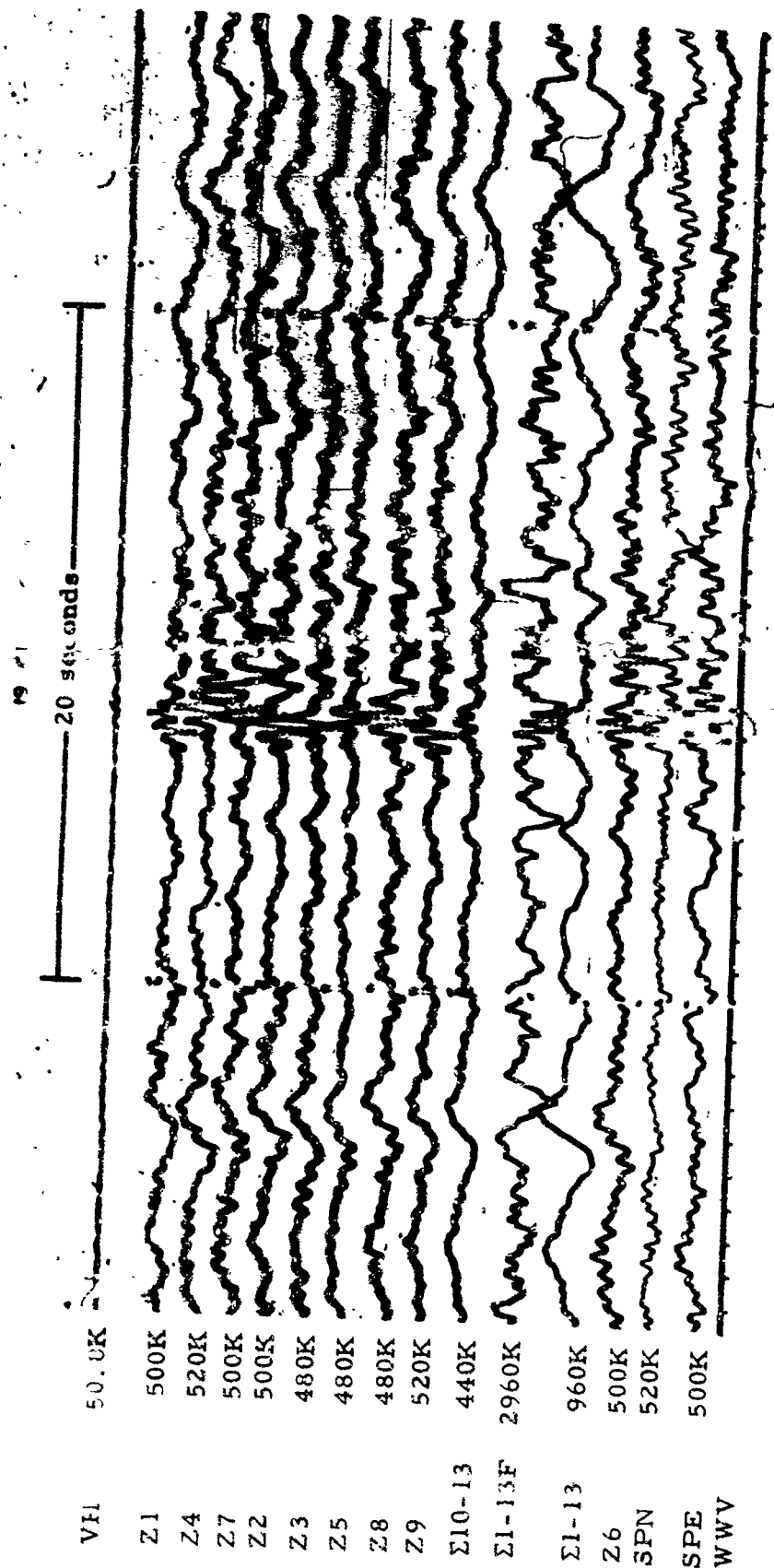


Figure 4-14. WMSO seismogram illustrating the Lg (Sur) phase from a near regional (?) event. The P phase was not recorded (X10 enlargement of 16-mm film)

WMSO  
Run 337  
3 Dec 1963  
Data Group 311

## INDEX

Acoustic Signals, 4-9, 4-10, 4-11, 4-12, 4-13

Aegean Sea, 3-26

Andreanof Islands, 3-16, 3-17, 3-18

Atlantic Ocean, 3-13, 3-23

Australia, 3-39

Banda Sea, 3-33

Bolivia, 2-8, 2-9, 2-19, 3-20

Brazil, 3-14, 3-20

California, Gulf of, 3-1

Chagos Archipelago, 3-38

Chile, 2-5, 2-6, 2-7, 2-20, 2-21, 3-11, 3-19

Easter Islands, 2-10, 3-21

Ecuador, 3-12

Fiji Islands, 2-17, 2-32, 2-33, 2-33a, 2-35, 3-27, 3-28

Galapagos Islands, 3-10

Guerrero, Mexico, 3-3

Hawaiian Islands, 3-15

Hokkaido, Japan, 3-24

Idaho, 3-2

INDEX, Continued

Indian Ocean, 3-40

Ionian Sea, 3-25

Iran, 3-31

Jalisco, Mexico, 3-5

Java, 2-23, 2-27, 3-34

Kamchatka, 2-4, 2-28

Kermadec Islands, 2-1, 2-29, 2-30, 2-38, 2-39, 2-42, 2-43

Kurile Islands, 2-3, 2-11, 2-16, 3-22

Lightning Spikes, 4-7

Loyalty Islands, 2-31

Luzon Island, 3-32

Macquarie Islands, 2-24

Mexico, Central, 2-41

Microseisms, 4-1, 4-2, 4-3, 4-4

New Britain, 3-30

New Guinea, 2-14, 2-15, 2-36

New Hebrides Islands, 2-12, 2-13, 2-34, 2-37

Ontario, 3-6

Oregon, Coast of, 3-7, 3-8

Peru, 2-2, 2-18, 2-19

INDEX, Continued

Phases

Lg, 4-14

Love, 2-40, 2-41

P, 2-1, 2-2, 2-3, 2-4, 3-1, 3-2, 3-3, 3-4, 3-5, 3-6, 3-7, 3-8, 3-9,  
3-10, 3-11, 3-12, 3-13, 3-14, 3-15, 3-16, 3-17, 3-18, 3-19, 3-20,  
3-21, 3-22, 3-23, 3-24, 3-25, 3-26, 3-27, 3-28, 3-29

PcP, 2-18

PcPPKP, 2-31

PKKP, 2-25, 2-26

PKKS, 2-37

PKP, 2-14, 2-22, 3-30, 3-31, 3-32, 3-33, 3-34, 3-35, 3-36, 3-37,  
3-38, 3-39, 3-40

PKPPKP, 2-28

PKPPKPPKP, 2-29

PKPPKPPKPPKP, 2-30

PKPPKS, 2-38

pP, 2-1, 2-2

PP, 2-12, 2-13, 2-14, 2-15, 2-16

PPP, 2-16

PFS, 2-34

PS, 2-32, 2-34

INDEX, Continued

Rayleigh, 2-40, 2-42, 2-43, 2-44

S, 2-5, 2-6, 2-8, 2-9, 2-10, 2-11, 2-20, 2-32, 2-41

ScP, 2-19, 2-20

ScS, 2-10, 2-20, 2-21

SKKKS, 2-39

SKKP, 2-27

SKKS, 2-36, 2-37

SKP, 2-23, 2-24

SKS, 2-32, 2-33, 2-33a, 2-34, 2-35, 2-36

SP, 2-11, 2-35

SPP, 2-35

sS, 2-5, 2-7

SE, 2-17

SSS, 2-17

Surface, 2-41

Pressure Noise, Barometric, 4-8

Prince Edward Island, 3-37

Quebec, 3-6

Revilla Gigedo Island, 3-4

Sandwich Islands, 2-25

INDEX, Continued

Santa Cruz Island, 2-26, 2-44

Sonora, Mexico, 2-40

Sumatra, 2-22, 3-35

Sunda Strait, 3-36

Train Noise, 4-6

Turkey, 3-29

Venezuela, 3-9

Wind Noise, 4-5